03

ERTS III

E7.6 - 1 0.3 3 1

CR-147212

(E76-10331) REGIONAL TECTONIC EVALUATION OF   N76-24656
THE TUSCAN APENINE, VULCANISM, THERMAL   HC $6.00
ANOMALIES AND THE RELATION TO STRUCTURAL
UNITS Final Report, Oct. 1972 - May 1975   Unclas
(Zentralstelle fuer Geo-Photogrammetrie)   G3/43 00331

ORIGINAL CONTAINS

COLOR ILLUSTRATIONS

/332A

ZGF - ZENTRALSTELLE FÜR GEO-PHOTOGRAMMETRIE UND FERNERKUNDUNG (DFG)

am Institut für allgemeine und angewandte Geologie der Universität, Luisenstr. 37, D-8 München 2

1. SR No. 332	2. Type of Report III	3. Recipient's Catalog No.

4. Title: Regional tectonic evaluation of the Tuscan Apenine, Vulcanism, thermal Anomalies and the relation to structural units	5. Report Data May 1975
	6. Period Covered Oct. 72 – May 75

7. Principal investigator Prof. Dr. J. Bodechtel	8. Number of Pages 133

9. Name and Adress of Principal Investigators Organization Zentralstelle für Geo-Photogrammetrie und Fernerkundung	10. Principal Investiga.Rept.No.
	11. GSFC Technical Monitor James Broderick

12. Sponsoring Agency and Adress Deutsche Forschungsgemeinschaft BONN-Bad Godesberg Kennedyallee 40	13. Key Words (Selected by PI) Geology, Land use, data processing

Supplementary notes

This report consists of the results of research work carried out at the Zentralstelle für Geo-Photogrammetrie und Fernerkundung der Deutschen Forschungsgemeinschaft (Central Laboratory of geophotogrammetry and remote sensing of the German Research Council)

Summary:
Based on LANDSAT-1 data (photographic products and CCTs) methodological and application oriented investigations were carried out. The geological interpretation on data exhibiting the Italian peninsula (lineament evaluation) led to the recognition of tectonic features which are explained by a clockwise rotation of various blocks along left-handed transform faults. These faults can be interpreted as resulting from shear due to main stress directed north-eastwards.
A landuse map of the mountainuous regions of Italy was produced on a scale of 1:25o.ooo. Several levels, I,II and III categories could be mapped.
For the digital treatment of MSS-CCTs an image processing software was written in FORTRAN IV. The software package includes descriptive statistics and also classification algorithms. Statistical investigations on redundancy and user-oriented application of LANDSAT-data led to investigations concerning data reduction and to analogue-digital data processing techniques. At least laser-optical processing techniques (Fourier-analysis) applied on LANDSAT-data were considered.

The following Report was prepared
by the Staff of the Zentralstelle:

Prof.Dr.J. Bodechtel

Dr.R. Haydn

Dr.J. Nithack

Dipl.Phys. R. Dittel

Cand. Geol. G. di Bernado

Dipl. Geol. K. Hiller

Dipl. Geol. F. Jaskolla

Cand. Geol. H. Leisen

Cand. Geol. U. Münzer

Dipl. Geol. A. Smolka

Dr. R.P. Gupta [+]

[+] Guest scientist from the Department of Geology
and Geophysics, University of Roorkee, India

CONTENTS

PART II

Methodological investigations
(Digital analog investigations)

PART I

SCIENTIFIC AND APPLICATION-ORIENTED INVESTIGATIONS

(GEOLOGY, TECTONICS, LANDUSE-MAPPING)

INTRODUCTION

This final report on LANDSAT-1 investigations is the re-
sult of activities conducted during the years 1973 - 1975.
With respect to our research activities in the LANDSAT
program and in the field of remote sensing in general,
this report must be considered an intermediate work state-
ment of progress to date.

It is necessary to continue and to intensify future work
on the following aspects: methological investigations
concerning the applicability of LANDSAT data for various
earth scientific disciplines; development of data handling
techniques, such as digital evaluation of LANDSAT data;
and the analog electronic treatment of images. From a pure
scientific point of view, LANDSAT data have delivered a
great deal of new information.

With regard to LANDSAT-2, we are optimistic that further
scientific results can be derived by evaluation data
acquired over a longer period of time.

Pure scientific investigations lead automatically to
practical applications and the practical use especially
of LANDSAT data. In order to define and to identify poten-
tial applications of spaceborne remote sensing techniques,
a first-order task is to bring to the attention of poten-
tial users the importance of such data.

The Zentralstelle für Geo-Photogrammetrie und Fernerkundung
has been founded and is funded by the German Research Council
in order to promote remote sensing activities in Germany and
to help establish this new technology for various potential
applications. The enclosed book on ERTS and partly on SKYLAB
(" Die dritte Ent eckung der Erde ") must be considered as
a step toward achieving this goal. The distribution of this

book has already resulted in increased interest by potential users, such as ministries and other agencies involved in environmental planning and surveillance.

The LANDSAT-1 data provides us, for the first time, with very high resolution sequential multispectral satellite data. Our first approach in the evaluation of this data has been carried out under earth scientific aspects using more or less conventional interpretation techniques. These activities consist of structure-tectonical investigations and also the evaluation of LANDSAT data for land-use planning purposes.

Investigations into the more methodological aspects concerning the digital treatment of LANDSAT data has been intensified after receiving the first tapes near the end of 1973

Within the scope of the above-mentioned investigations, the following activities were conducted: software development for the treatment of MSS-data, the application of analog digital and optical techniques.

According to our various activities, the following report is subdivided into two main parts entitled: Part I, scientific and application-oriented investigations and Part II, methodological investigations.

A) GEOLOGIC EVALUATION OF CENTRAL ITALY

The geological investigations described are based on
conventional photo interpretation techniques applied to
LANDSAT imagery. For some demonstration purposes also
EREP data were applied.
The methods described were used to investigate the tectonic
significance of identifiable linear features by utilising
multistage imagery and the results of fieldwork (Fig. 1).
The geological field investigations are restricted to some
areas near Volterra and Siena in the Central Tuscany.
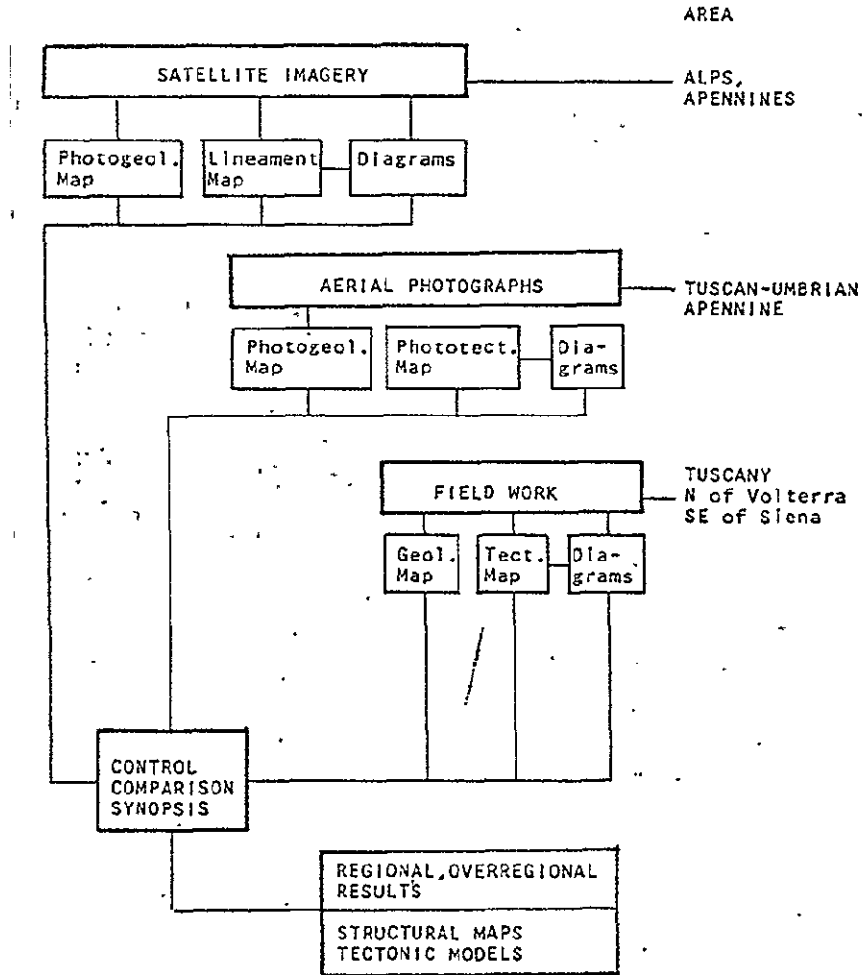
Fig. 1 Scheme for the geologic-tectonic research in the
        Apenines

1. Methodological Aspects of Space-Imagery Interpretation

1.1 Multitime Image Interpretation

The ability to recognise and interpret linear features within mountain regions strongly depends on shadow effects provided by the distinct relief. As shadow effects are also a function of Sun angle. ERTS images offer optimum possibilities for the statistical comparison of lineament maps with respect to seasonal illumination conditions.

Figure 2 shows a statistical representation of lineament directions derived from three sequential ERTS images of the Molise, northwest of the Gargano Peninsula, Italy (ERTS-1, 8.8.72, 27.8.72, 5.2.73). Comparison of the three histograms shows that all possible linear-feature directions are present in each ERTS frame. The distributions of the maxima, however, have shifted to a certain degree. Depending on the azimuth and elevation of the Sun, this effect has to be taken into consideration, especially when performing tectonic interpretations on the basis of statistical lineament distributions.

In order to minimise the above effects, it is necessary to superimpose the results of as many multitime lineament evaluations as possible as in the following table.

The significance of the distribution maxima obtained by combining sequential data is discussed in Chapter 4.

-10°	-20°	-30°	-40°	-50°	-60°	-70°	-80°	-90°	sector
3,9	14,6	9,5	15,5	14,2	23,4	12,5	2,7	2,2	relative value
-100°	-110°	-120°	-130°	-140°	-150°	-160°	-170°	-180°	sector
3,0	8,6	1,4	4,5	3,7	9,1	5,0	7,1	9,7	relative value
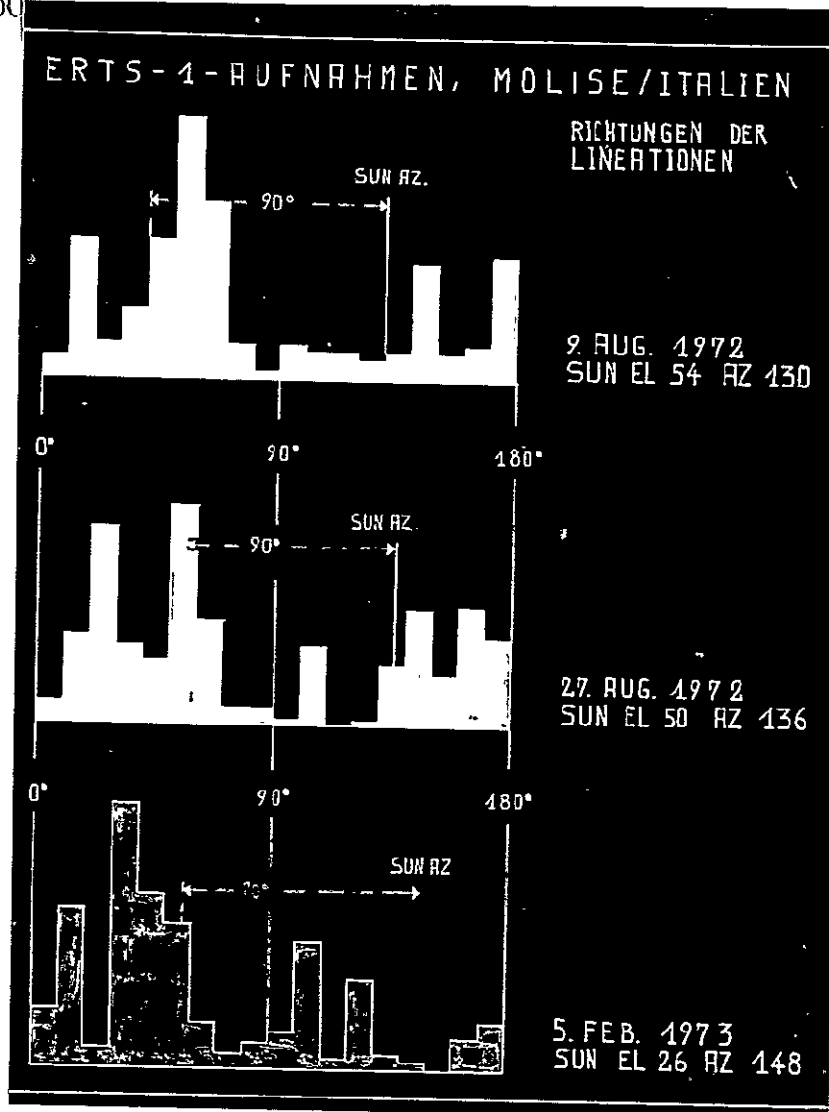
Fig. 2 Histograms of lineament distributions derived from
        sequential images

The need for multitime evaluations is also apparent from
Figure 3. Many linear features could be identified and
traced over large areas by using images from different
seasons. The reason for this is that, in Central Europe
at least the detection of lineaments depends on morpho-
logy and vegetation. When using multitime imagery,
regional patterns become more obvious.
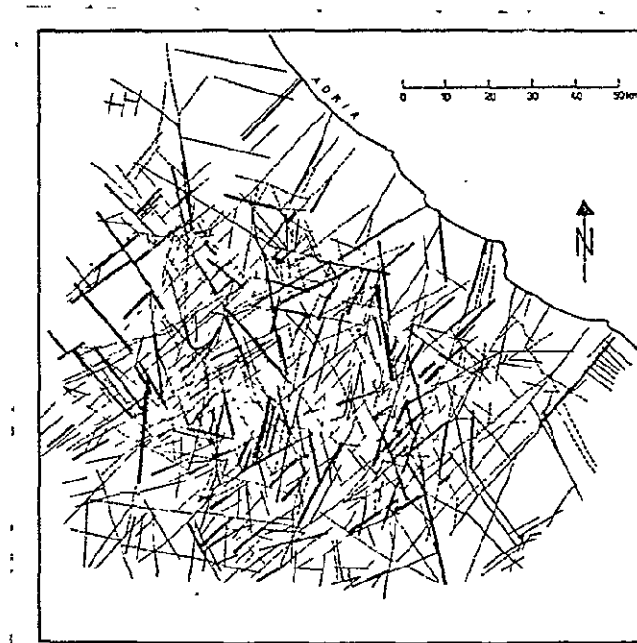
Fig.3   Composed lineament map of temporal · imagery
        LANDSAT-1 images
        MOLISE/ITALY

        Lineations (MSS 7)
        ——— 9.Aug.1972
        ------ 27.Aug.1972
        -------- 5.Feb.1973
        ———overlapping lineations

1.2 Detection of Tectonic Movements from Morphological Features

By using morphological features for the evaluation of
synoptic satellite imagery , it is possible to obtain
information on tectonic movements along fracture systems.
Regions comparable in terms of petrography and tectonic
stress fields are characterised by a similar morphological
pattern if the same climatological conditions can be assumed.
If a displacement of such comparative units is detectable
along a linear feature in a first approach, it can be des-
cribed as a fault. A more detailed description of the fault
is only feasible if the dipping direction of the strata
can be detected, because vertical displacement of tilted
strata results in a pseudo-horizontal displacement at the
surface. Vertical movements can be determined only for
fold structures, basin or graben fringes. Sigmoidal
oriented valleys and mountain ridges can mask younger
horizontal movements. Furthermore, it can be observed
that fold structures cut by faults often show displace-
ments with respect to the movement of the fault.

Examples of the above phenomena are shown in Figure 4,
which represents part of a Skylab image (S 19oA, Septem-
ber 1973) showing the Umbrian Apennines between the
Lago di Trasimeno and the Adriatic coast.

Figure 5 clearly shows the feasibility of thematic mapping
of geologic tectonic phenomena. This map, which covers the
the Latium volcanic region and the northeastern area bet-
ween the Umbrian Apennines and the Abruzzi, shows the
advantages that synoptic satellite imagery offers in this
field. Besides different volcanic phenomena and the strike
and dip of strata, regional relationships between distict,
identifiable linear features are also evident.

Two types of faults in particular can be differentiated:
transform or shear faults and vertical fractures.
In this area, the shear faults from a narrow-angle system.
The first, approximately north-south oriented, is represen-
ted by a zone which cuts the Apennines east of the well-

known Rieti line. Along this fault, horizontal movement
can be detected, with a relative dislocation of the western
part towards the south. Forming an angle of about 45°, this
system is cut by southwest-northeast directed shear faults.
For the north-west oriented faul system, clockwise rota-
tion of the western and eastern blocks is assumed.

Fig. 4   Umbrian Arc, Skylab S 190 A; Examples for de-
tecting faults by morphological features

Further detectable northwest-southeast striking vertical
fault systems are correlated with the chain of Tuscan-
Latium volcanoes. These vertical faults, together with
the above northeast-southwest oriented transform faults,
form a system of bc and ac joints that were originated
by a southwest-northeast directed stress field.

Fig. 5: Geologic tectonic map of LATIUM, ITALY
LANDSAT-1, 6.Feb.1973, MSS 7

geologic morphological limit

volcano area

lava

volcano complex

small volcano

caldera

lineament

horizont.faul

vertical faul

sedim. beddin
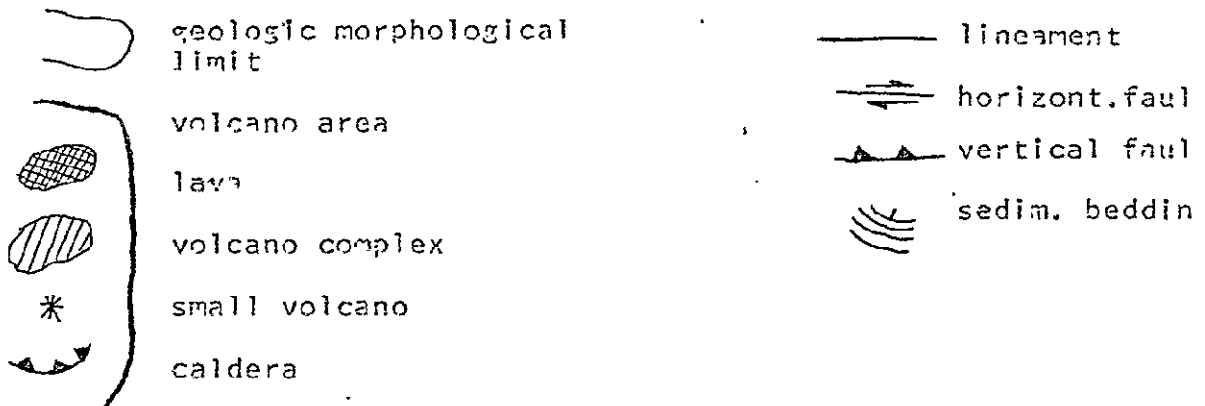
2. Lineament Patterns of the North and Central Apennines

Owing to the synoptic nature of satellite data, the exten-
sive major fault systems could be identified and explained
in relation to stress directions and fold systems.
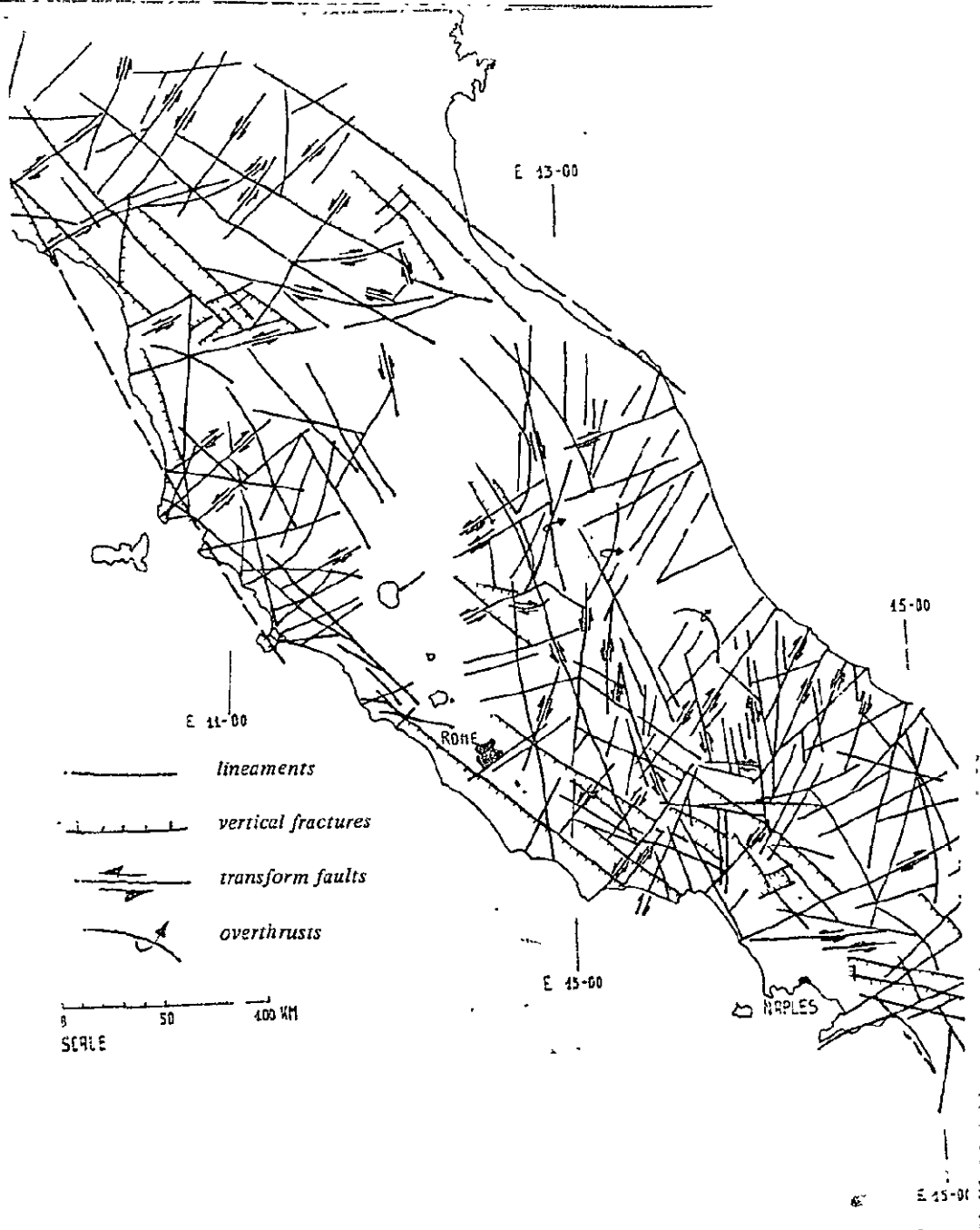
Fig. 6 Main faults in Italy revealed by ERTS-1

Regional Lineaments Evaluated from LANDSAT - Data

Figure 6 shows a view of the main lineations in the northern and central Apennines. The arrows indicate the senses of the horizontal displacements (see Chapter 1). The statistical distribution of the transform and vertical faults corresponds with the results derived by aerial photo-interpretation and fieldwork (Fig.7). Of importance for the further interpretation are the distribution peaks at 40°, 70°, 130° and 160° (see Chapter 4).

Intensive ground studies have proved that these directions can be correlated directly with an older tectonic system, with a-axis 70° and b-axis 160°, which was rotated clockwise from a primary system (b 140°), and with a younger system again in the primary stress with a = 40° and b = 140°.

The excellent correlations between the results derived from satellite images, aerial photographs and ground truth serve to demonstrate the feasibility of the evaluation methods applied.

AERIAL PHOTOGRAPHS | ERTS-1-DATA
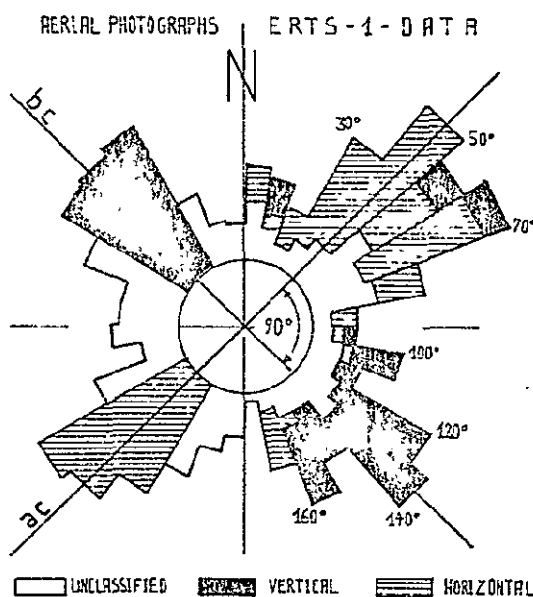
Fig. 7 Rose-diagram of fault directions revealed by aerial photographs and ERTS-1 data

2.2 Lineament Tectonic Evaluation of the Tuscan-Umbrian Apennines

The complex tectonics of the Umbrian arc are demonstrated by Fig. 9 which shows the main lineaments and accompanying minor lineations. Taking into account also the information derived from ERTS data (Fig. 7), the same tectonic systems as above ($a_1 = 70°$, $b_1 = 160°$; $a_2 = 40°$, $b_2 = 140°$) could be derived. In addition to these main lineations, shear faults at $10°$ and $110°$ can be observed.

E 12-/00

N 42-00

E 12-00

SCALE

0   10   20   30   40   50 KM

——————— lineaments

(C)   partly volcanic, partly undefined circular structures

——————— lineations
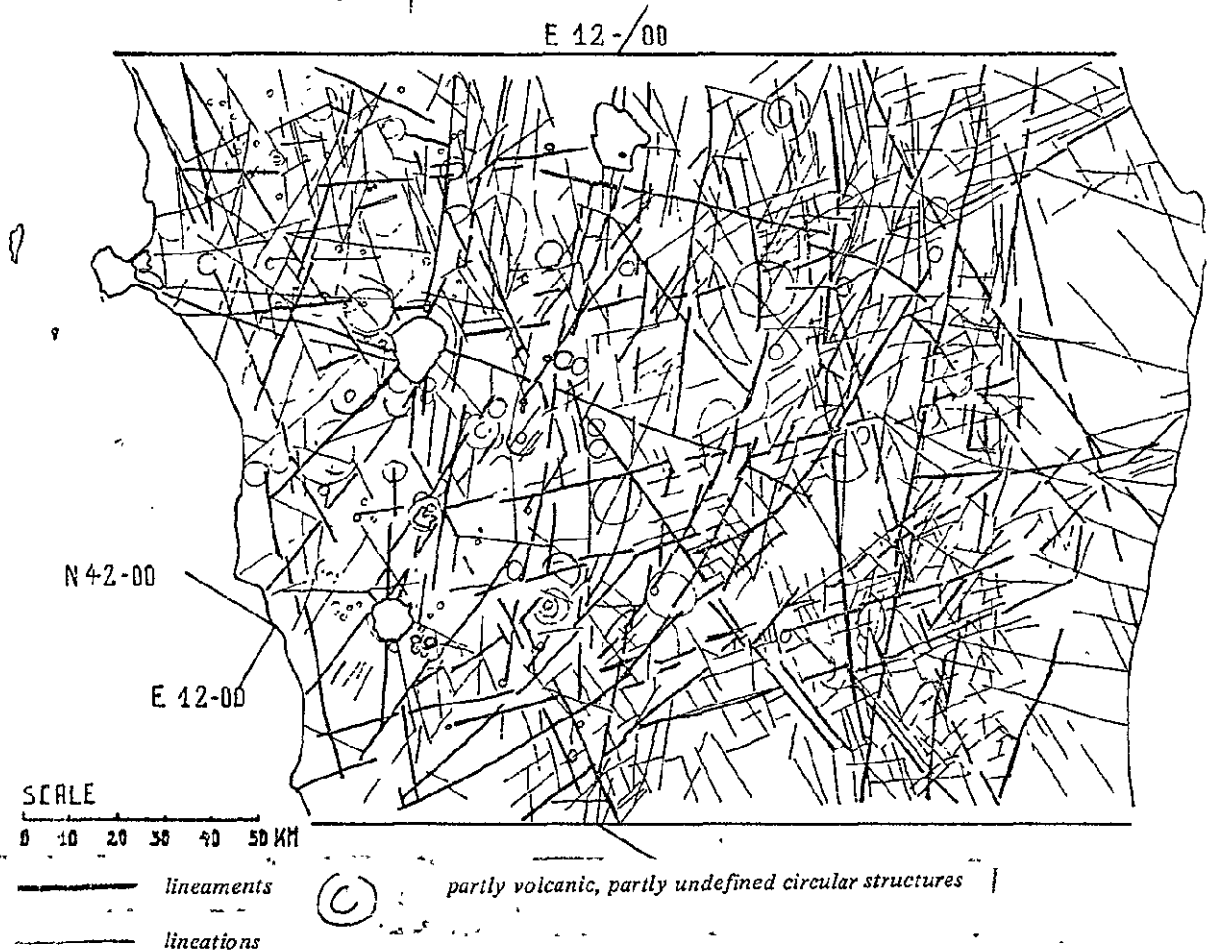
Fig. 8 Photo-tectonic interpretation, Tuscan-Umbrian Apenines

Some information could also be derived concerning the age
of the various systems. A sequential description could be
drown up for the latest movements. A model for a "tectonic
schedule" is illustrated in Figure 1o and can be described
as follows:

1) Beginning of the folding phase, which is characterised
   by northwest-southeast oriented fold axis and a per-
   pendicular striking ac-system (primary 14o$^{\circ}$ b and b$_2$).

2) With respect to the further compression, displacement
   of the various blocks occurs along the ac-system.
   This results in a relative displacement towards the
   northeast of the northwestern part.
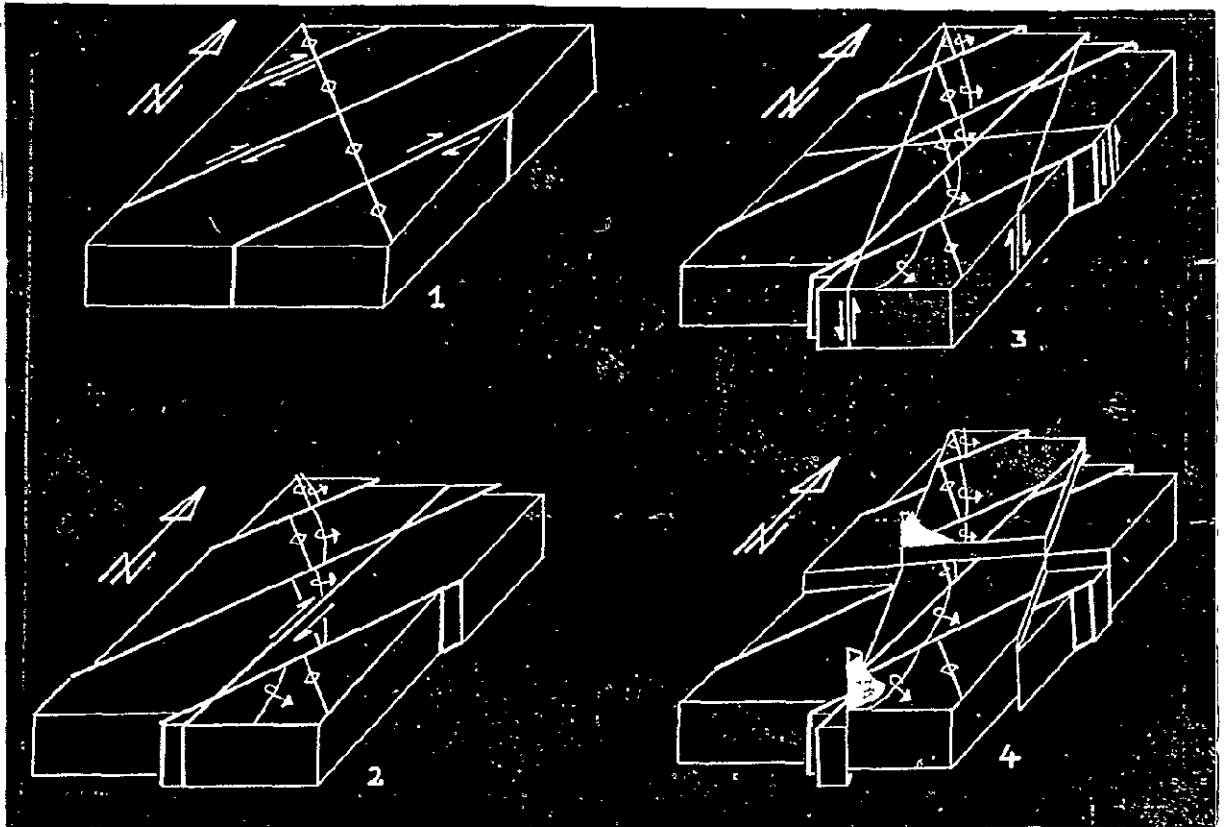
Fig. 9   Fracture development in the Tuscan Umbrian Apenine

3) Besides north-south oriented transform faults, a con-
tinuation of the shearing process causes a north east
directed displacement of the southeastern part. The
repeated displacements of the folds and overthrusts
from the "Umbrian Arc".

4) In a last phase, vertical movements occur especially
along 70°, 110° and 160° striking planes. Along these
fractures, the region of the Latium and Tuscan vol-
canoes was depressed.

3. General Tectonic Model for the Northern and Central
3.1 Apennnines

Tuscan-Umbrian Apennines

As is clearly shown in Figure 7, the directions of the
main lineations of the region between the Arno River and
the Abruzzi Mountains differ from those in the northern
and southern areas. The tectonic unit of the Tuscan-Umbrian
Apennines is bordered by the following fracture zones:

- In the north, a transform fault striking about 80° and
following the Arno Valley. Along this fault, the
Tuscan-Umbrian block was displaced to the east.

- In the east, a north-south striking transform fault,
beginning east of the city of Latina and ending at
the Adriatic coast northwest of Ancona. The relative
movement of the Tuscan-Umbrian unit was directed to
the south.

A clockwise rotation of the Tuscan-Umbrian Apennines
results from the combination of movements described.
Diagrams* obtained from fieldwork show two rectangular
joint systems: and older ($b_1 = 160°$) and a younger
($b_2 = 140°$) system. In his theory of the orogenesis of
the Apennnines, Wunderlich (1966) postulates an anti-
clockwise rotation of the main stress from west to
southwest. Such a rotation could have caused the diffe-
rence between the older and younger b-axes. As regards

* see next chapter

tectonic movements revealed by satellite data, it must, however, be pointed out that such studies mainly high-light features of relative movements.

Assuming the Tuscan-Umbrian region to be a static block, the forming stress would have shifted from west to south-west. However, taking the direction of stress as a stable element, the Tuscan-Umbrian block must be rotated clock-wise (Fig. 11). This second possibility is confirmed by:

- the movements along the bordering main transform faults,

- the internal fault pattern of the block,

- the overthrusts in the Abruzzi Mountains,

- the reduction in overthrusting intensity from north to south along the border between the Umbrian Apennnines and the Abruzzi.

Stress direction SW - NE
Primary fracture system
b $\approx$ 140°
$_1$

Same stress direction
Clockwise rotation by movements
along the great transform faults
$b_1 \approx 160°$, $b_2 \approx 140°$

vertical movements parallel to b_2
overthrusts in the north
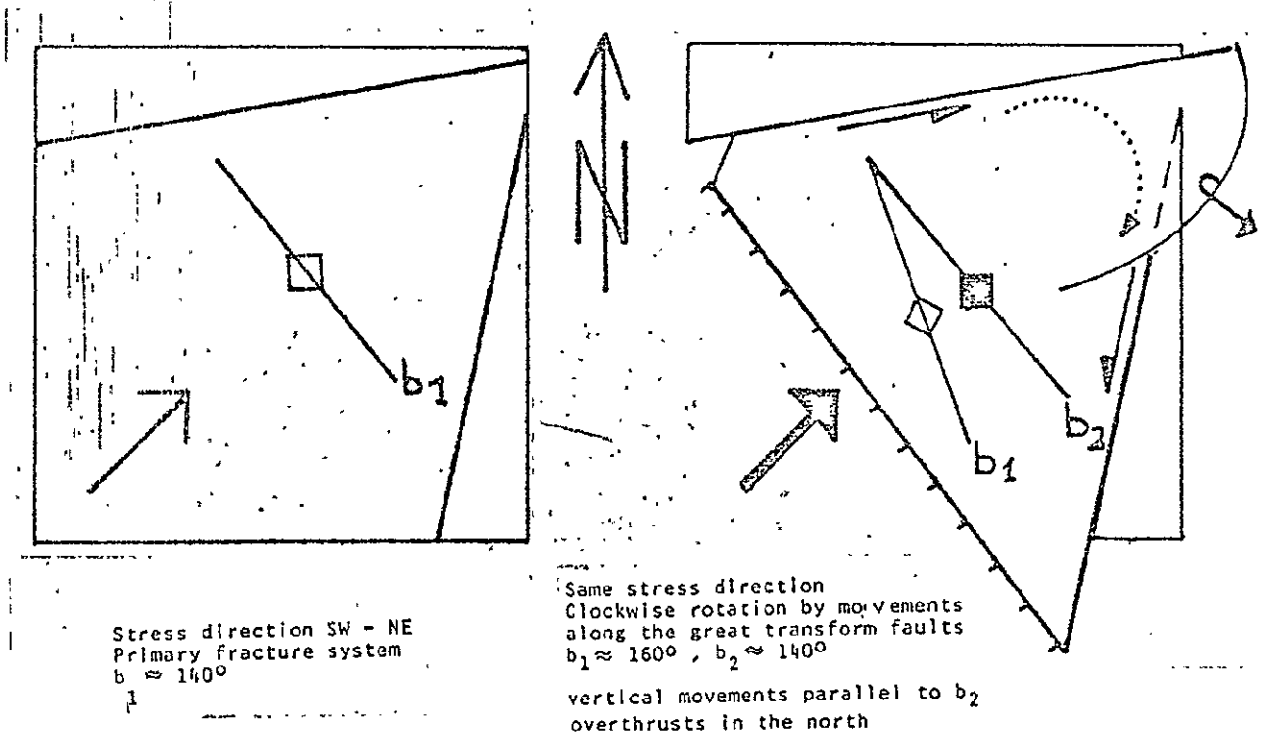
Fig. 1o   Tectonic model of the Tuscan - Umbrian Apennines

3.2 Central Apennines (Abruzzi Mountains)

The tectonic concept, described for the Tuscan-Umbrian
Apennines based on the relative movement observable in
ERTS and Skylab data has to be seen in connection with
the neighbouring areas north and south.

Based on the tectonic map (Fig. 7), a movement of the
Central Apennines, the Abruzzi Mountains, similar to
that of the Tuscan-Umbrian block can easily be derived.
But the Abruzzi are further southwest than the Tuscan-
Umbrian Apennines. This could be caused by a combination
of clockwise rotation and northeastward drift tendency of
the Tuscan-Umbrian Apennines, whereas the Abruzzi block
was a relatively stable element.

3.3 Northern Apennines

In the west, the Northern Apennines are cut off by a NNE
striking transform fault beginning in the Gulf of Genoa
and forming the eastern border of the Monferrato. The
southern limit is the Arno Valley fault, which borders
the Tuscan-Umbrian Apennines.

According to the relative movements along the two bordering
transform faults, the Northern Apennines must also have
been rotated clockwise. In this case too, the rotation
could be combined with drift in a northeastern direction.

These movements may explain the triangular shape of the Po
Valley, the northwestern part of the Northern Apennines
being moved further northeast than their southwestern part.

A sketch of above tectonic model, evaluated from ERTS and
Skylab data, is shown in Figure 12. The "block-bordering"
transform faults can be interpreted as a shearing system
with a main stress lying SW-NE. This stress caused a general
drifting of the Apennines to the northeast. The drift

intensity decreased from northwest to southeast and caused
clockwise rotation of the three blocks of the Northern
Apennines, the Tuscan-Umbrian Apennines, and the Abruzzi
Mountains.
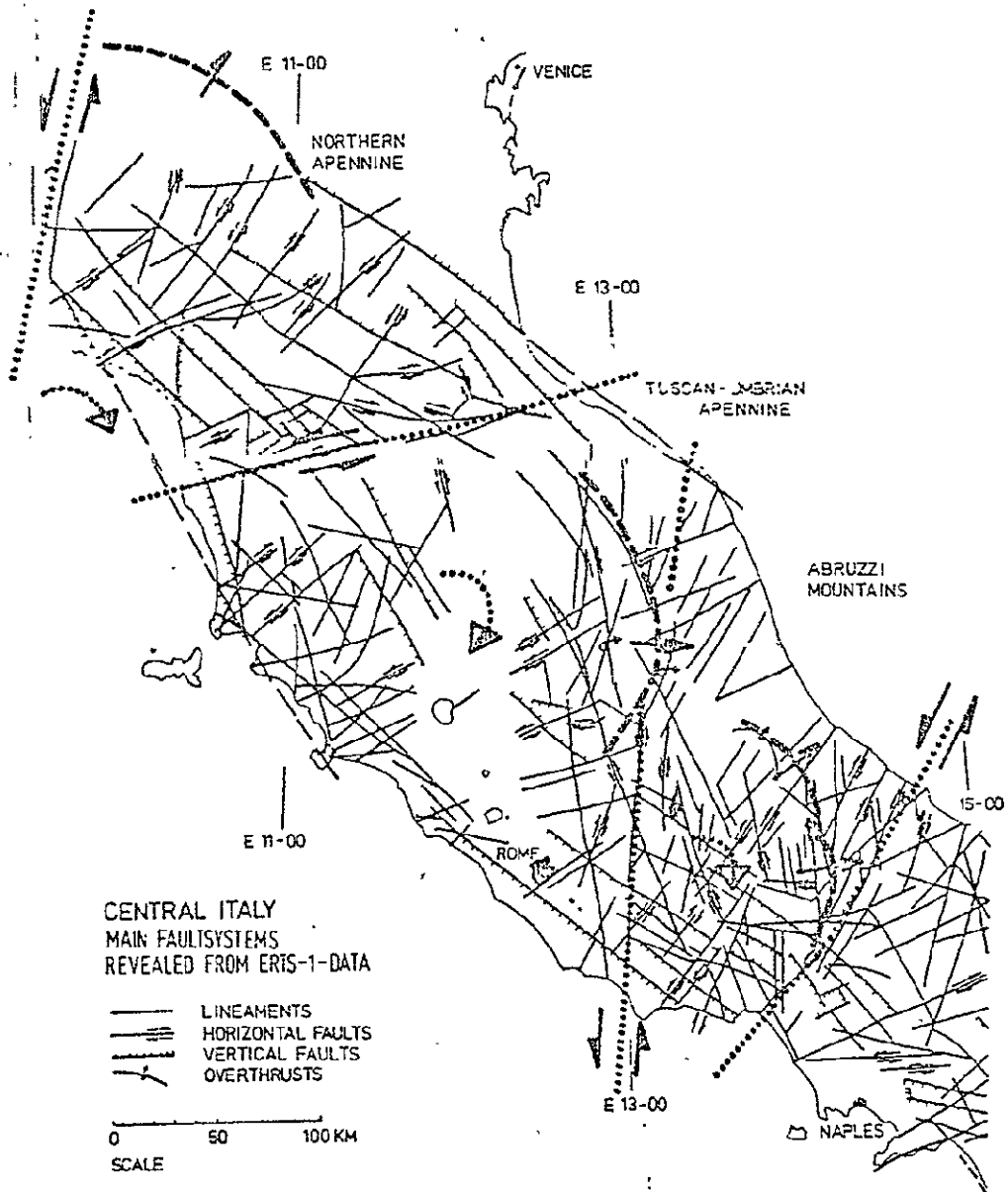
Fig. 11   Main fault systems in Central Italy

4. Relationship between Northern Apennines Po Valley and the Southern Alps

It is understood that the extensive tectonic fractures must have their origin in the deeper crystalline basement. These large scale movements result in a system of fractures revealed only by a subtitle lineament pattern in the sedimentary cover, interpretable on the basis of space and aerial images.

However, the exact location of the fracture planes, revealed by the lineaments, is difficult to detect.

But for the geologist, the knowledge of the relative position of the fracture planes, obtainable through evaluation of photolineaments is, especially, of great importance.

In the area of the northern Apennines, SW-NE and NW-SE striking parallel fractures are known and can be traced as lineations through the bordering Po Valley. Some of these lineations even extend into the southern Alpine body.

From geological investigations, it is known that swales and ridges existed during Triassic time. These features resulted from NNE-SSW striking fractures in the crystalline basement (Auboin, 1967; De Jong, 1967; Nithack, 1968). Furthermore, it is proven that there is a stepwise downward progression from the southern Alps to the Po Valley, created by WNW-ESE stepwise faults.

It can be expected that the above-mentioned prevalent vertical movements within the crystalline basement are present also in the basement of the Po Valley area. This conclusion is reached on the basis of the lineament evaluation (Figure 13) and the morphology of the Quaternary basin, described by the map of Figure 12 (Beder ke & Wunderlich, 1968).

The characteristic morphology of the Quaternary basin in the region of the Po Valley suggests that the large scale lineaments exist throughout the Apennine-Po Valley and

southern Alps and that they are an expression of actual faults.

Based on this conclusion, a schematic block diagram could be constructed for the above-mentioned area (Fig. 14).
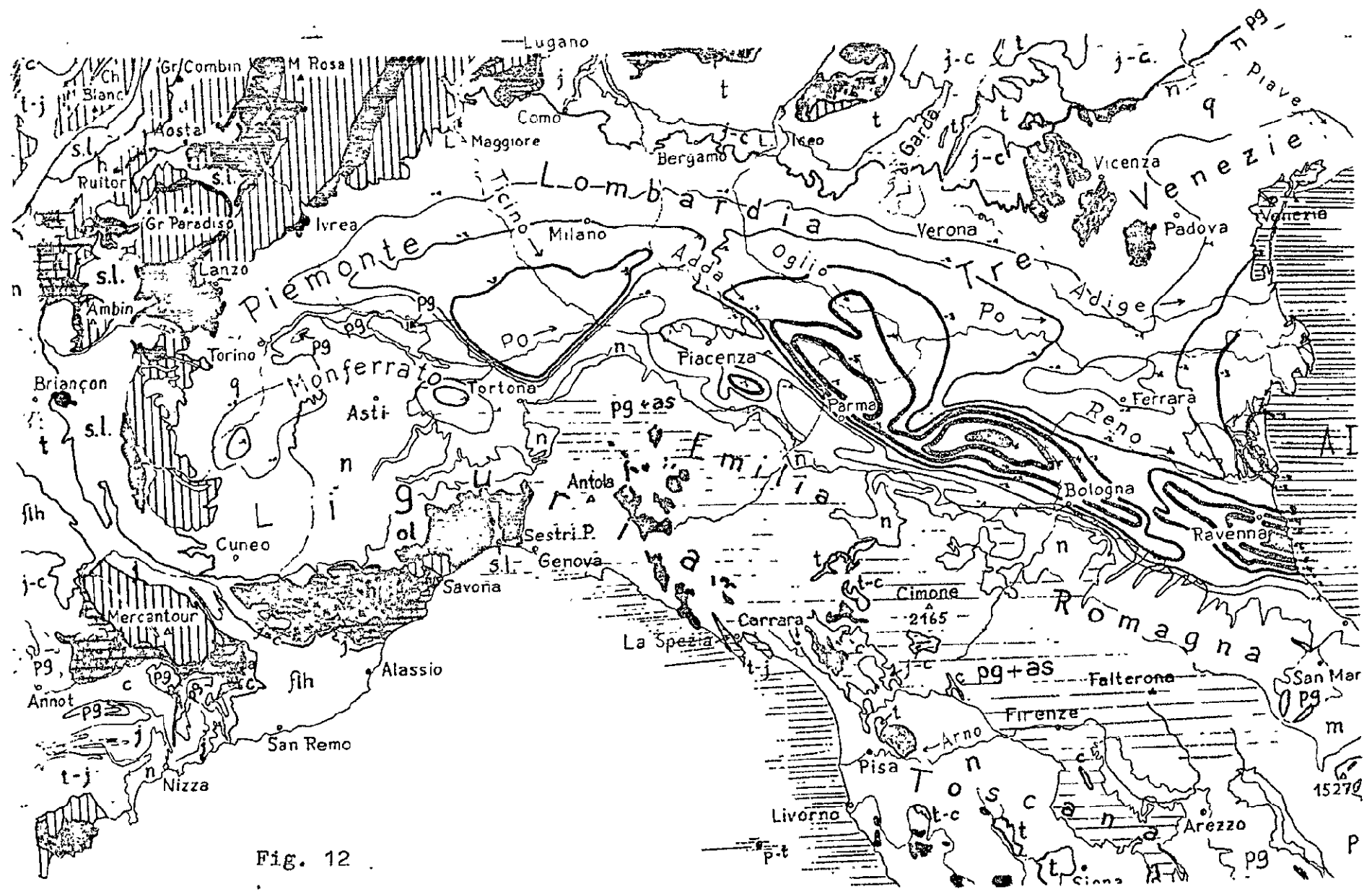
Fig. 12
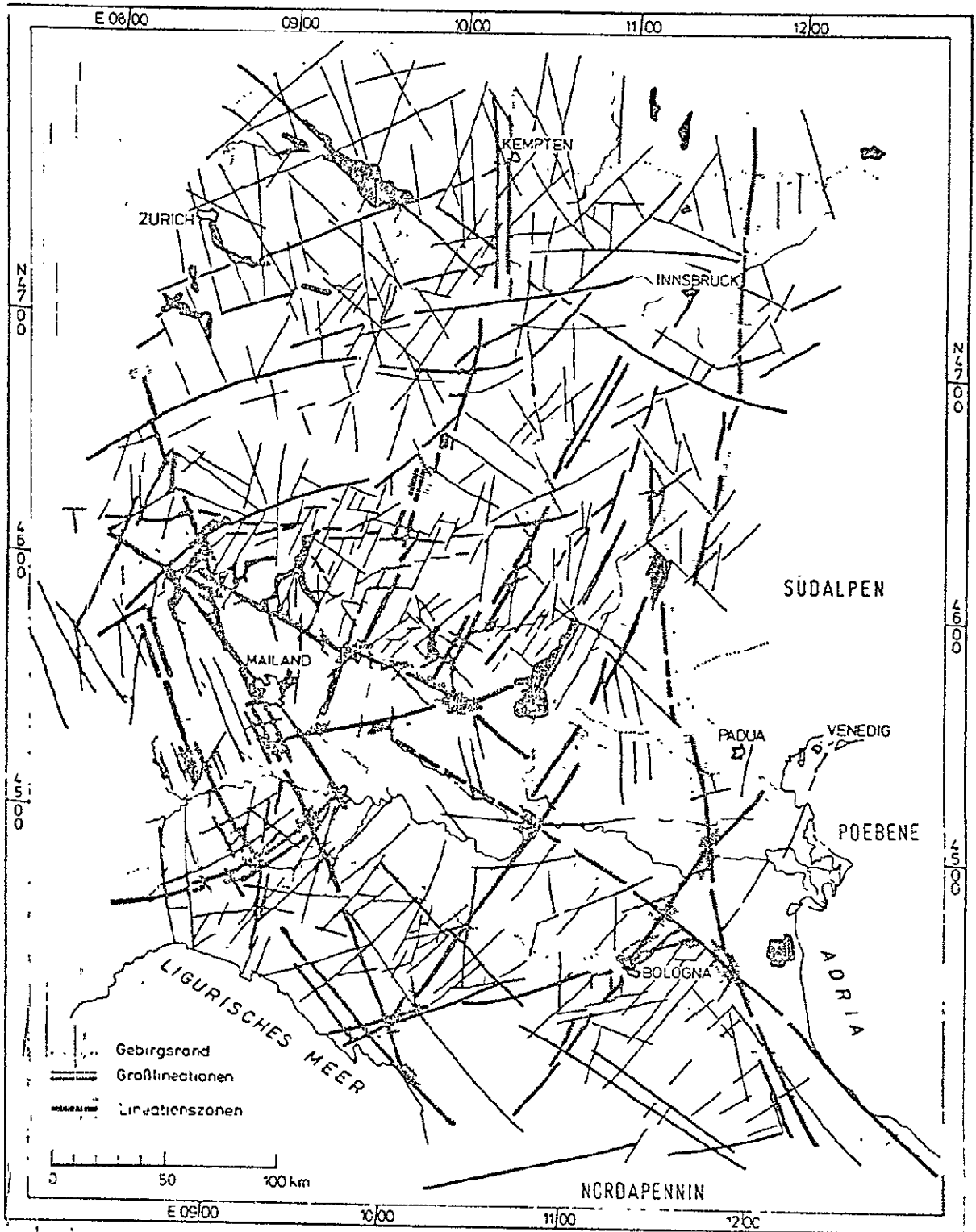
Fig. 13
Northern Apennines, Po Valley, Southern Alps
Lineations derived from LANDSAT imagery

S Ü D A L P E N

COMERSEE   ISEOSEE   GARDASEE

POMÜNDUNG

NORDAPENNIN
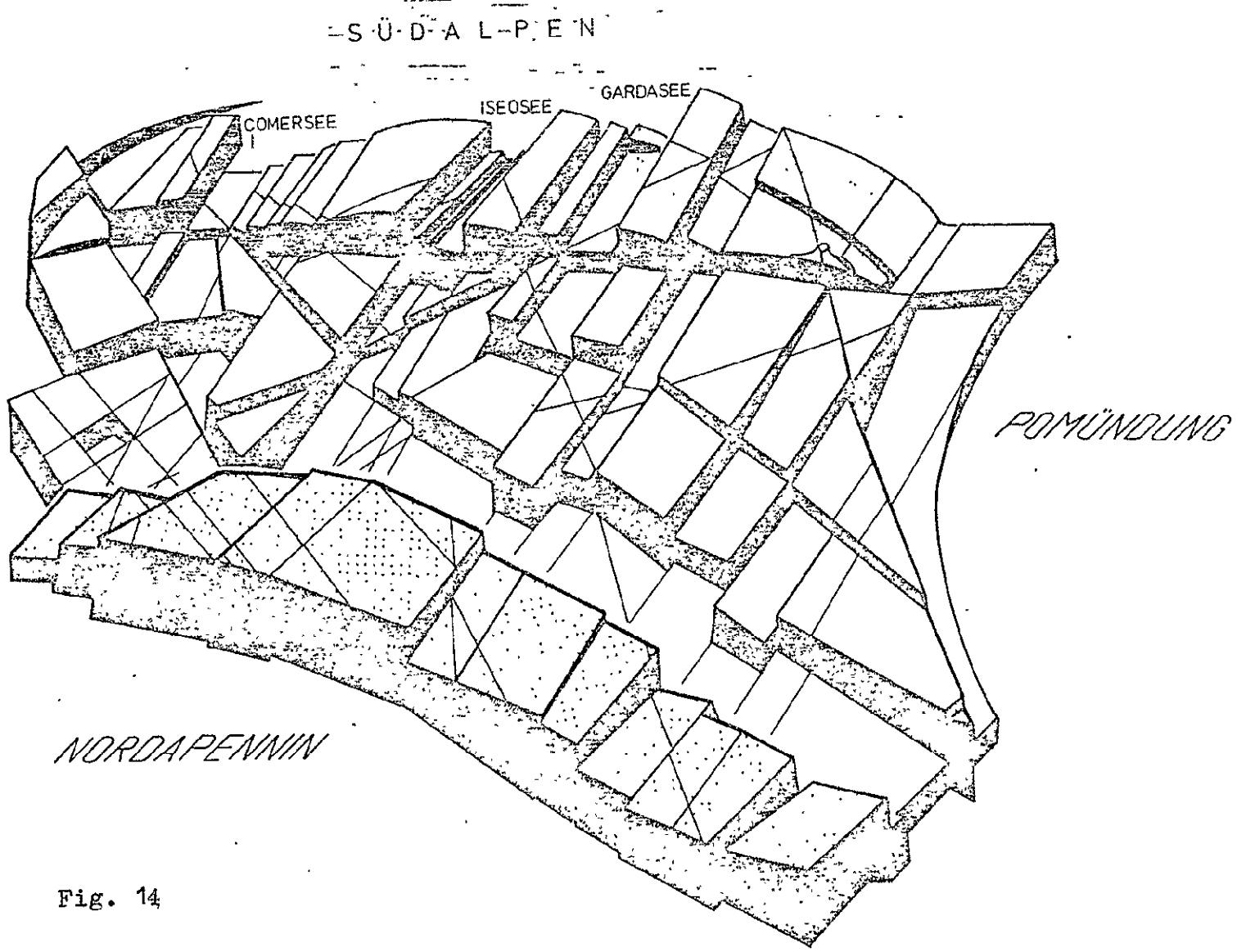
Fig. 14

5. Comparison of Lineament Pattern with Tectonic. Ground Truth Measurement

Satellite imagery can be regarded as an optimum base for
a large scale lineament and structure analysis. By
utilizing the unique synoptic view over large areas, the
interpreter is able to delineate linear features and to
recognize subtle structural elements on the earth sur-
face, detectable by aircrafts or by ground investigations.
Because of the above-mentioned advantages of space imagery,
it is not surprising that many scientists, and especially
geologists, have concentrated their efforts on preparing
detailed lineament maps. This kind of evaluation is of
great scientific importance, especially with respect to
the understanding of inter-regional structural relation-
ships. In addition to the above-mentioned aspects, a
further evaluation procedure is to verify the interpreted
structural elements from space imagery by intensive field
work. Within this approach a first order task is to assess
the influence of interregional structures on the meso-
tectonic fabric.

The mesotectonic fabric of rocks is the result of certain
tectonic stress conditions. During geological time, stress
patterns have changed their orientation and intensities
several times. The above-mentioned changed stress conditions
often are reflected by typical symmetrical configurations
of joints. A careful interpretation of the fabric enables
the geologist to draw conclusions on former stress condi-
tions. That is not only of scientific, but also of great
economic importance. Quite often a close relationship
exists between a specific tectonic situation and the occurrence
of ore deposits. In order to investigate the possible influence
of lineament features to be seen on LANDSAT data to the
meso-fabric, a test site in the southern part of the
TUSCANY near SIENA was chosen.

Fig. 15:

Geological Map of the test area and its
surroundings

   Signatures in darker grey: Mesozoic rocks

                    | O | Oligocene rocks

                    | Mp | Miocene/pliocene rocks

                    - - - - - - - Faults
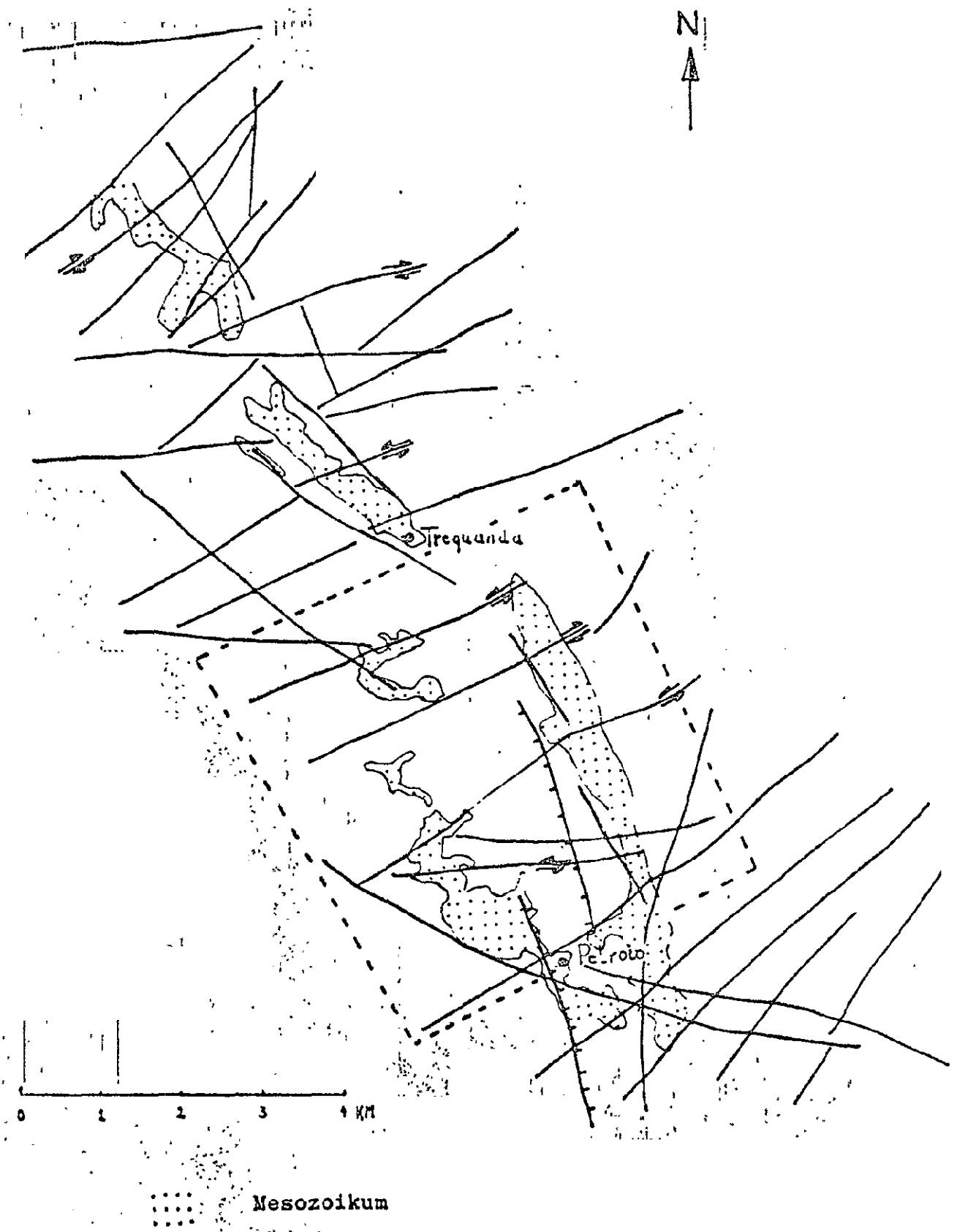
Fig. 16
Photolineations derived from aerial photographs

5.1 Geology at the Test Site

The ground truth area is part of a very important
orogenetic structure with Apenninic strike direction,
whose nature is still open to discussion. This struc-
ture is known as Cetona – Orsaro – line (the most
suitable name without genetic significance).
Morphologically, the Cetona-Orsaro-line forms a 260 km
long ridge of variable altitude and extension. In the
North of the Arno River, it represents the main crest
of the Apennines. With respect to geology, the ridge is
built up in its southern part by Mesozoic limestones,
dolostones and alternating cherty--calcareous-marly strata
and in its central and northern parts mainly by the
Macigno sandstones of Oligocene age. (Fig. 15) In
general, the structure in the mapping area could be ex-
plained as a sequence of two overturned anticlines being
replaced by thrust faults. The original fold-structures
appear now to be disturbed by synkinematic shearing and
postkinematic block-faulting. Such block-faulting revived
the old fracture pattern and created the horst-like up-
lifting of the ridge as a whole. The ridge is divided by
several horizontal faults transverse to the strike of the
folds (Fig. 16). The largest displacements have taken
place on ac-direction, as revealed by satellite images
and aerial photographs (Fig. 16, 17). On the contrary,
shear directions are less important with respect to large
scale displacements.
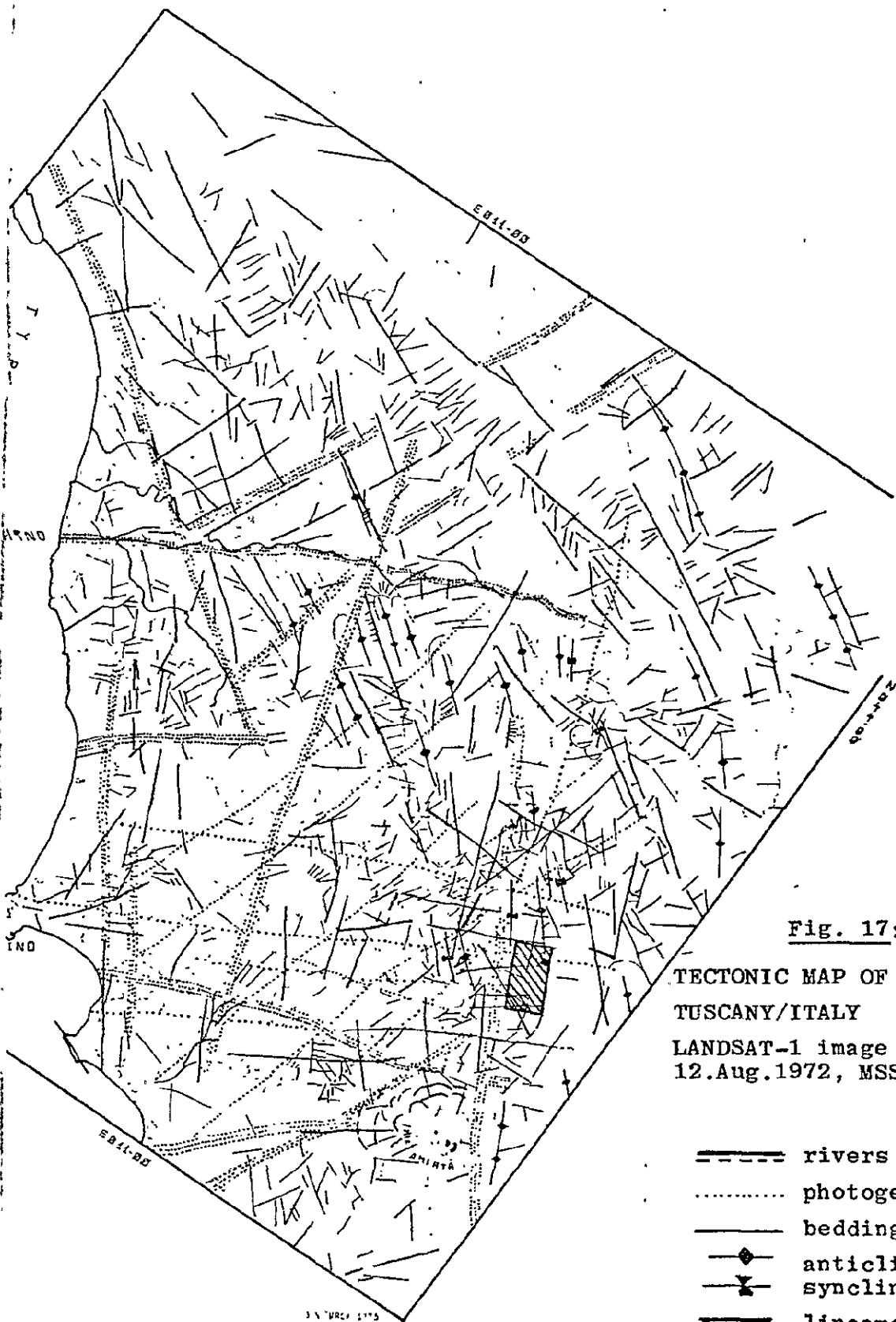
Fig. 17:

TECTONIC MAP OF
TUSCANY/ITALY
LANDSAT-1 image
12.Aug.1972, MSS 5

rivers
photogeol. units
bedding traces
anticlines,
synclines
lineaments
main lineations

Fig. 18

LANDSAT image of Tuscany

□ · : test area

5.2 Evaluation of a LANDSAT-1 Image of the Tuscany, with Special Regard to the Ground Truth Area

The following Figure 17 is based on a LANDSAT-1 image of the Tuscany taken on August 12, 1972 (Fig. 18). The ground truth area is demarcated by dotted lines. The interpretation map (Fig. 17) shows all the large lineaments touching the calcareous ridge situated between Rapolano and Montepulciano. The important ESE-WNW-striking horizontal faults can be followed almost to the Thyrrenian coast. In the same way, the bc-fault-traces (representing reverse faults) reach far to the North and South. In aerial photographs (Fig. 16), a third important fault direction striking 110° can be recognized which does not appear on the LANDSAT image. This is probably explained by the fact that scan-lines run nearly parallel to this direction. For this reason the recognition of those linears is impossible. In addition, the LANDSAT image indicates some lineaments, unrecognizable by ground truth or by evaluation of aerial photographs. Examples are the lineament W of the ridge, the result of the uplifting of the ridge, and the other one N of Trequanda, the result of the displacement of the ridge by about 4oo m transverse to its strike direction. Another one, only in part recognizable on aerial photographs, but well-identified in the satellite image, marks the boundary of the western part of the horst structure. All the large horizontal faults in the ac-direction ("antiapenninic"), seen in the aerial photos, are more difficult to recognize on the LANDSAT image.

The Large Scale Structure

The existence of two different b-axes (see chapter:"Examples of Characteristic Pole Diagrams out of the Test Site") indicates two deformation stages, the first of which, at least, is active still in the upper Triassic, but no longer is active in the Oligocene. A multistage deformation is postulated by several scientists investigating the Geology of the Apennines (Baldacci, et al., 1967, Bortolotti, 1966, Giannini, 1962, Sestini, 1970, Reutter, 1968). A possible explanation for the

N

Trequanda

Fig.20

Petroio

0   1   2   3   4 KM
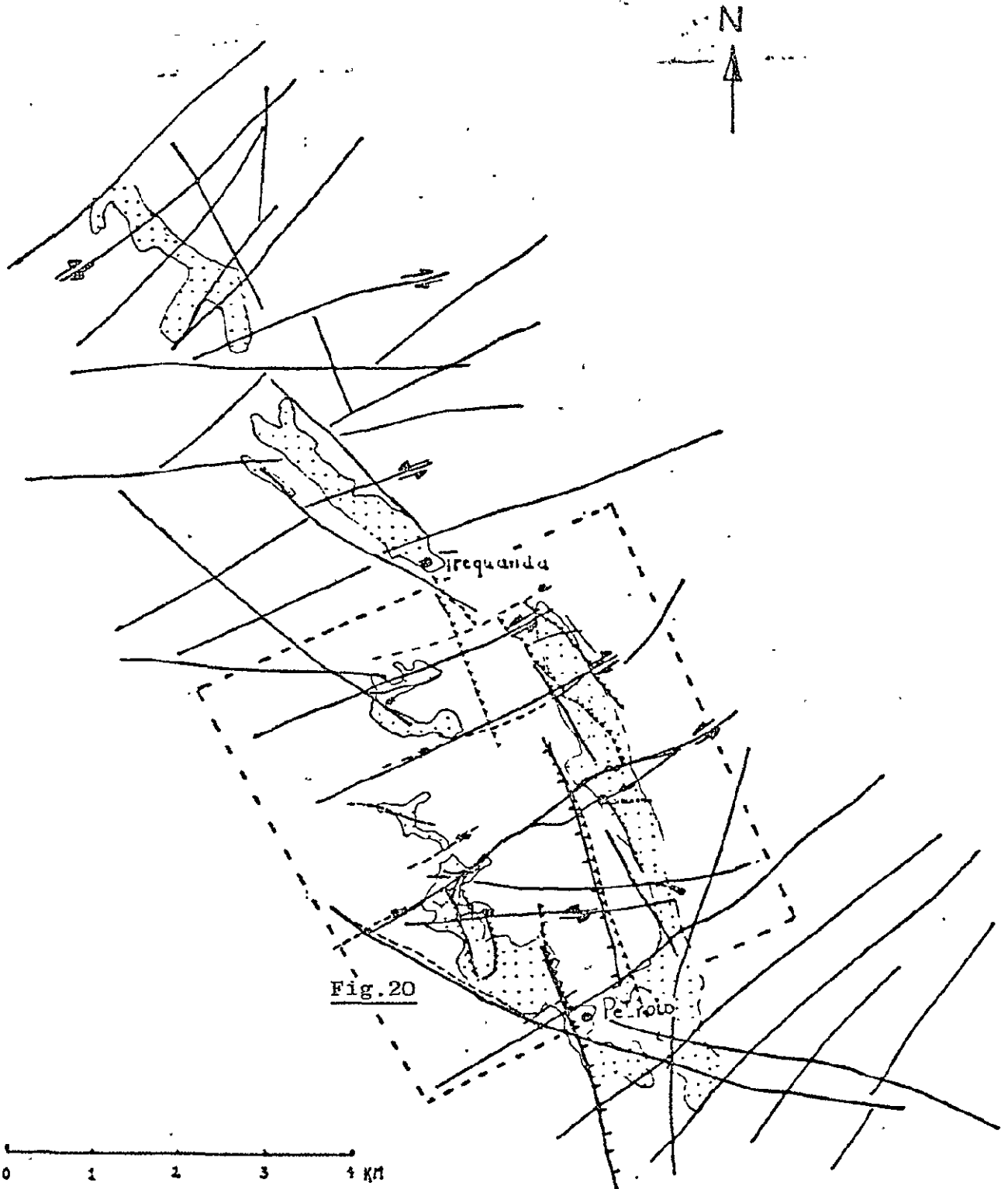
Fig. 19

```
. . . .
: : : :    mesozoic rocks
: : : :
. . . .
```

Fig.19 : Photolineations derived from aerial photographs
Fig.20 : Faults mapped by field work

difference of the two b-directions is given by Boccaletti,
Guazzone (1968, 1970). They postulate an anti-clockwise
rotation of the Italian Peninsula, which brought the axes
to their present directions. The structural data reported
by these authors (e.g. the E-W stress direction in the
Tuscany, corresponding to N-S fold axes) cannot be con-
firmed in our mapping area. Wunderlich's (1966) opinion
that the stress direction rotated counter-clockwise to the
WNW-ESE trend on the margin of the Po plain is better
suited to the structural facts. A new concept was proposed
by our research team: based on the interpretation of LANDSAT-
1 images we contend that a clockwise rotation of a block
formed Tuscany and part of Umbria. Such a rotation results
from a lefthanded horizontal fault following the Arno valley
and another N-S striking left handed horizontal fault between
the towns Ancona and Latina (see previous part of this
report).

5.3 Relation between Field Work and Phototectonic Interpretation
of Aerial Photographs

The relations between field work and aerial photointerpreta-
tion are demonstrated in figure 19 and 20. Figure 19 shows the
main lineaments touching the Mesozoic ridge in the area
around Trequanda, as seen on aerial photographs.
Recognizable displacements are marked as well. Figure 20 is a
structure map of the study area S of Trequanda. This map was
prepared from data supplied by intensive field investigations
which paid special attention to large lineaments visible on
aerial and satellite images. Such combined work applied to a
small ground area has provided a solid base for the inter-re-
gional interpretation of LANDSAT images (as performed in the
previous chapter). The combination of field measurement and
lineament analysis indicated the existence of two fabric
systems with different orientation and suggested the concept
of clockwise rotation of Tuscany-Umbria.

Fig. 21: Rose diagrams of the photolineations of the test aerea
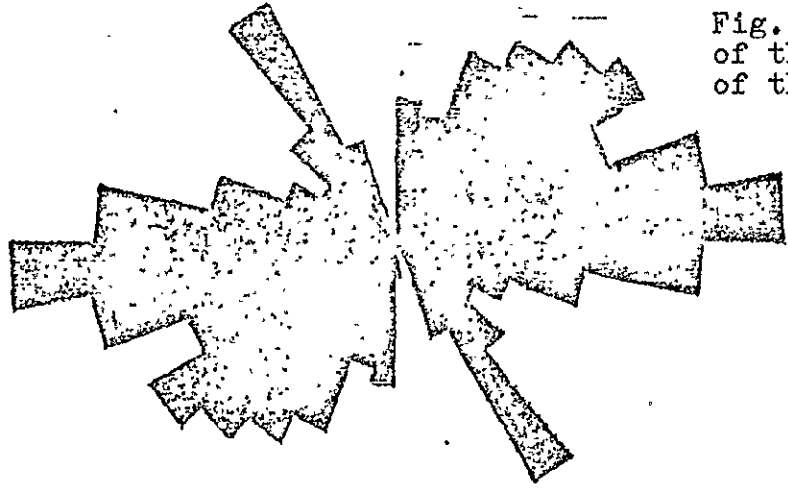
Mesozoikum   19,06 km
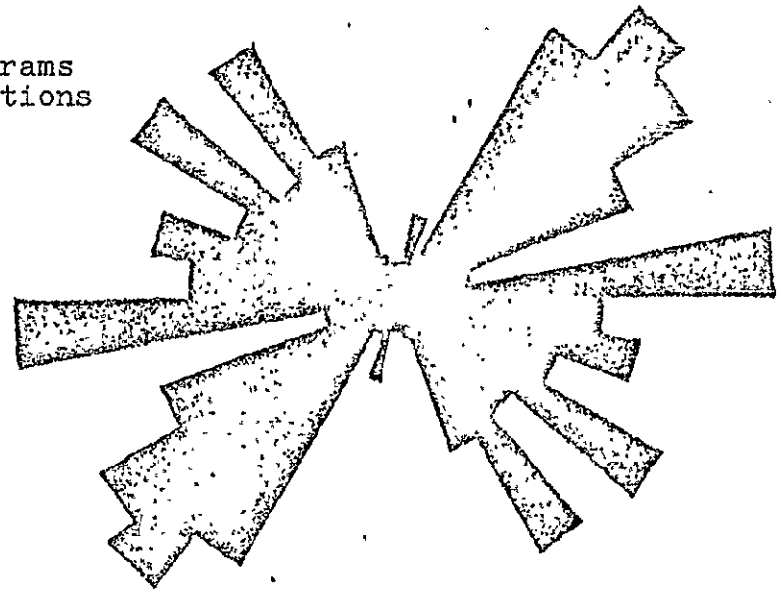
Macigno + Argille   23,16 km
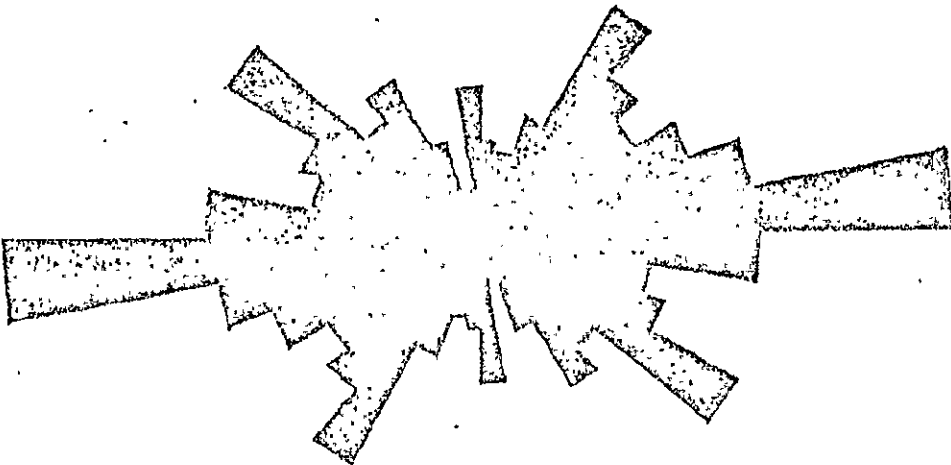
Pliozän   242,2 km
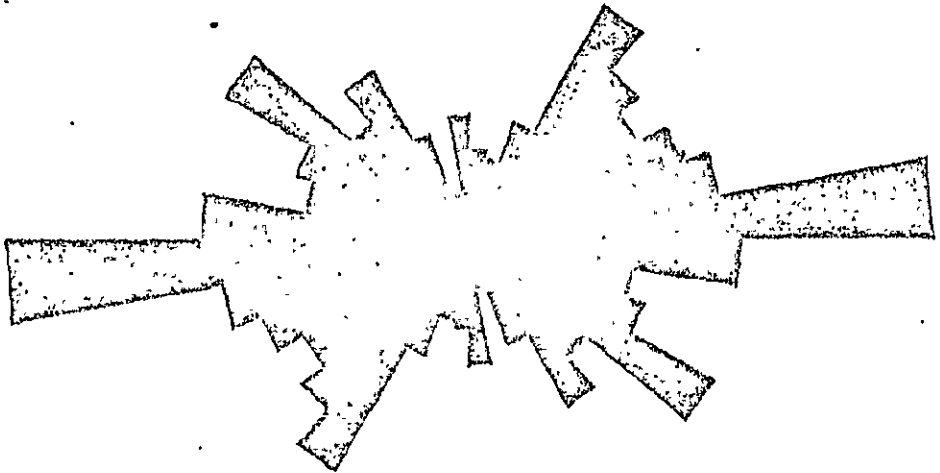
Gesamtgebiet   280,4 km

The Photo Lineaments

The lineament map (Figure 19) has been statistically
evaluated in three separate zones:

    zone 1: formed of Pliocene sands

    zone 2: formed of Mesozoic limestones and cherty-
            calcareous-marly alternating strata

    zone 3: formed of Macigno sandstones and Argille
            Scagliose

The rose-diagrams show the percentage of all the lineaments
for 10°-classes. Looking at the four rose-diagrams (Fig.21) (one
for each specific zone and one for the whole region) the
most striking feature is the similarity of the diagrams
for the whole region and for the Pliocene. This is caused
by the fact that Pliocene in this region covers by far
the largest areas. So it has great influence on the percen-
tage of lineaments of the whole region. The evaluation of
the three zones agrees with the conclusions reached by the
interpretation of equal area projection diagrams of joint
poles.

In the Mesozoic limestones the early deformation stage is
reflected by lineaments in ac_1-direction accompanied by
hko_1 shear directions. The stratification was nearly hori-
zontal during this early deformation stage. The younger
stage (during upfolding) is represented by ac_2 and bc_2.
Very important are E-W-striking hko_2-lineaments reaching
the absolute maximum in this zone. Zone 2 (Agrille Scagliose
and Macigno) show especially ac_2, bc_2 and hko_2 formed by
the younger deformation stage. The scattering of the maxima
can be explained by the different competences of arenaceous
and argillaceous beds. A last stage with 125° striking bc-
traces seems to have been important in late orogenic
block-faulting. In zone 3 (transgressive Pliocene sediments)
the fracture traces are not statistically distributed, but
the directions of the underlying Mesozoic rocks seem to
penetrate through the younger sedimentary covering.

Model of a
"Stress Cube"

main stress
a-axis

Fig. 22

Presentation of the
"Stress Cube" in the
Schmidt'sche Net
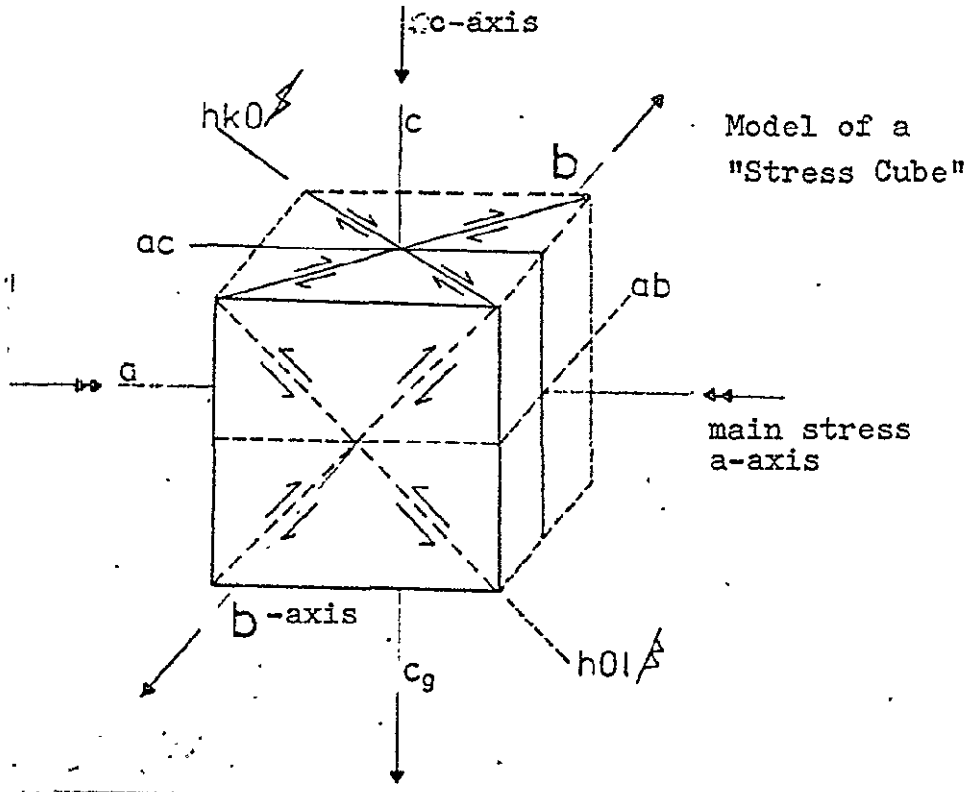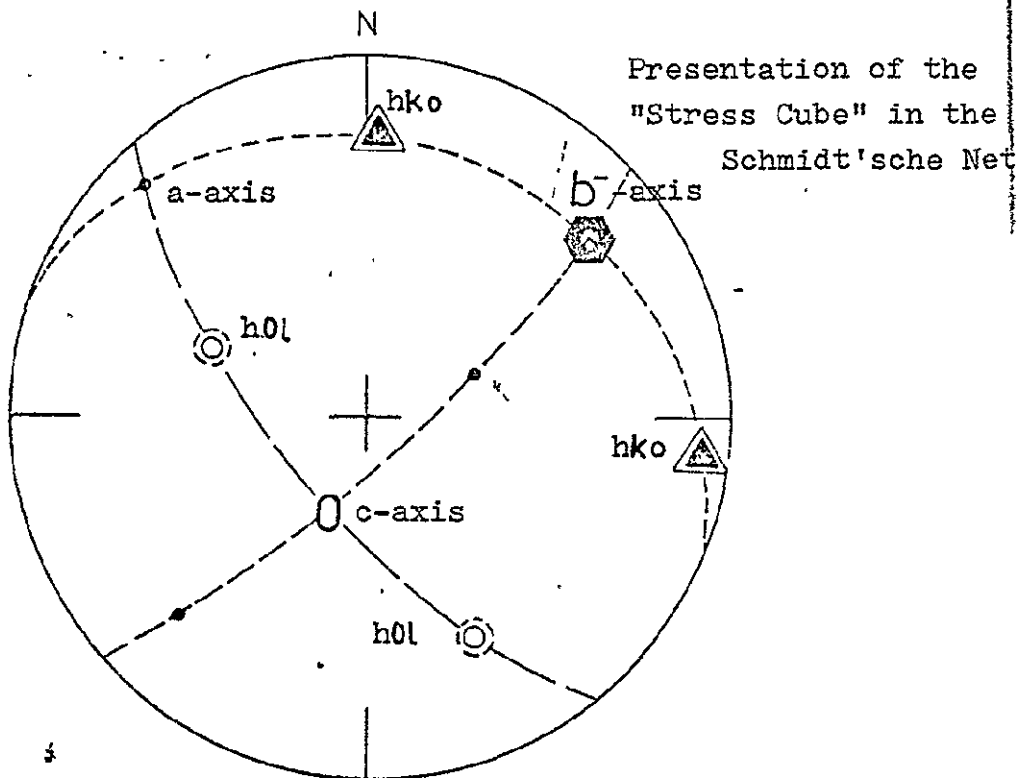
Fig. 23

5.4 Some Methodological Aspects on the Evaluation of Meso-Tectonical Measurements

Aproximately 15oo joints and 5oo bedding planes were measured in the field. These measurements were plotted in pole-diagrams (equal area projections). Interpretation of the diagrams is based on theoretical principles developed by R. Adler et al. through intensive research in the coal district of the Ruhr Region, Western Germany. Adler found, by the measurement of several hundred points, that two deformation systems, corresponding to two deformation stages, always existed. In the younger stage, the older joints and faults are only revived, forming suitable angle s to the new main stress direction. In the other case, totally new parting planes have originated. In addition to these two systems in most cases a third system is recognizable, caused by a special stress field in the surroundings of large scale faults. One aspect of the field work was to verify the influence of such large lineaments on the tectonic deformation system, as can be seen in LANDSAT-images.

Figure 22 shows an ideal stress-cube with the corresponding positions of the dividing surfaces. Figure 23 illustrates how a surface appears as a great circle in the equal area projection diagram (Schmidt'Net). For statistical evaluations the use of the projection poles of the surfaces is more suitable since numerous great circles on a single diagram are disturbing to the interpreter.

The following symbols are used in the pole-diagrams:

$\bigcirc$ = ac $\triangle$ = hko

$\diamondsuit$ = bc $\bigcirc$ = hol

0 = ab $\square$ = ohl

N
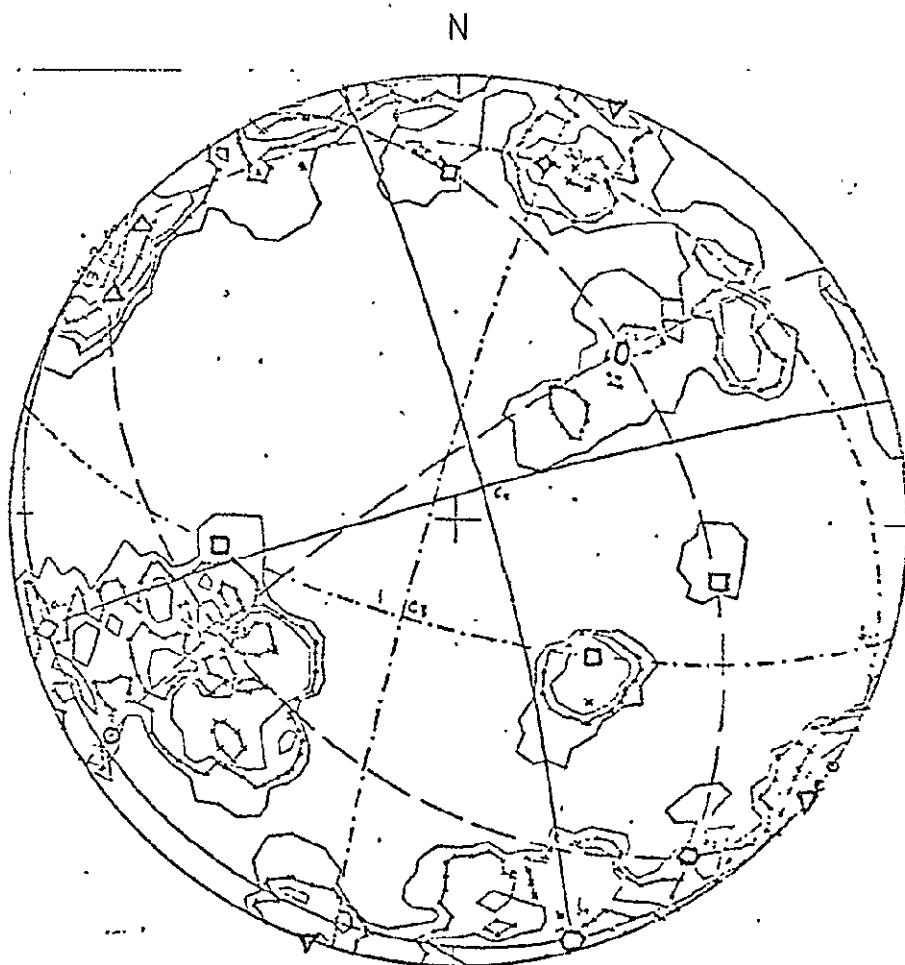
Fig. 24
Piazza di Siena, 166 joint poles
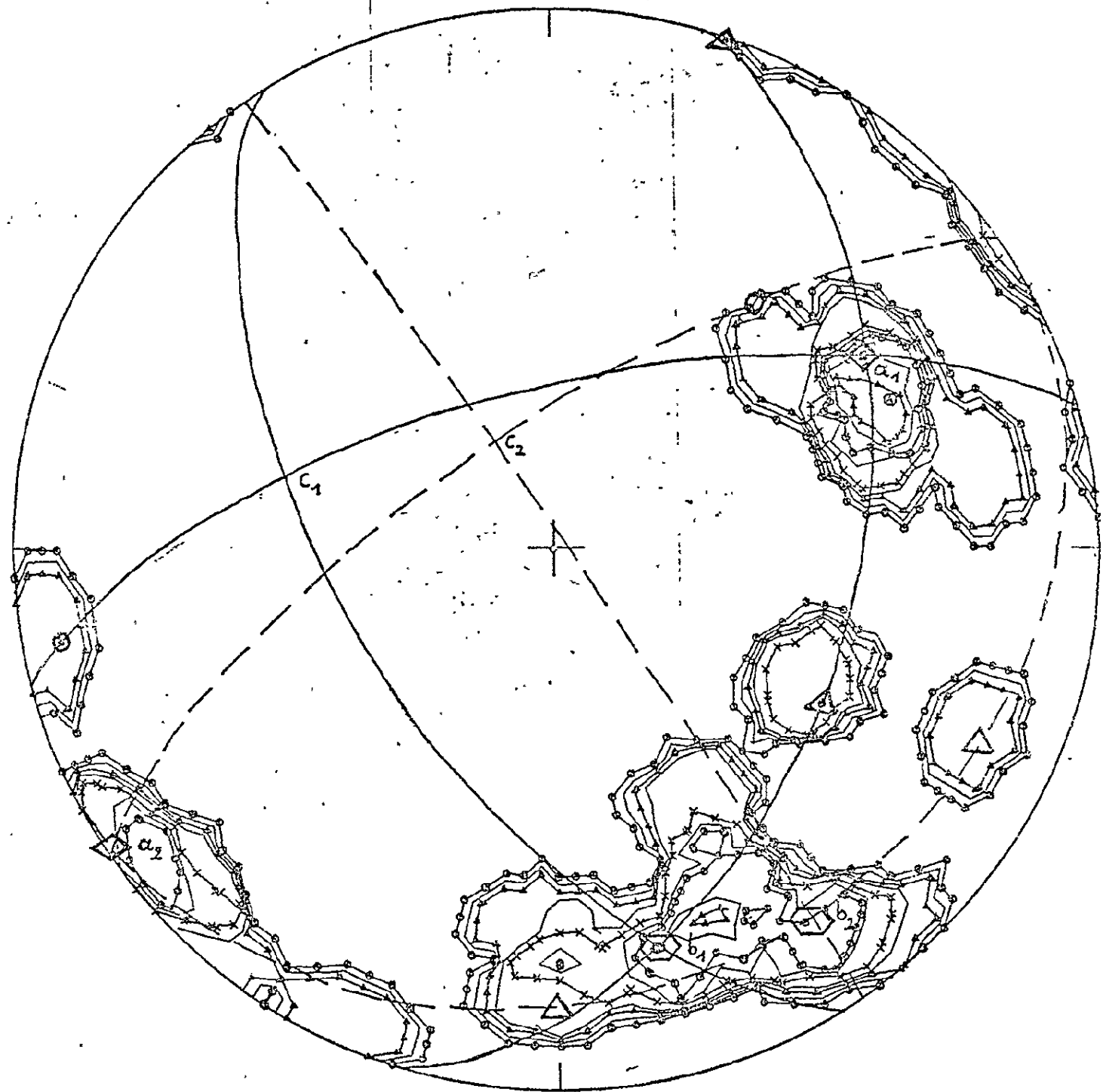
Fig. 25
S. Pietro a.M., 44 fault poles

5.5 Tectonic Systems Derived from Pole-Diagrams

The following pole-diagrams (Fig. 24 - 26) are only 3
characteristic examples for the tectonic data, which were
taken directly or photogrammatrically.

The joint-pole diagrams (Fig. 24,25)clearly show
the existence of two deformation systems, characterized
by typical configuration of parting planes, as follows:

System 1 is characterized by well-developed ac-fractures,
whereas bc and hko are less important. Furthermore, hol
and okl can be seen. The b-axes of the various diagrams
have a strike between 166° and $17o^{\circ}$. This fabric can
surely be attributed to the stratification (ab great-circle
representing bedding planes) and for this reason it must
have been formed before folding.

On the contrary, the second fabric system is composed
mainly of ab-jointing. Ac and hko are represented less
or are totally lacking. On the other hand, hol and ab
(in the massive Liassic limestones) are well-developed.
The b_2-axes show strike directions of 142-158°. They are
identical with the β-axes of the bedding-pole diagrams.(Fig.26)
The above-mentioned characteristics of the b_2-axes and
the significant assembling of joints indicate the origin
of the second fabric in a later deformation stage, during
upfolding of the strata.

In addition to those two basic deformation systems, a
special fabric can be related to important fault structures
(thrust faults and horizontal faults). Such systems are
defined by secondary shear jointing, as described in the
introductory chapter.
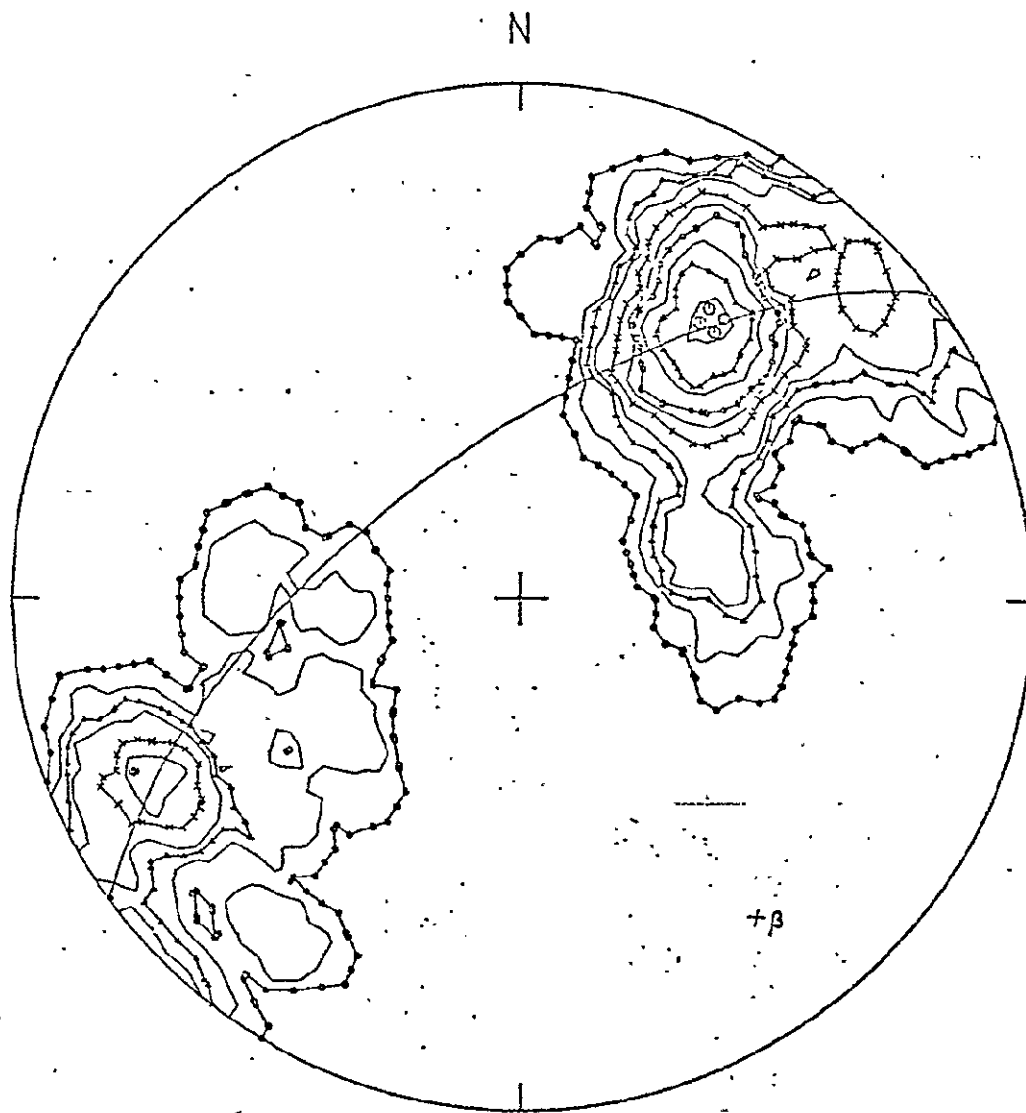
Fig. 26
Piazza di Siena, 160 bedding poles

The evaluation of the tectonics of the Northern and
Central Apennines as described in the previous
chapters is based on field work, interpretation of
aerial photographs and satellite imagery. Aerial
photographs and especially field work cover small
areas. Therefore only, the synoptic view of the
satellite images allowed to gain the results, which
partly lead to new ideas on the tectonic systems of
the Apennines.
The methods applied during this work are not only of
scientific value but also give a basis for the ex-
ploration of tectonic controlled mineral deposits by
satellite imagery.

B) GEO-TECTONIC STUDIES IN EASTERN ALPS[+]

INTRODUCTION AND METHOD

A section across the eastern Alps has been analysed
using the imagery from the LANDSAT-1 and 2. It has been
shown, as a result of the present studies, that a great
potential of these satellite images lies in delineating
active movement zones of today. Presence of such move-
ment zones along with their sense of movement can be
deciphered, on the satellite images, by very accurate
and detailed mapping of lineations and study of deformation
of landform structures and river courses.

Conventional methods of photo-interpretation utilizing
texture, tone and morphology, have been applied to these images
for delineating faults and lineaments. (Fig. 27, 28) Special attention was
paid to the trends and their deformation, if any, of the landform
structures and river courses which has helped in deciphering
direction of movements along the faults. For example, study
of the courses of tributaries of the Adige river in the Bolzano-
Merano region has indicated presence of an active fault (sinis-
tral sense of movement) along the river valley. The main Adige
river flows NW-SE in this tract. Tributaries on the eastern side of
the Adige river turn southwards while approaching the main river,
whereas those on the western side turn northwards, thus simula-
ting a typical drag-effect (Fig. 29). The southwards turn of the
tributaries on the eastern side may be accounted for also due
to general loss of elevation southwards. However, the fact that
the tributaries on the western side turn anomalously northwards -
towards the region of general higher elevation and against the
direction of flow of the main river - brings clearly out the
presence of active movements along the Adige river valley in

[+] This work has been carried out by Dr. R.P Gupta, guest
   scientist from the Department of Geology and Geophysics,
   University of Roorkee, India.
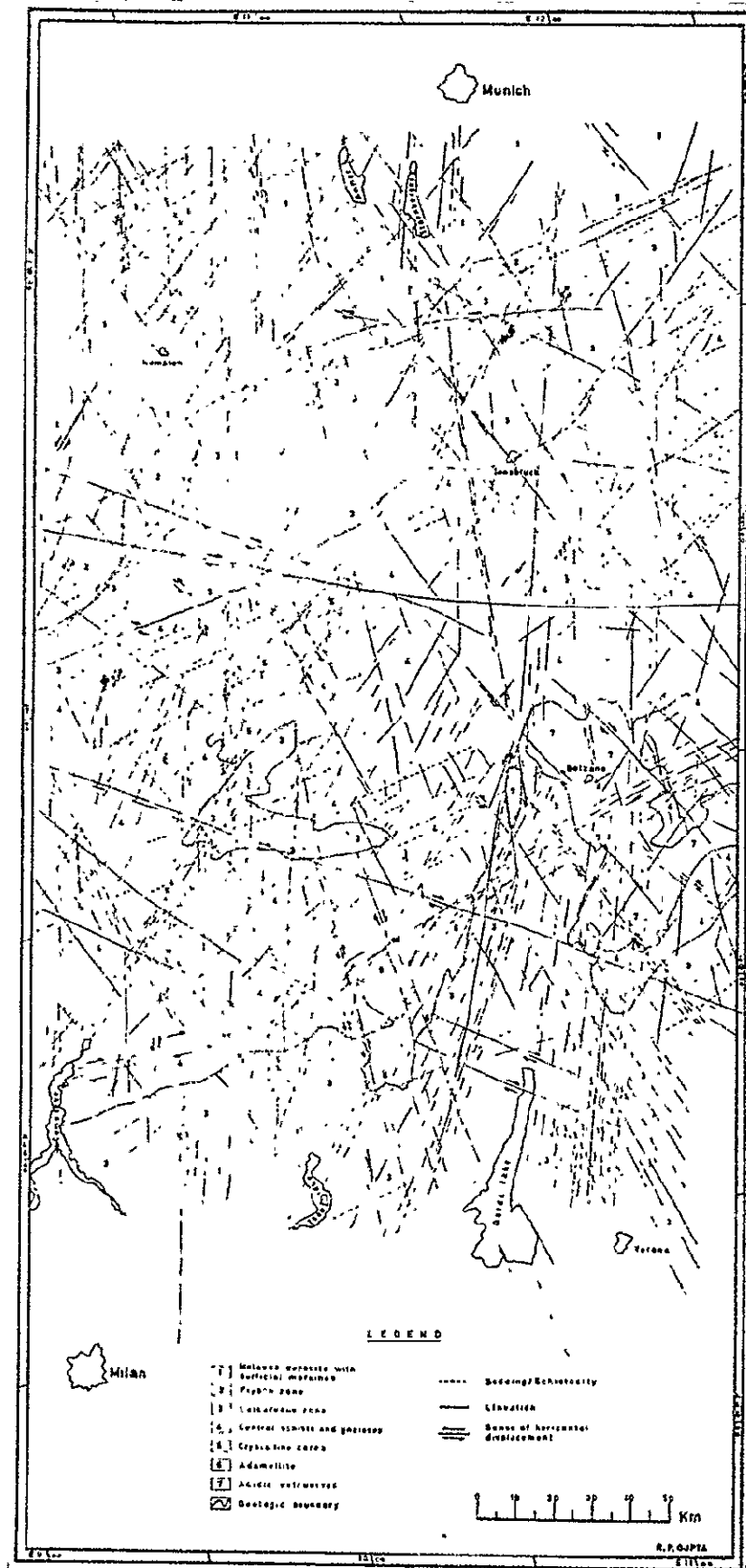
Fig.27: Lineation map of the eastern Alps as inter-
preted from the LANDSAT-1 and 2 images
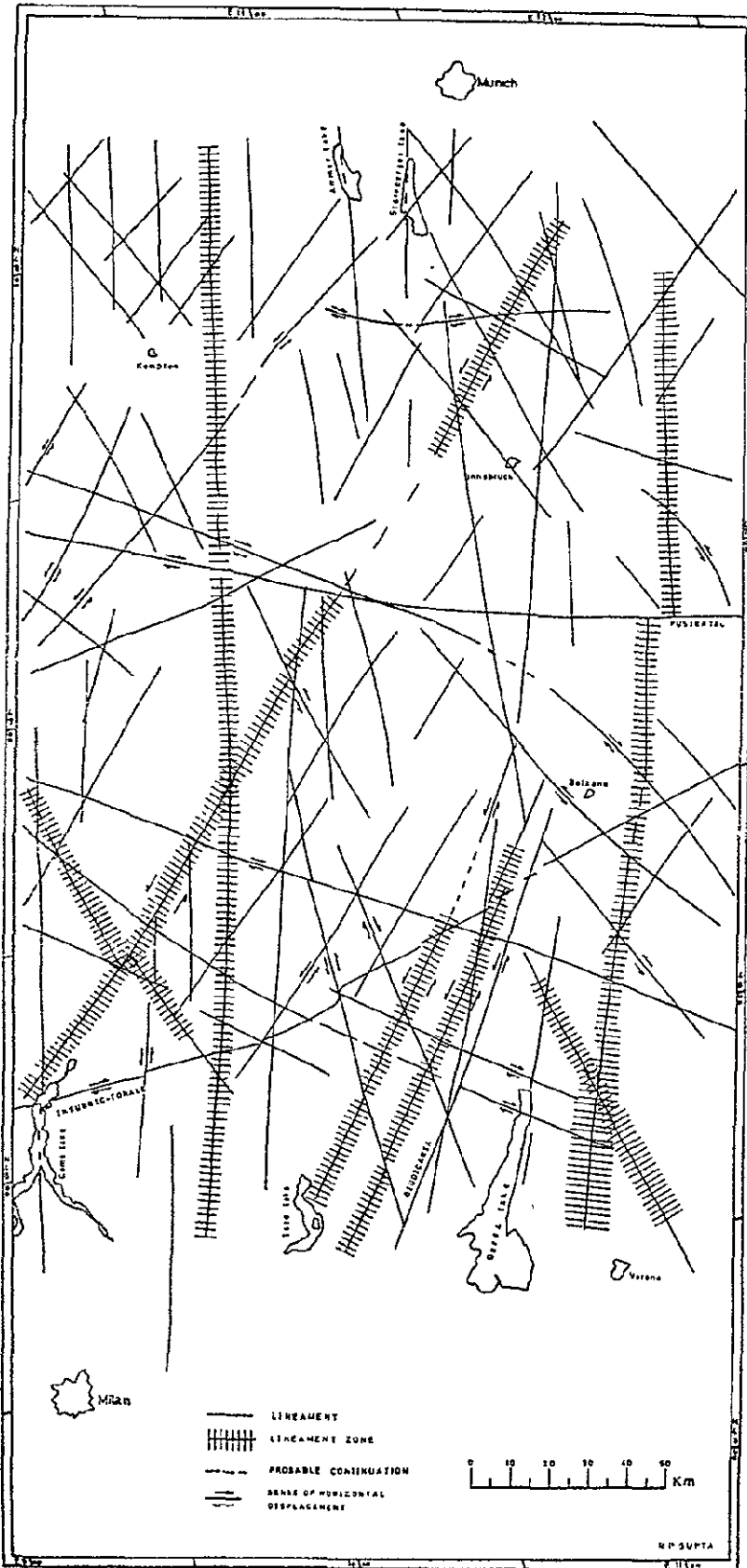
Fig. 28 Major tectonic zones and lineaments in the eastern Alps
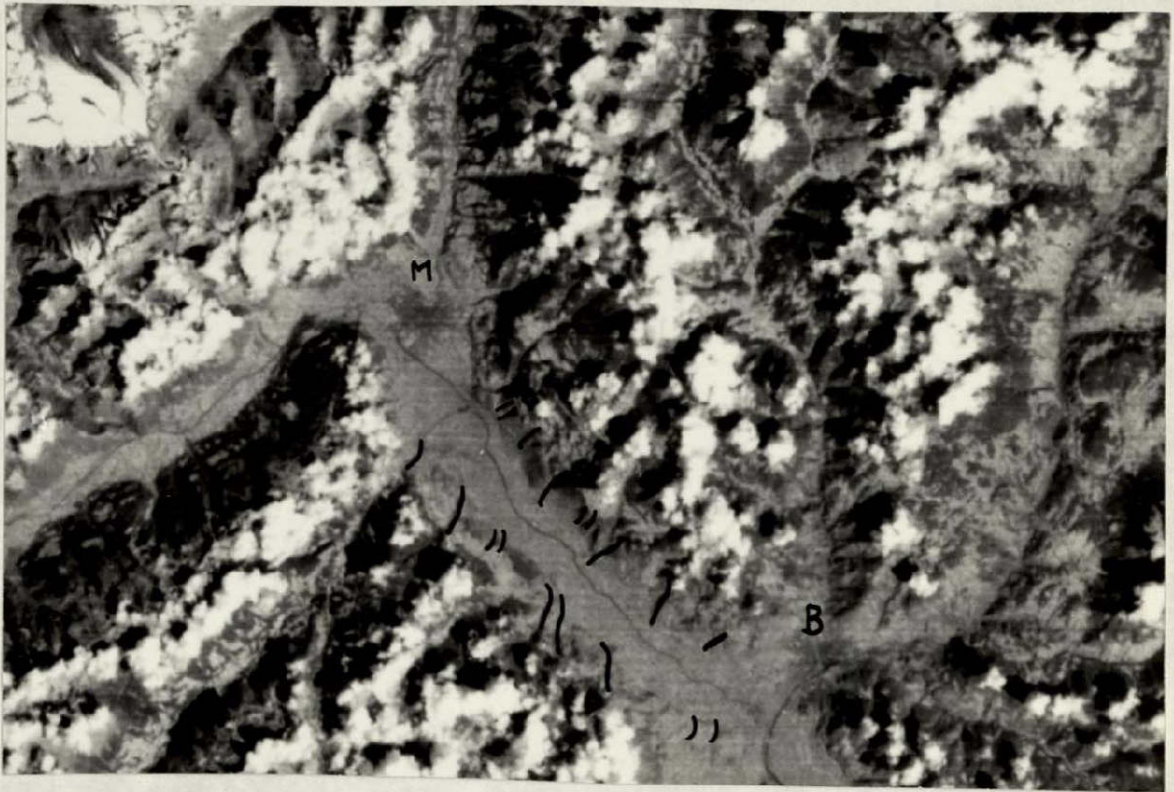
Fig.29:Turning of the tributaries indicating active sinistral
        faulting along the Adige river valley in the Bolzano (B)-
        Merano (M) region.
        LANDSAT-1, dated 31.8.72, channel 7

this area, the sense of movement being sinistral. The lineament
can be traced and extended in the mountainous tract on either
side, on the imagery, where also movements with sinistral
sense along the lineament are confirmed. It may be added here
that as the satellite images provide vertical views, only hori-
zontal movements can be deciphered on the images. However, the
swampy areas occurring in the south-western part of the river
valley in consideration indicate that the possibility of con-
currant vertical movements with western block as downthrow side,
is also not ruled out. Similarly, accurate detail mapping
of photo-lineations representing geomorphological features
has shown the presence of drag-effects pertaining to dextral
movements along the Insubric-Tonale Line (Fig.30).

Fig. 30: Drag effects along the Insubric-Tonale Line suggesting
         movements with dextral sense.
         LANDSAT-1, dated 7.1o.1972,   = 0,8 - 1,1

Interpretations have been made by superimposing observa-
tions on multi-time imagery. Images obtained on 13.8.72, 31.8.72
and 7.1o.72 by LANDSAT-1 and those on 7.8.75 by LANDSAT-2
have been made use of. This, on the one hand, has helped in
removing errors due to illumination conditions, such as
position and angle of sun leading to shadows (e... Bodechtel
and Nithack, 1974), and on the other hand, has strengthened
validity of the observations and interpretations therefrom.

RESULTS AND DISCUSSION

It is apparent (Fig.27) that nearly all lineaments are
characterized by several long to small en-echelon minor linea-
tions constituting a zone. So, basically we have to visualize
zones rather than planes such that each zone is comprised of
numerous small to large parallely arranged en-echelon minor zones
and surfaces. Fig. 28 shows a generalized map with major tectonic
zones and lineaments. A few of the lineaments are seen to be
very extensive, being traceble from one end to other end of the
investigated area and running across the entire section of the
Alps. Some of the lineaments have been off-set by others. Besides,
as mentioned earlier, several lineaments have been found to be
active(Fig. 29,30,32)Results obtained in the present investigations
render it necessary to make a special mention, among many others,
of the Insubric-Tonale Line and Pustertal Line-- the two recognized
major geotectonic boundaries in the eastern Alps (Fig.31)
Insubric-Tonale Line :On the satellite images, this lineament
appears to consist of a number of minor overlapping lineations
and shows displacements along other intersecting presumably later
lineaments (Fig.27,28)The present investigations, as shown (Fig.30,
indicate   ·ı   movements (dextral) along this Line.
It is worthwhile to recall that Gansser(1968,p.139)on the basis
of field investigations in this region wrote about temptations
to postulate lateral displacements and Laubscher(1971) based on
palinspastic restorations involving the Dinaride Alps and the
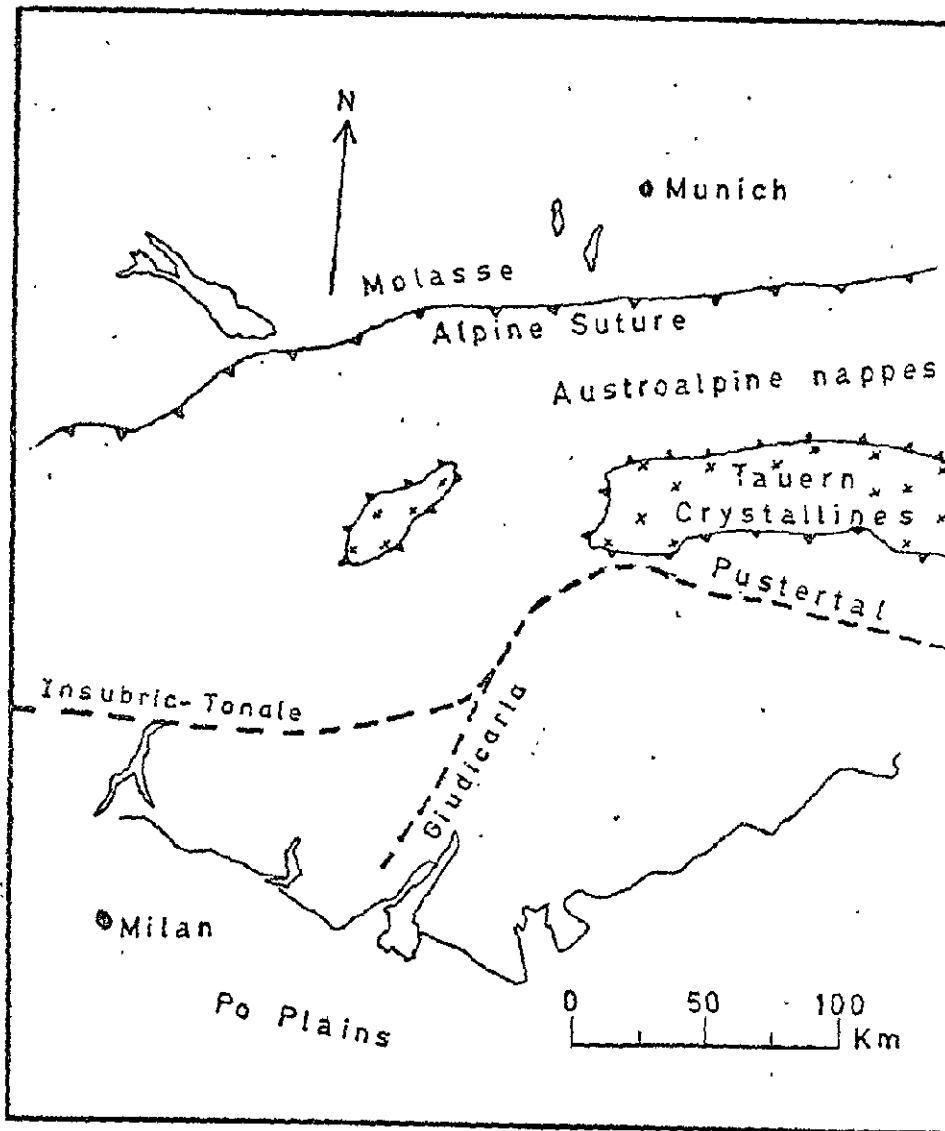
Fig. 31: Regional tectonic map

Apennines inferred 3oo km. of post—Oligocene slip, both suggesting
similar sense of displacement as deduced above (also c.f. Laubscher,
1973; Ernst,1975$_{a,b}$).Further, the Insubric-Tonale Line is commonly shown
to be abruptly terminated on the east by the Giudicaria Line (Fig.31)

However, the present investigations indicate continuation of this
trend in the acidic extrusives lying on the eastern side of the
Giudicaria Line and the Adige river(Fig. 27) Though the intensity
of development of this lineament in the acidic extrusives
is not so pronounced, the mere presence is striking. In the
geological past, the Insubric-Tonale Line,of course, seems
to have been cut-short (or displaced) by the Giudicaria Line.
However, later movements along the Insubric-Tonale must be
postulated to explain its eastward continuation in the acidic
extrusives. Further, though the seismic investigations have
failed to record movements along this Line (in Gansser, 1968),
the results of the present investigations that all along this
Line the geomorphological features are aligned simulating drag
effects, strongly suggest that this geotectonic boundary is still
active or at least has been active in the recent past.

Pustertal Line: Similar to the Insubric-Tonale Line, the Pustertal
Line is a major geotectonic feature(Fig.31) The geological
field mapping shows no indication of continuation of this Line
into the area of present study and therefore it has been,by and
large, considered to be abruptly terminated by the Giudicaria Line
on the west. Continuation of this Line westwards across the
Giudicaria Line was first detected on the ERTS-1 imagery by
Bodechtel and Lammerer(1973). In the present study it has been
further established that this Line constitutes a zone of active
movements as accurate mapping of the geomorphological features
adjoining this lineament on the imagery
has revealed drag-effects with dextral sense of movement. Its
westward continuation across the Giudicaria Line and presence of
drag-effects indicate its later rejuvenation and still active
nature (dextral). It may be of interest here to mention that
on the basis of repetitive precise levelling measurements over
time, active vertical movements along this zone at the rate of
nearly 1 mm./year have been found by Senftle and Exner (1973).

System of Post-Alpine Faults - Relation to the Present Day
Stress Field

An interesting feature is the presence of several W-E to
NW-SE trending lineaments some of which have been neither
mapped so far, nor could be visualized earlier (Fig. 27, 32)
On the satellite imagery, they appear as rather unprominent fine
lineaments which failed to make an impression during the first
hand study for major lineaments. It was only during detailed
analysis that their presence became clear and thenceforth has
been confirmed on separate observations on both LANDSAT-1 and 2
images. It is important to note that it is not   the case of an
isolatory occurrence; on the contrary they appear to form a set
and hence certainly demand attention.These lineaments are fine
but extensive and cut across all earlier trends and boundaries
thus indicating that they are post-Alpine in age. Often along
their length they are marked with geomorphological evidences,
in the form of drag-effects, indicating movements of evidently
recent nature. Some of these lineaments partly follow the old
major tectonic zones, like the Insubric-Tonale Line and the
Pustertal Line, apparently extending and rejuvenating them.
Further, a relation between these lineaments and the stress field
leading to folding and uplift of the Alps (maximum principal
stress at N 15-20, in this area   , see page 51-53) is difficult to
arrive at. On the other hand, it is easy to link these lineaments
to the   .   stress field of the present times. On the basis
of in-situ stress measurements and fault plane studies of earth-
quakes, maximum principal stress of the present day stress field
in central .Europe has been found to be W-E to WNW-ESE (Ritsema,
1969; Illies, 1974,1975; Ranalli and Chandler, 1975), which
taking the intermediate principal stress to be vertical, would
fairly well explain the development of these post-Alpine seemingly
active zones of movements (Fig.32).

MUNICH

ZURICH

Innsbruck

A L P I N E   R A N G E

MILAN

Venice

P_1

P_1

0   50   100   Km

E 8 00   9 00   10 00   11 00   12 00   E 13 00

N 48 00   N 48 00

47 00   47 00

46 00   46 00

N 45 00   N 45 00

E 9 00   10 00   11 00   12 00   E 13 00
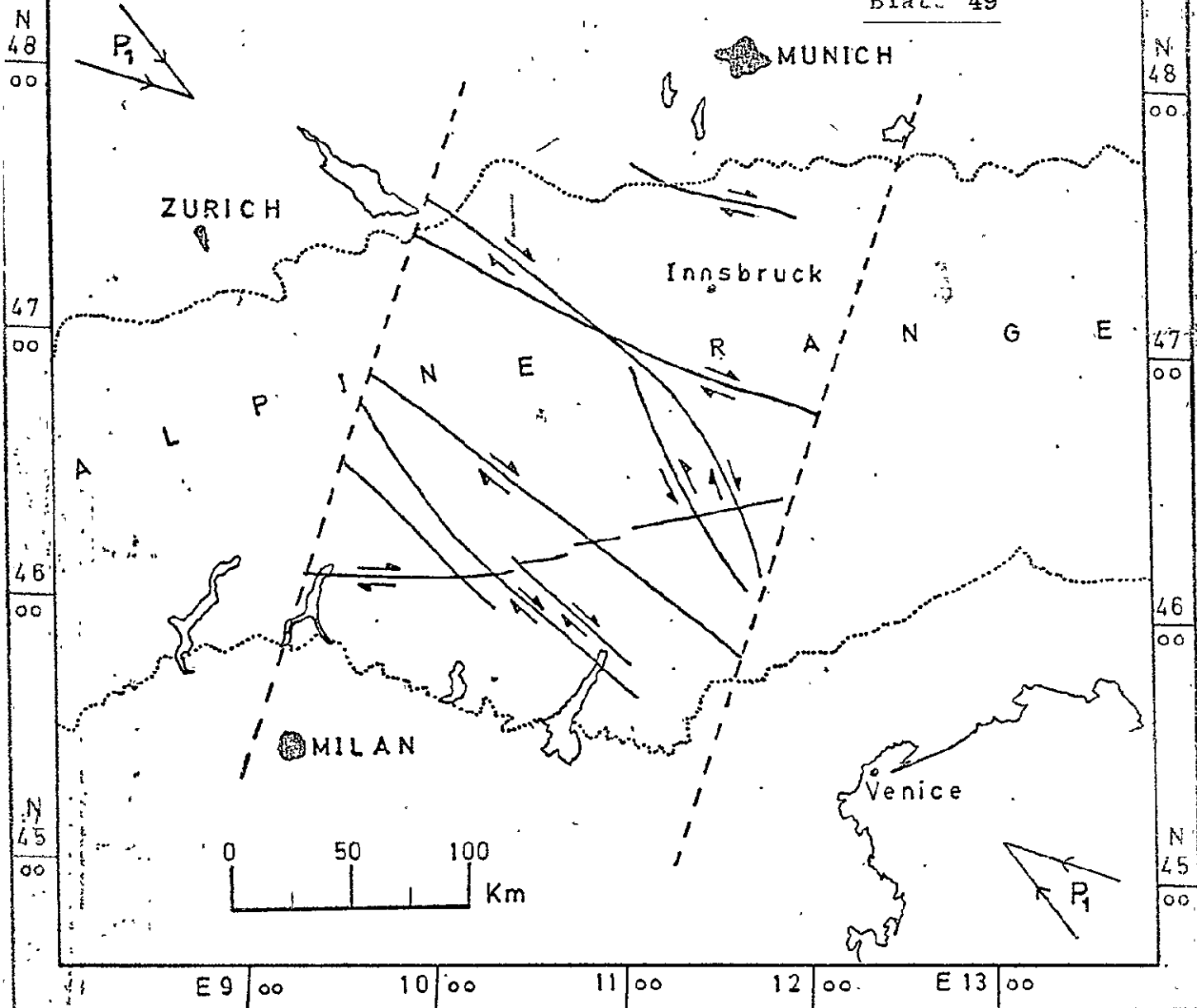
I N D E X

Section studied
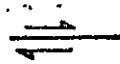
Post-Alpine movement zones with
sense of horizontal displacement

P_1

Direction of the maximum principal
stress of the present day stress field
in Central Europe

Fig.: 32: Relation between post-Alpine movement zones
and the present day stress field

Predominant Lineation Trends – Relation to Stress Field

A trend diagram depicting relative predominance of various lineation trends observed on the satellite images of the area, is shown in Fig. 33. Clearly three major directions stand out:(i) N 45-225, (S_1); (ii) N 15-195, (T); and (iii) N 345-165, (S_2). Out of these three lineation groups, the two S_1 and S_2. oriented at N 45 and N 345, respectively are considered to be of shear origin and the third, T, trending N 15. to be of tensile origin (all the three being of cogenetic nature) on the basis of following arguments:

(i) A number of movements planes are observed, oriented at nearly N 45 (fig.27 and hence the lineation group S_1. is of shear origin.

(ii) The lineation groups S_1 and S_2 appear to form a conjugate set. Here a few additional remarks seem warranted. The pile of rocks involved here range from rather incompetent sedimentary deposits with surficial loose moraines to low to high grade metamorphics and crystallines(Fig. 27) Regional geology after Carte tectonique internationale de l'Europe, 1:2,500,000). Evidently, they have wide diversity in their failure characteristics. However, a corollary to the Coulomb-Navier criterion for shear failure widely applied to rocks (c.f. Anderson,1951; Farmer, 1968; Price, 1959,1966) states that under normal stress conditions the dihedral angle of the shear fractures (2θ) is related to the coefficient of internal friction (μ) as follows:

$$ \tan 2\theta = \pm \frac{1}{\mu} $$

$$ \text{or:} \quad \theta = \pm \frac{\pi}{4} \mp \frac{\phi}{2} \quad \text{where} \quad \phi = \tan^{-1}\mu $$
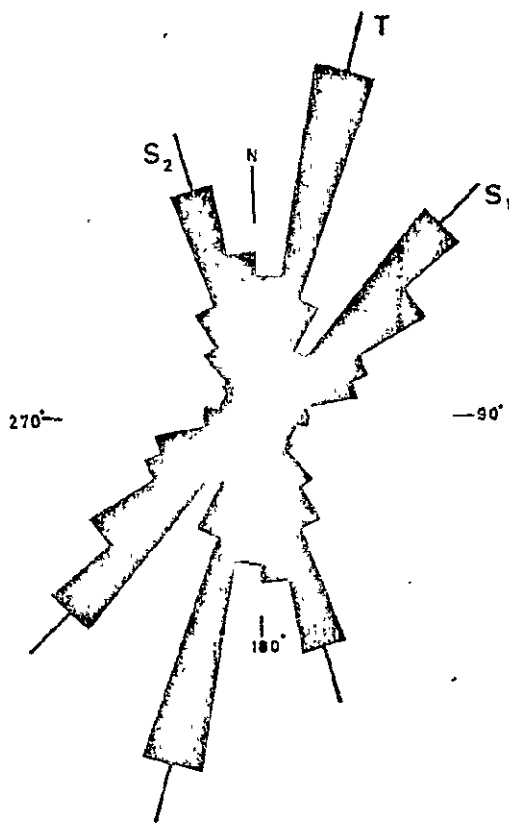
Fig. 23: Trend diagram of lineations
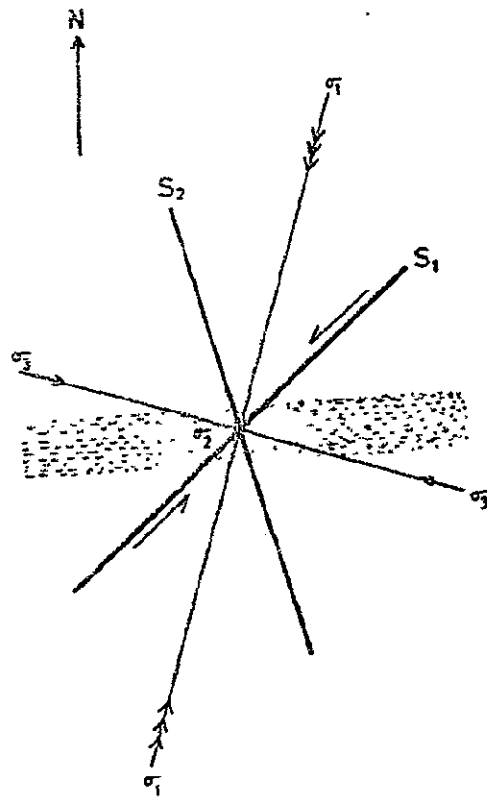
Fig. 34: Preferential sinistral movements on the NE-SW trending lineaments

For most natural rock substances the angle of coefficient
of internal friction (ϕ) being around $30\text{-}45^o$, the dihedral
angle (2θ) ranges around $45\text{-}60^o$, which is in conformity
to the angle between S_1 and S_2 (taking intermediate
principal stress to be vertical). Further, the above
relation between the dihedral angle and the coefficient
of internal friction implies that the dihedral angle
increases with decreasing frictional resistance. This fea-
ture seems to be corroborated in the present study as the
S_1 and S_2 lineations seem to widen out towards the northern
tract from the central parts of the Alps (fig.27).This
"refraction" observed in this area, is attributable to the

decreasing competency of the medium, as the northern tract
is underlain by largely molasse and surfial moraine deposits
and the central mountainous range is underlain by competent
sedimentary and crystallines rocks.

(iii) A third set of lineament (T) is oriented at N 15^c. Few
displacements are noted parallel to this set. On the other
hand, many of the larger lakes are observed to lie along this
set of lineament, for example, Starnberger Lake and Ammer
Lake in the North and Garda Lake (?) and Como Lake in the South
(fig.27).Further, this trend (N 15^c) coincides with the di-
rection of maximum principal stress as derived from the
orientation of S_1 and S_2 conjugate shear sets . Therefore,
it seems logical to conclude that the lineament set T has
cogenetically developed as a result of tensile failure.

       Hence, the above interpretations that the S_1, S_2 and T
groups of lineaments have cogenetically developed and that
S_1 and S_2 are of shear origin and T of tensile origin, are well-
interknit and appear to be logical. It is interesting to find
how the direction of maximum principal stress deduced
as above from the lineament analysis of Alpine section
compares with that independently inferred for the adjoi-
ning areas by other workers. A major geotectonic

feature adjoining the Alps is the Rhinegraben system, con-
sidered to be more or less contemporaneous with the Alpine
orogeny. The Rhinegraben trending NNE-SSW, evidences crustal
dilation normal to the graben axis, of about 4.8 km. and an
average direction of maximum principal stress of about N 20 (NNE)
must be concluded for the beginning of rifting in Middle Eocene
times (Illies, 1974, 1975). This is in striking conformity to
the direction deduced as N 15 from the above lineament analysis
for the Alpine section.Further, the above inferences regarding average
direction of maximum principal stress in late Mesozoic - early
Tertiary times from the macrotectonic observations are corroborated
by the results of statistical evaluation of field measurements
on horizontal stylolites in unfolded Mesozoic platform sediments,
made all over Central Europe (Beiersdorf, Wagner, Wunderlich
and Plessmann,in Illies, op.cit.)

The presently concluded situation that the then prevalent
maximum principal stress seems to have been not perpendicular
(and hence the minimum principal stress not parellel) to the
general trend of the rocks in this Alpine section needs
explanation.It seems that this abnormality has been caused by the
presence of a hindering block on the south-east. The alternative
possibility is by postulating two different phases of deformation ,
the first phase(with average maximum principal stress trending
N 350) bringing about the regional folding and uplift of the
Alps, followed by a second phase(with average maximum principal
stress oriented at N 15-20) causing largely translational
movements, shearing and faulting but retaining the pre-existing
strike trends. The author tends to favour the first possibility
as separate phases of folding and faulting are difficult to
visualize. Often the two phenomena are found to be concurrant and
closely associated with each-other.   If the main phase
of deformation had maximum principal stress at N 350 , the
related tectonic impressions which would have been of the same
degree of magnitude and intensity, should have been visible
and thus borne evidence to that. Further, uplift of the Alps
associated with northwards movement of the Adriatic block

has been long postulated (for example, Aubouin, 1964) and the
same block, which lies to the south-east of the area, could
have also provided the hindering resistance referred to
above. Besides, the presence of such a block would be further
in conformity ` to the observed predominance of NE-SW (S_1)
lineations with sinistral sense of horizontal displacement,
described below.

S_1 Lineations and the Giudicaria Line

A striking feature is the large number of   NE-SW trending
lineations (S_1) with predominantly sinistral sense of movement,
observed throughout the region of study (Fig.27).They are
developed with varying intensity in the area and are more
prominently developed in the vicinity of Giudicaria Line.
From field investigations Trevisan (in Laubscher, 1973)
reported the large system of NE-SW trending sinistral faults
in Giudicaria. Evidently , intense development of S_1 set of
shear planes and zones seems to have controlled the development
of Giudicaria Line.
The reasons why movements have taken place   largely on the S_1-set
of shear surfaces and not on the S_2-set and that too with
predominantly sinistral sense are also clear. The general strike
of rocks is N 75-80° (Fig.27).The maximum principal stress has
been concluded to be directed at N 15, giving the conjugate set

of shear surfaces at N 45 (S_1) and N 345 (S_2). Thus, the shear
surfaces S_2 trend nearly perpendicular to the general strike
of rocks whereas those of S_1-set make acute angle (30-35) with
the latter(Fig.34).In such a state, movements on the S_1- group
of surfaces,with sinistral sense, would be evidently preferred.

CONCLUSIONS

On the basis of above studies on LANDSAT-1 and 2 images of
eastern Alps, the following broad conclusions may be drawn :
 (a) A number of W-E to NW-SE trending post-Alpine active
     lineaments are present, These lineaments can be logically
     related to the present-day stress field.
 (b) There are three dominant lineation-sets in the eastern
     Alps. They have co-genetically developed as a result of
     shear and tensile failures, due to stresses with maximum
     principal stress averagely trending N 15^c.
 (c) The Giudicaria Line seems to have been controlled by the
     NE-SW trending lineaments over which movements with sinistral
     sense have been preferred.
It goes without saying that as the satellite images provide very
accurate map of ground features, a great potential of these
images lies in their detailed and accurate mapping. This can
unearth valuable information of local and regional importance,
unobtainable from any other source.

C APPLICATION OF LANDSAT DATA FOR LAND USE MAPPING BY
CONVENTIONAL INTERPRETATION ·TECHNIQUES

For many earth scientific activities, land use maps form
the basis for further planning and inventory preparation.
Very often the existing land use maps are more than 2o to
4o years old and do not correspond any longer to the
existing situation.

In order to prepare a land use map on a conventional basis,
many man-years are necessary to conduct intensive field
work and supporting aerial photointerpretation. The Italian
authorities are faced with the problem of producing new
land use maps of the mountainous regions on a scale of
1 : 5oo'ooo. Especially in mountainous regions, the cost
factor has always been a severe constraint, hampering
completion of this project. Preliminary evaluations of
LANDSAT-data, has indicated the high potential of multi-
spectral satellite data and its suitability for land use
mapping. On the basis of our background experience in
aerial photointerpretation and satellite data evaluation
techniques, we approached this problem by determining the
feasibility of vegetation mapping through application of
conventional interpretation techniques to LANDSAT-data.The
tasks seem to be solvable with respect to the small scale
and the few main or level one categories that have to be
determined. The different categories of interest are:

1. barren land (rocks, gravel)

2. permanent snow cover, glaciers

3. urban areas (including industrial areas and larger
transportation patterns - streets)

4. pastureland (areas covered by grass)

5. agricultural areas (including plantations)

6. forested areas

7. water bodies, rivers and lakes

1. Data Source

LANDSAT-1 MSS images taken during '72 and '73 were used
as the data source. The nine inch negatives (scale 1:
1.000.000) were photographically enlarged on a scale of
1:25o.ooo. For most of the areas the information loss
acquired through repeated photographic processing of the
images did not interfere with the detection of level 1
categories. For some key-areas a direct production of
images from tape were carried out by PRAKLA-Company.
These images, showing maximum information of the MSS
data, were generated on a scale of 1:2oo.ooo. Furthermore
for some middle Italian and Sicilian areas Skylab photo-
graphic data in panchromatic and false colour were pro-
duced. By this means a total cloud-free-coverage of the
areas of interest was obtained.

2. Evaluation Techniques

2.1. Background Information

The basis of any photointerpretation is not only the
experience of the interpreter, but also detailed background
information. The background information for our project
consisted of:

    a) existing land use maps on a scale of 1:2oo.ooo,
       produced 2o - 4o years before

    b) existing field data obtained through intensive
       field investigations of the last ten years

    c) detailed vegetation profiles.

Information gained through field work proved to be the
most actual information and could be utilized with high
confidence.

2.2. Interpretation Key

2.2.1 LANDSAT-1 multispectral scanner data

For conventional photointerpretation there are no sig-
nificant differences of information between MSS 4 and 5
and between MSS 6 and 7.

On the other hand MSS 5 and 7 show the best contrast of
grey tones in vegetated and non-vegetated areas. There-
fore images of these two bands were chosen for the land-
use mapping.

From an earth scientific point of view, the utilization of
data representing different vegetation cycles would be the
optimum.
This requirement could not be fulfilled over all areas
because of insufficient continuous data. It turned out that for
the production of a preliminary base map, channel 5 was op-
timally suited. Band 7 was utilized in order to obtain
additional information for discriminating various types
of surface features. So, for example, the use of band 7
allows for the separation of coniferous forest from mixed
forest, the better delineation of agricultural areas and
the clear identification of barren land. For the level 1
classification the sensitivity of band 7 to soil moisture
has been somewhat disadvantageous.

The diagrams of figure 35 represent a qualitative comparison
of grey tone classes obtained from band 7 and 5. In the co-
ordinate-system the land use categories were plotted as a
function of their grey tone in both channels. It is evident,
that such schematic representations only gives a very rough
idea about the principles of evaluation. Of course such
diagrams do not reflect the experience of the interpreter,
his ability to differentiate subtle grey tones or his
analytic ability under various environmental conditions.
Furthermore both diagrams do not express important criteria
such as texture and morphology and also the synoptic know-
ledge of the geological conditions. An interpretative
decision can be made by a combined analysis of all criteria,
as shown for grass in figure 36 .

SUMMER

MSS 7

LIGHT

MOISTURE

DARK

CLOUD SNOW

VINE OLIVES DRY

LARCHES

HUMID URBAN AREAS HUMID

SHADOW-SUSPENSION

LIGHT MSS 5

MOISTURE

LEGEND

1 DECIDUOUS

2 CONIFEROUS

3 1+2

4 AGRICULTURE

5 GRASSLAND

6 4+5

7 BARREN LAND

8 WATER

WINTER

MSS 7

LIGHT

MOISTURE

DARK

CLOUD SNOW

MEDIT OAKS DRY

URBAN AREAS HUMID

SHADOW-SUSPENSION

LIGHT MSS 5

MOISTURE
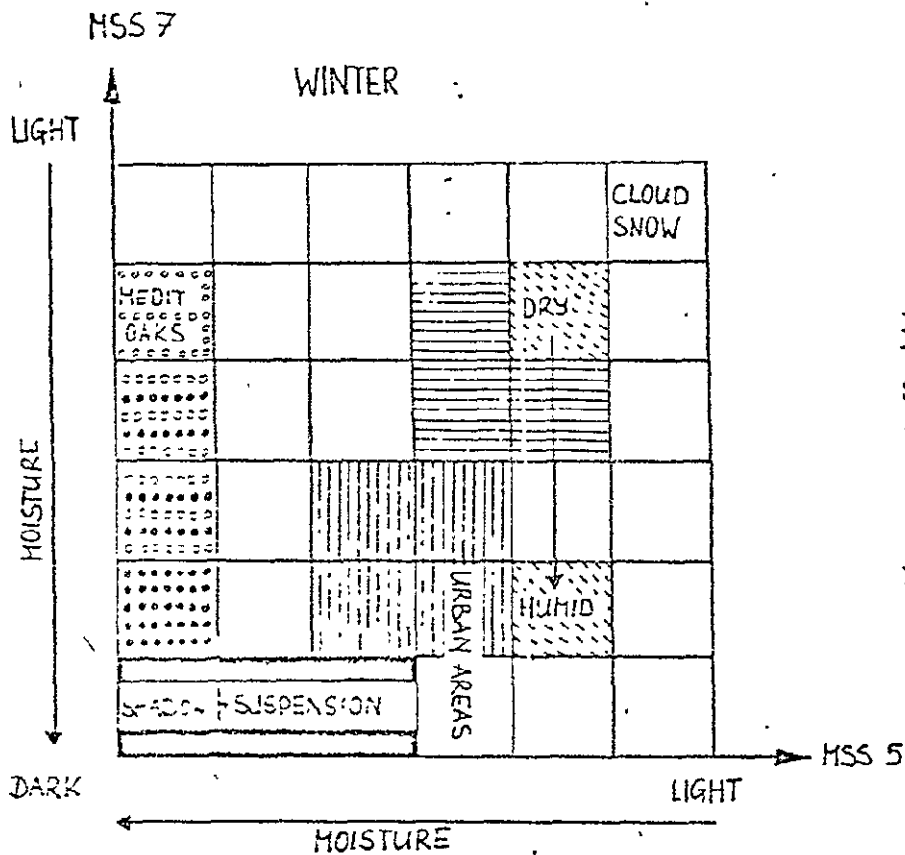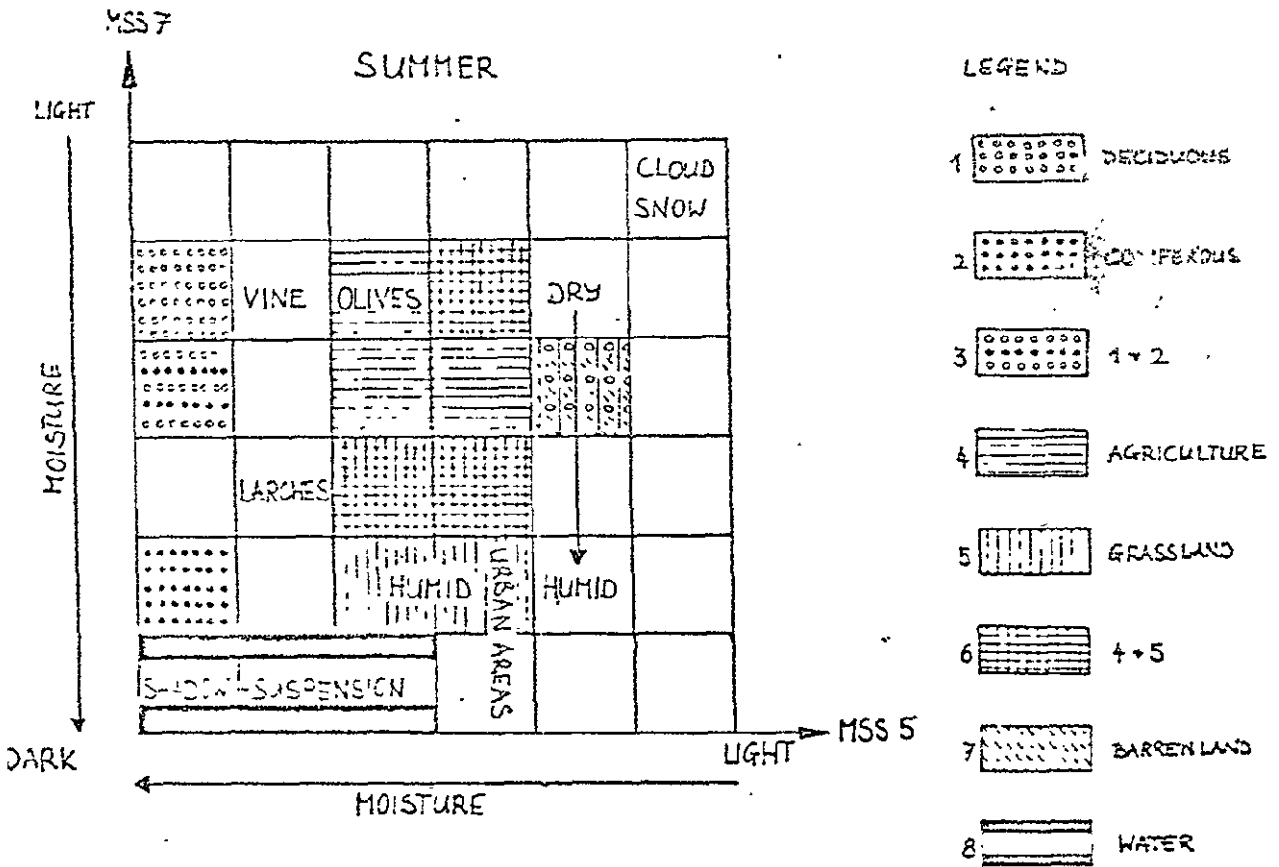
Fig. 35

Schematic position of land use categories in a coordinate system based o the grey tone in images o MSS 7 and MSS 5
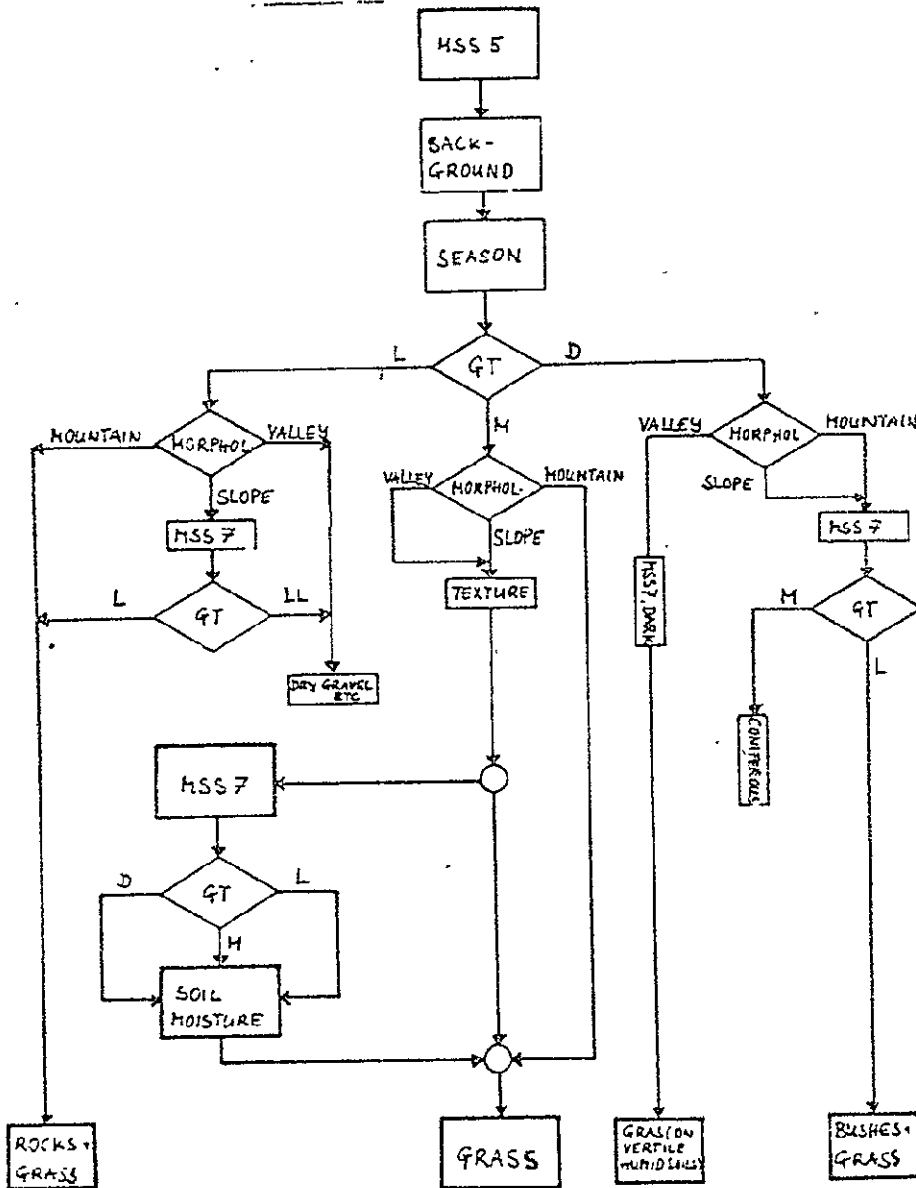
Fig. 36

Identification of grass land

Schematic diagram for the Interpretation of LANDSAT MSS-data

(Legend: GT = grey tone, L = light, LL = very light,

        M = medium, D = dark)

2.2.2 Skylab data (colour and false colour images)

Colour photographs of Skylab (for example 19o a, taken in
September 1973), were projected on a scale of 25o.ooo. Due
to the outstanding colour quality of these images, the
following surface features could be clearly identified:
forested areas, agriculturally used areas, grassland and
barren land. False colour composits of Skylab data and also
of LANDSAT-1 MSS data served as basic information for
differentiation areas with grassland from agricultural
use regions. The determination of borders between those
two features has been very difficult with black and white
images taken during late autumn, summer or winter. During
these seasons, the fields are not planted or are already
harvested. In relatively dry areas grassland and agri-
cultural areas appear in relatively unidentifiable grey
tones when the field patterns are far below the resolution
capabilities of the sensor system. The only reliable cri-
terion for differentiation is a distinct red colour re-
presented in false colour images.

2.3 Gray Tone and Colour Tone

In respect to the physical properties, various surface
features reflect incoming radiation in different inten-
sity levels. The reflection intensity is translated on
photographic data into a gray or coloured tone. Therefore
the photographic density is one of the most important inter-
pretative criterion. In addition, the density is very
sensitive to uncontrollable factors, caused by natural
phenomena or by photographic processing techniques.

2.3.1. The Impact of Natural Parameters on the Photographic Density

In general pictorial representations of our earth surface
are a combination of all possible factors of which the
image density only plays one part. Problems arise con-
cerning the identification or surface features, regarded
to be homogeneous from any earth scientific point of view.
This is due to the fact that such a homogenity does not
necessarily correspond to a homogeneous distribution of
gray tones. Therefore in order to decide whether to deal
with category a or b, further decision-making criteria
have to be introduced. So for example, a well cultivated
fertilized medium humid meadow may have a darker grey tone
than an uncultivated grassland under the same environmental
conditions. Grassland in an Alpine valley, for example,
has a different grey value from grassland in a south
Italian Apennine valley. Grass growing on clay has a
different dark grey tone than grass on limestone. The grey
tone, the intensity of reflections, is mainly dependent
on natural factors such as soil moisture, soil type, cli-
matic zone and local climate. The image, figure 37, re-
presents some of the basic relationships between environ-
mental parameters and grey values. Another important
factor, not taken into account, is the exposure of the
surface to an illumination source – the Sun. In areas
with great relief the identification of surface features
is extremely difficult, not only due to the shadows
themselves, but also to the change of the relative sunangle.
Another important factor is the changing state of vege-
tation during the year, i.e. the change of reflectance
depending on the seasons. Therefore multitime imagery
allows better identification and further differentiation
of land-use categories.

2.3.2. Impact of Tecnical Factors on the Photographic Density

The main technical factors influencing the density of
images are related to the image generation itself.
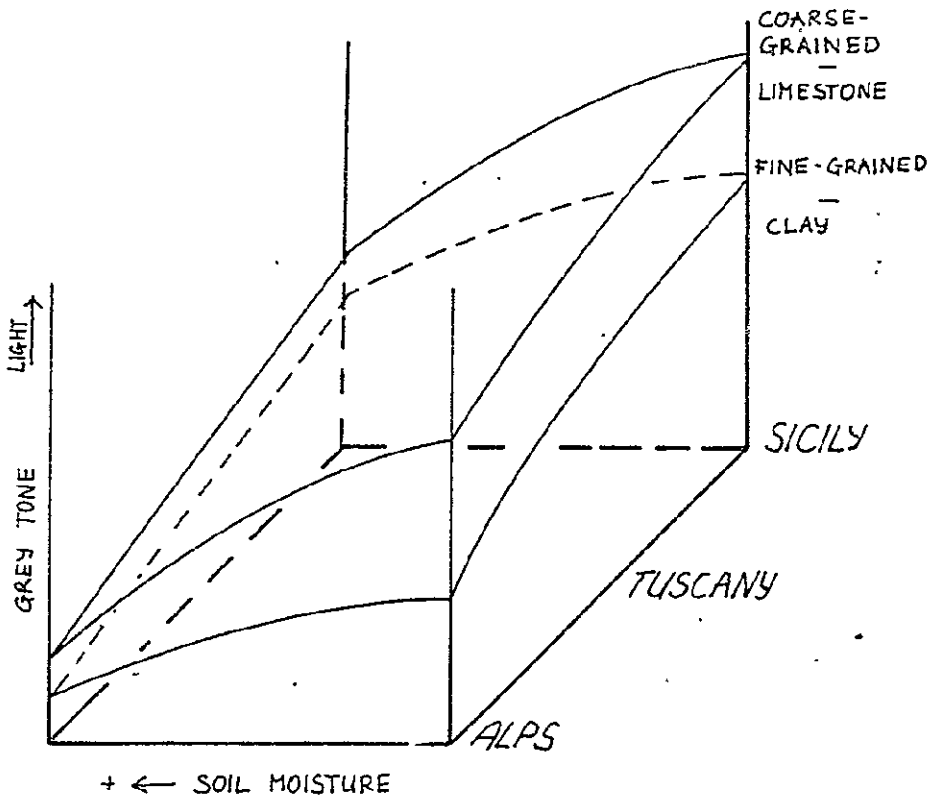
Fig. 37 Grey-tone levels of grass
        Schematic representation for the factors soil,
        soil-moisture and climatic zone

Concerning the generation of images from a digital tape,
restrictions result from the dynamic range of the output
devise. The equipment used for data generation has an
overall dynamic range of 16 grey levels. In comparison
with the theoretical performance of the MSS scanner, with
a dynamic range of 128 (MSS 5) and 64 (MSS 7) grey levels,
the applied generated images represent reduced informa-
tion. In order to minimize this effect the available inter-
val of 16 grey tones was adapted to the actual sensitivity
range of the scenes. In order to obtain maximum grey reso-
lution for the areas of interest, the adaption was carried
out on scenes that did not show maximum reflective contrasts,
such as snow and water, in infrared images. A second important
parameter which influences the quality of the film material
is the degradation effect resulting from photolab processings
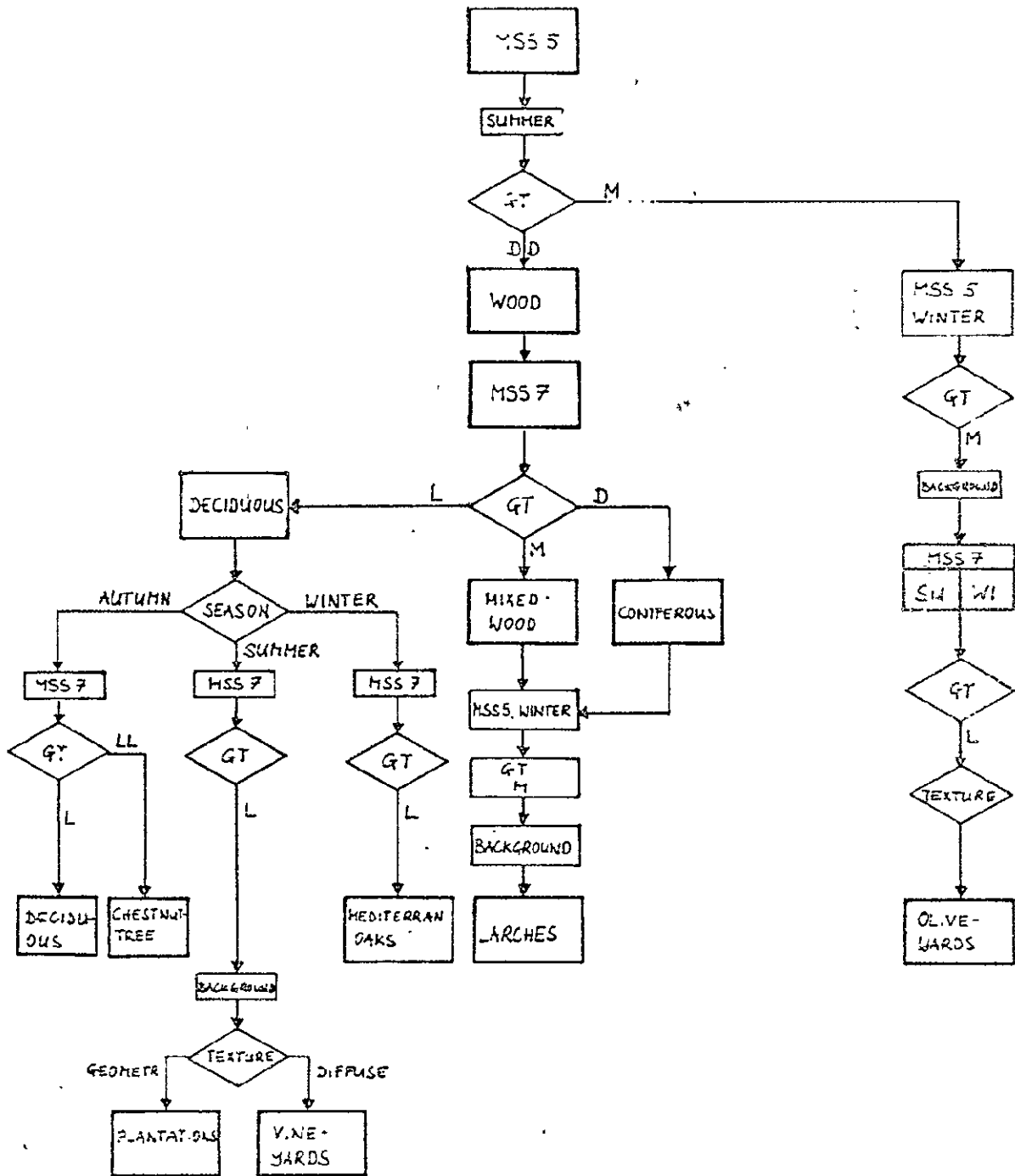
Fig. 38

Identification of wooded areas

Schematic diagram for the interpretation of LANDSAT MSS-data

(Legend: GT = grey tone, L = light, LL = very light,
         M = medium, D = dark, DD = very dark)

such as enlarging etc. During these processes the grey
tones are influenced by the various film emulsions, by
various exposure times and by the state of the chemical
ingredients.

Another degradation effect which occurs mainly in channel
7 is caused by the high contrast between water and land
masses. The extreme dark water areas interfere in such a
way that the coastal areas always appear in darker grey
tones. The above-mentioned photographic factors may es-
pecially degrade the possibilities and the accuracy of
conventional photointerpretation techniques. In other words
the interpreter has to revise his interpretation results
not only from image to image but also within the evaluation
of one scene.

3. Possibilities and Limitations of the Conventional
    Classification

The possibilities of identifying surface features is
extremely dependant on the resolution capabilities of the
sensor and on the target size. Figure 38 demonstrates to
what degree under optimum conditions, the differentiation
of trees can be made. With regard to trees or tree-cones,
two points have to be taken into consideration. With
respect to the resolving power to the multispectral
scanner, larger areas with a dense tree population can
be identified as uniform reflecting areas. It is under-
stood that with a dense population of trees there is no
interfering reflection from the ground. Furthermore be-
cause of the poor resolution of the satellite data, the
differentiation between bushes and forests, can not be
made.

Furthermore conventional definition based on the percen-
tage of trees within a certain area can not be made.

To a certain degree, grey tone and background information
enable the interpreter to map areas with different densi-

ties of wood. But the geometric resolution of LANDSAT-1
images does not allow to map woods by quantitative measure-
ments of percentage of trees per area. Therefore areas
with for example 10 % trees, which are conventionally de-
fined as wood do not appear on the evaluated land-use map.

Further difficulties arise when comparing forsts and
plantations. Densely planted hazels agrumenplantages
and vineyards have the same reflection characteristic as
deciduous forest, at least for the eye. A basic local
knowledge and the experience in examing textural infor-
mation may sometimes help to overcome above-mentioned
difficulties.
Plantations, for example, are very often characterized
by geometric borders, and in contrast, vineyards often
show a kind of chaotic texture.

Cultivations with clearly separated rows of plants such
as oliveyards are characterized by a uniform medium grey
value. These grey values are originated by intensities
reflected from the ground coverage and the foliage of
the trees. The following images demonstrate areas with
plant units which have characteristic signatures. Figure 39
shows coniferous and deciduous forest near Pratomagno,
mountains south east of Florence, figure 40 mediterranean
oaks in the Apennine west of Rieti, figure 41 oliveyards
of the Tuscany, figure 42 an area with bush and grassland
near Valle Taleggio (Begamasc Alps).

Especially the last example (fig. 39) indicates the diffi-
culties which result from the poor geometric and spectral
resolution of LANDSAT-1-images.

Areas with mixed reflections are very difficult to classify
without knowledge of the local conditions. Normally in such
cases textures can not be detected any more and the surfaces

appear rather uniform. The limitations of differentiating
between various surface features becomes evident if we
are looking at interface regions between meadows and
areas with dried-out grass and barren rocks. Barren rocks
are clearly detectable but a distinct tracing of the
border between the grass land and areas without vegetation
is impossible.

a)   b)
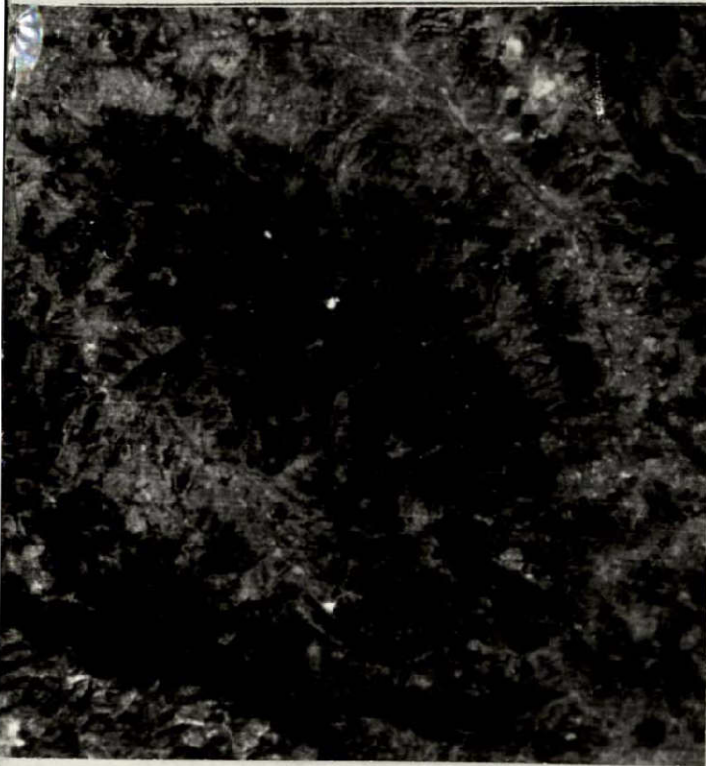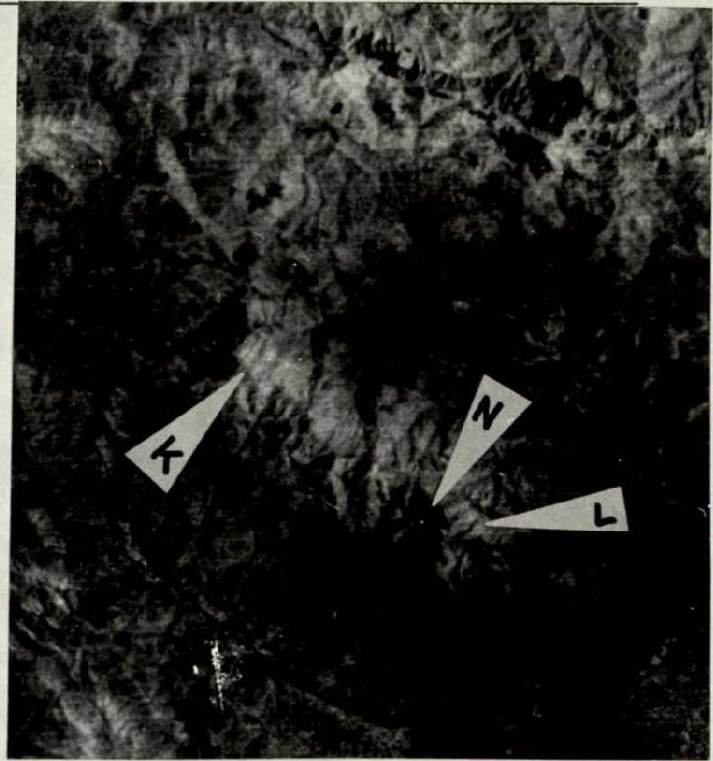
c)

Fig. 39

Pratomagno Mountains (detail from LANDSAT-1 image of 12. Aug. 1972)

a) MSS 5   (dark = wooded areas)

b) MSS 7; light = deciduous wood (L = in general, K = chestnut)
        dark = coniferous (N)

c) Ground truth photograph, showing coniferous (dark) surrounded
   by deciduous wood
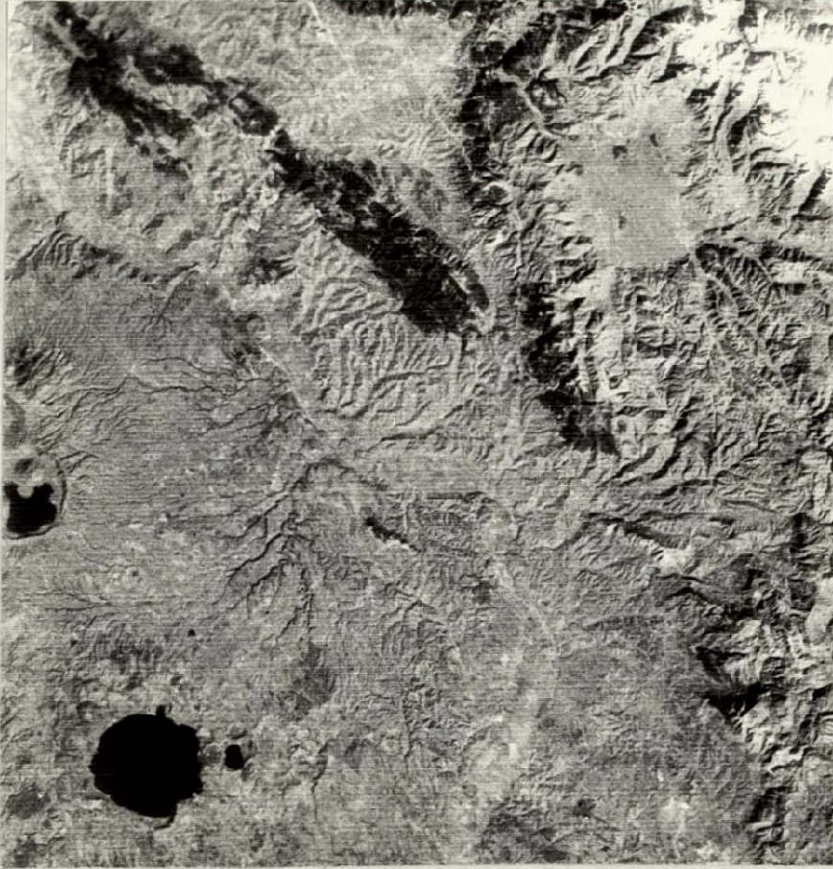
Fig. 40:

Mountain ranges west of Rieti (detail from LANDSAT-1 image
of 6.Feb. 1972)

a) MSS 5   (dark = mediterranean oaks)

b) Ground truth photograph taken in June 1973 near Amelia.
   Dark = mediterranean oaks

Fig. 41:

Lower valley of the Cornia
River, east of Piombino
(detail from LANDSAT-1 image
of 12 Aug. 1972)

MSS 5: dark = woods
        middle grey = olive yard;
                        (arrow)

a)
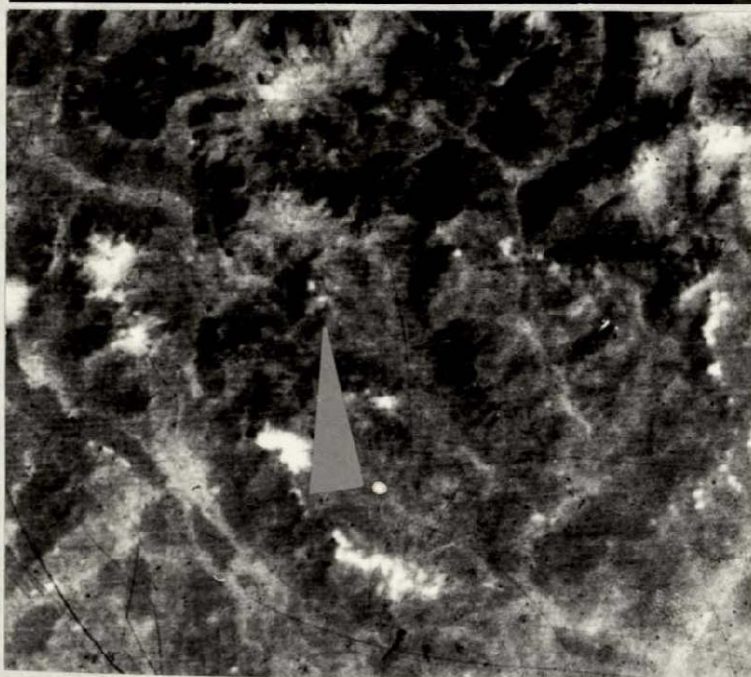
Fig. 42:
Valle Taleggio (Bergamasc
Alps)

LANDSAT-1, MSS 5, 7.Oct.1972

(a) does not show the distinct
vegetation pattern as the
ground truth photograph (b)

b)

Discussion of the Results

The possibilities of conventional interpretation mentioned above base on extreme situations. With respect to the 7 level I categories the results are good.

Mapping of Land-Use Categories

The land-use classification followed the USGS-system which ANDERSON, HARDY & ROACH (1972)* established for the interpretation of remote sensing data.
For our special problems there was introduced the level I category "grassland", which in the USGS-system belongs to "agricultural land", if it is pasture, and to "range land" if it is uncultivated.

The following table (Fig. 43) shows to which degree LANDSAT and SKYLAB images can be used for mapping land-use categories of level I and II. The table is based on our experiences during this work and therefore is valuable for European mountainous regions.
Good satellite data and good background information enable the interprete to subdived the level I categories no. 2, 4, 5 and 6 in level III and IV categories. The following schemes show these subdivisions, which are not included in the above USGS-system.

---

* J.R. ANDERSON, E.E. HARDY & J. T. ROACH: A Land-Use Classification System for Use with Remote Sensing Data. - Geol. Surv. Circular, 671, 1-16, Washington 1972

LEVEL I	LEVEL II	LANDSAT MULTISPECTRAL IMAGERY	SKYLAB
1) BUILT UP LAND		++ o	++
	Residential	+	+
	Commercial	+	+
	Industrial	+	+
	Communications	+	+
2) AGRICULTURAL LAND		+++ o	+++
	Fields	+++ o CIR	+++ HP/A
	Plantations	++ o CIR	+++ HP/A
3) GRASSLAND		+++ o CIR	+++ CN/CIR/A
	Pasture	+ o CIR	++ HP/CN/CIR/A
	Uncultivated	+ o CIR	++ HP/CN/CIR/A
4) WOODS		+++ S	+++ S/A
	Deciduous	+++ S	+++ CIR
	Coniferous	+++ o	+++ CIR
5) WATER		+++	+++
	Streams, Waterways	+++ (o)	+++
	Lakes	+++	+++
	Reservoirs	+++	+++
6) BARRENLAND		+++	+++
	Beach	+++	+++
	Sand	+	+
	Rocks	+	+
7) PERMANENT SNOW/GLACIERS		+++	+++

Fig. 43: Quality of Landsat- and Skylab-imagery for land-use mapping if
level I and II categories are wanted (Legend see fig. 22 a)

Fig. 43 a

<u>LEGEND</u>   for fig. 43

+++   Identification $\geqslant$ 90%

++   Identification $\leqslant$ 90%

+   Identification only
         in special cases

o   sequential imagery

S   Images taken in Summer

A   Images taken in Autumn

HP   High Precision Photograph

CN   Natural Colours

CIR   False Colours

÷ Ground truth knowledge

LEVEL I	LEVEL II	LEVEL III	LEVEL IV
2. agricultural land	acres	—— grain	—— wheat
			rice
		—— truck crop	
	plantations	—— vineyards	
		orchards	
		oliveyards	
		citrous	
		nut-plantations	
4. woods	deciduous	—— deciduous	—— deciduous
		evergreen	—— mediterranean-
		deciduous	oak
			Macchia
	coniferous	—— spruce	
		pines, stone	
		pines	
		larches	
5. water	lakes	natural	—— shallow
		artificial	deep
			+ suspension
	rivers ————————————————————————		
	channels		
6. barren land	barren rock	—— volcanic	
		—— sedimentary	—— limestone
			sandstone
			marles,
			shales

Many categories, however, are not sharply bordered because
of a gradual change of grey tones i.e. a zone of mixed vege-
tation. Even if the categories can be identified, such cases
produce a great uncertainly and mistake in bordering different
land-use categories, especially if the scale is large.

4.2. Cartographic Accuracy

Besides methodological problems and their solution it is
important to calculate the cartographic accuracy.

If the geometric accuracy in the scale of 1:1'ooo'ooo there
is regarded mostly no important differences between LANDSAT-
1 images and topographic maps. During mapping the enlarge-
ments squares of 1o cm x 1o cm were rectified by using exact
topographic features identical in the images and in the
topographic maps.
Finally the geometric accuracy was a good as it is required
for maps of a scale of 1! 25o'ooo. Areas of 1 mm x 1 mm, i.e.
25o m x 25o m, were mapped, so that the geometric resolution
of topographic maps, too was obtained.

4.3. Comparison with other Methods of Mapping

The quality of new methods are generally compared with the
results of former, "conventional" Techniques.

Especially with respec t to woods the borders taken from
satellite images were more accurate than those of existing
land-use maps. This can be explained by this reasons:
Those areas which were mapped from aerial photographs lost
their initial accuracy by the generalization necessary for
a scale of 1:25o'ooo. If the map is based on field work
the borders can only be drwan roughly.

4.4. Comparison with Automatic Digital Classification

Because of the difficulties described in the above chapters
and because of the digital original MSS-data there must be
asked whether an automatic digital classification would not
be preferred to the conventional methods of photointerpre-
tation. Only a time-cost-calculation can answer this question.

At first, there are two important facts:

- A European mountainous region of ca 2oo'ooo km^2 was mapped. This area would be covered by 6 LANDSAT-frames.

- Level I categories were mapped. They include a great lot of sub categories which had to be combined. The subcategories result from differences of vegetation and soils.

Next we must have a look at the time needed for the conventional interpretation.

2 months	mapping	5 photogeologists
1 month	photographic laboratory work	1 photographer
1 month	ground truth	2 geologists

Because of the overlapping of processes the whole map was done in 3,5 months.

Furthermore, at the recent state of automatic digital classification there must be done some premises:

- All necessary computer programs must be established - i.e. programs for the statistics and programs for the correction of grey tones, which is very important especially in mountainous areas with an intensiv relief and with a small scale pattern of different soils.

- The computer must be capable to combine the level I categories from the very great number of subcategories often very similar to one another.

Although automatic digital classification is already done for small European areas and just because of the intensive experiments on this field, it is obvious without an exact calculation:

1. The computer will probably classify much quicker than than a interpreter.

2. The classification pixel by pixel will be much more exact
   than a conventional interpretation.

3. The costs for computer time will be much higher than the
   costs for interpreters, materials and field work.

Furthermore the high degree of resolution is not necessary
because areas of 80 m x 80 m can not be figured out in a
scale of 1:250'000 or less.

In spite of the possibilities offered by statistics and by
computers the automatic digital classification must solve
the same problems as the conventional photointerpretation.
A computer needs background information as well as the human
interpreter. But it is very difficult to code all important
background informations in a way that a computer can work
with them.

This short discussion shows that, at least for large moun-
tainous areas in Europe, the conventional photointerpretation
is and, for the near future, will be the only operational
method for land-use mapping.

LAND-USE MAP OF ITALY

Montaimous regions

Position of the map sections

1) Mount Etna (black and white)
2) Eastern Sardinia (black and white)
3) Sardinia (colour photograph)
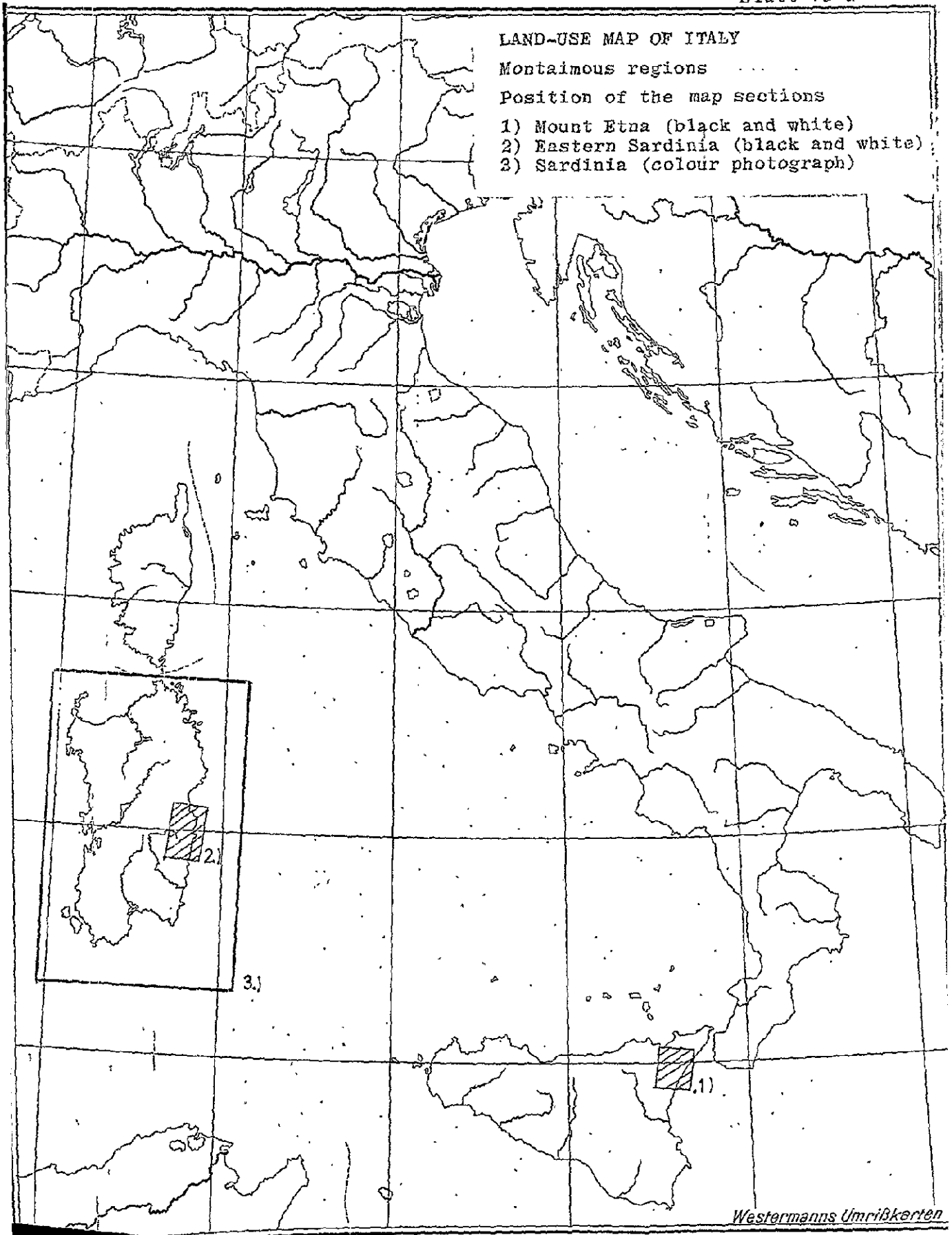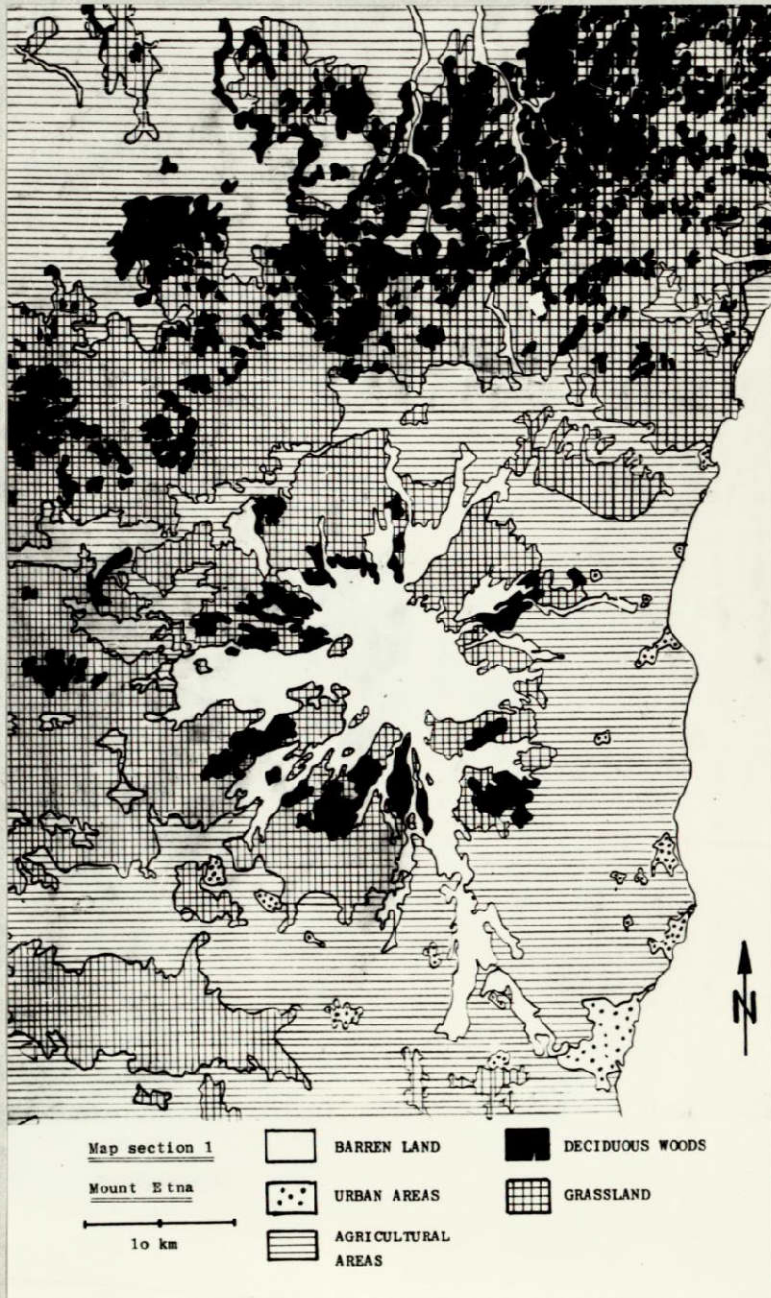
2.)

3.)

.1)

Map section 1

Mount Etna

10 km

	BARREN LAND		DECIDUOUS WOODS
	URBAN AREAS		GRASSLAND
	AGRICULTURAL AREAS		

Map section 2

Eastern Sardinia

|‑‑‑‑‑‑‑‑‑‑‑‑‑|
10 km

LAKES

CONIFEROUS

GRASSLAND

AGRICULTURAL AREAS

DECIDUOUS WOODS

PART II

METHODOLOGICAL INVESTIGATIONS
(DIGITAL ANALOG INVESTIGATIONS)

Methodological investigations concerning the various techniques of processing multispectral data have been emphasized during the last two years.

Within the scope of this activities the following methods have been applied:

1) Digital treatment of MSS data including the development of software programs

2) Combined digital analog treatment of multispectral data

3) Analog electronic data processing

4) Fourier analytical evaluation of LANDSAT data by an optical computer

A   Digital Image Data Processing

Due to the relatively late delievery of LANDSAT CCT's we went into the field of digital data processing only towards the end of 1973.

The digital treatment of multispectral data involved not only data processing in terms of automatic classification but also all data handling and preprocessing techniques for a more quantitative evaluation of spectral information.

The required soft-ware development for above mentioned approach has been carried out at our institution without adapting existing programs.
Today the ZGF is in a position not only to have a reliable program package for data pre-processing but also classification algorithms are implemented.
The flow-diagram for data processing and the applied systems is shown in Fig. 44

1. Image data processing package -IMAGIN-

1.1 Preparation of data for digital evaluation

At the beginning of the evaluation activities no computer
programs and arithmetic models were available to the ZGF.
For these reasons, it was necessary to create data files
on types which could easily be handled by computers of
different producers. The tapes could have been read in
the original format, but this would have required the
creation of ASSEMBLER-Routines for each type of computer
used. On the other hand evaluation programs in ASSEMBLER
seemed useless for this user-oriented application. There-
fore a conversion routine for the data conversion from
the original 8-bit-format to a universal FORTRAN-executable
13-Format was implemented.

During the whole activities of digital data evaluation the
following computer types have been used:

- Siemens 4oo4/151
- CDC 64oo
- CDC 17oo (for type conversion from 9 to 7 track
           and vice versa)
- IBM 36o/9o
- TR 44o (which will be used in the future)

Although the utilisation of different computers for the
evaluation activity was anything but economical, it had
the advantage that all programs have been tested and were
executed on either one of these. Therefore program caused
discrepancies between different systems and compilers are
very unlikely. In fact, discrepancies never did occur once
the programming work terminated.

The advantages of the FORTRAN programming, although in
execution a little slower than ASSEMBLER routines, became
evident once the programs are given to users, or are
integrated to different data service system.

	NASA - Tapes	**Tape Conv** $9 \rightleftarrows 7$ **Track**

Control Data 1700

Assembler	Parity - Error- Correction	Siemens 4004 / 151
Assembler	Convers. to FØRT. read. Format	Siemens 4004 / 151
FORTRAN	Quick Look Area Ident. & Extraction	Siemens 4004 / 151

(A)

FORTRAN	Ratio / Channel Clustering	Siemens 4004 / 151 CDC 6500
FORTRAN	Area Mapping Feature Extract.	Siemens 4004 / 151
FORTRAN	Statistics of Intensities	Siemens 4004 / 151 CDC 6500

(A)

FORTRAN	Factor Analysis	IBM 370
FORTRAN	Factor - Axis - Clustering	Siemens 4004 / 151
FORTRAN	Object Ident. & Extraction	Siemens 4004 / 151

Fig. 44 Flow diagram of data processing

1.2   Check of Data Quality

LANDSAT CCT'S have been the only multispectral information
in digital form. Therefore until now, all activities to-
wards the development of a data processing software have
necessarily been based on this data.

At the beginning we had to face problems concerning the
data quality.

One principal failure which eventually occured were parity
errors on the original data tapes. The maximum number of
events that occured were about 12oo parity disturbed re-
cords in the 234o records of tape data file. In order to
correct these data, a parity correction routine was
created. All parity errors up to now proved correctable.

An analog display of either one of the multispectral bands
showed a systematically increased intensity value for each
sixth scan line. This effect became particular evident
for low level intensities as for example for water bodies.

For analog processing such as density slicing, the sixth
scan line effect was very disturbing.
For the automatic classification it did not result in the
expected reduction of quality because of its high corre-
lation to all spectral bands.
Therefore no special processes for eliminating the sixth
scan line effect were applied.

1.3   Description of IMAGIN Routines (see Apendix 1)

The software routines developed can be separated into 4
groups representing

- descriptive statistics
- data manipulation
- classification periodicity analysis
- support routines.

The full program check is listed in Apendix 1.

The programs involved are:

1. Category: Descriptive statistics

1.1 HDAR   Calculation of mean, standard deviation, and
               variance for a set of multispectral data
               including graphic display

1.2 KORR   Calculation of correlation, covariance matrix

1.3 REGR   Determination of the regression function for
               one or several sets of data in linear, quadra-
               tic or cubic dependance and graphical display
               of the clusters and the regression function

2. Category: Data Manipulation

2.1 WIFU   Weighting of spectral intensities for contrast
               enhancement and illumination (for graphical
               presentation)

2.2 HAKAN   Principal Component Analysis for the selection
               of those axes with the high variance and the
               controlled illumination of those containing
               with the highest degree of systematic errors

2.3 FAKTR   Factor analysis -Principal components

     FAZEN   Factor analysis -Centroid method

     VARMX   Varimax rotation

3. Category: Classification

3.1 DISK   Discriminant analysis for the supervised
               classification of multispectral signatures

3.2 AUKLA   Clustering for the unsupervised classification
               of multispectral signatures

4. Category: Periodicity analysis

4.1 FORAN   Fourier analysis for the determination of one
             or two dimensional periodicities within an image
             (of only one spectral region)

5. Category: Support routines

             Supporting subroutines for matrix inversion,
             the generation of gray scale maps, matrix
             multiplication etc.

On the basis of above described software package, LANDSAT
data were processed under the following aspects.

1) Statistical evaluation with respect to the
   information content of MSS bands

2) Data Reduction

3) Automatic classification

2.   Selection of Data Material and Test Sites

Concerning our activities on digital data processing
during the last year, we were mainly involved in learning
about the significance of the spectral information gathered
by the MSS scanner and in developing and updating software
programs. For this basic research and software development
the selection of test sites has not been carried out
with special regard to our LANDSAT test area in Italy, but
more under the following requirements.

- they should all be very close to the location of ZGF
  (not more than 15o km). Thus it would be possible to
  visit them regularly.Then only a short time would be
  needed for comparison of results obtained by the
  computer evaluation to the real situation;

- they should show significant features for the central
  European user;

- to obtain results concerning the resolution to be
  obtained by a pixel-by-pixel selection, areas were
  chosen which contain featuresof high neighouring
  contrast.

All test areas were chosen of the same size and the same
geometry: 98 lines and 12o pixels per line = 1176o pixels
per test area. This geometry of the frame has been selected
simply for particular reasons of computer display, not
for any other purpose.

The areas in particular are as follows (fig.45,46)

Scene Nr.	Name of area	Data taken
1.	Ostersee Area	
2.	Ammersee-North	
3.	Hofolding Forest	ERTS 1o21-o938o
4.	Landsberg Fields	Date: 13 Aug. 72
5.	Valli di Comacchio	ERTS 1218-o9341
6.	Marina di Carrara	Date: 26 Feb. 73
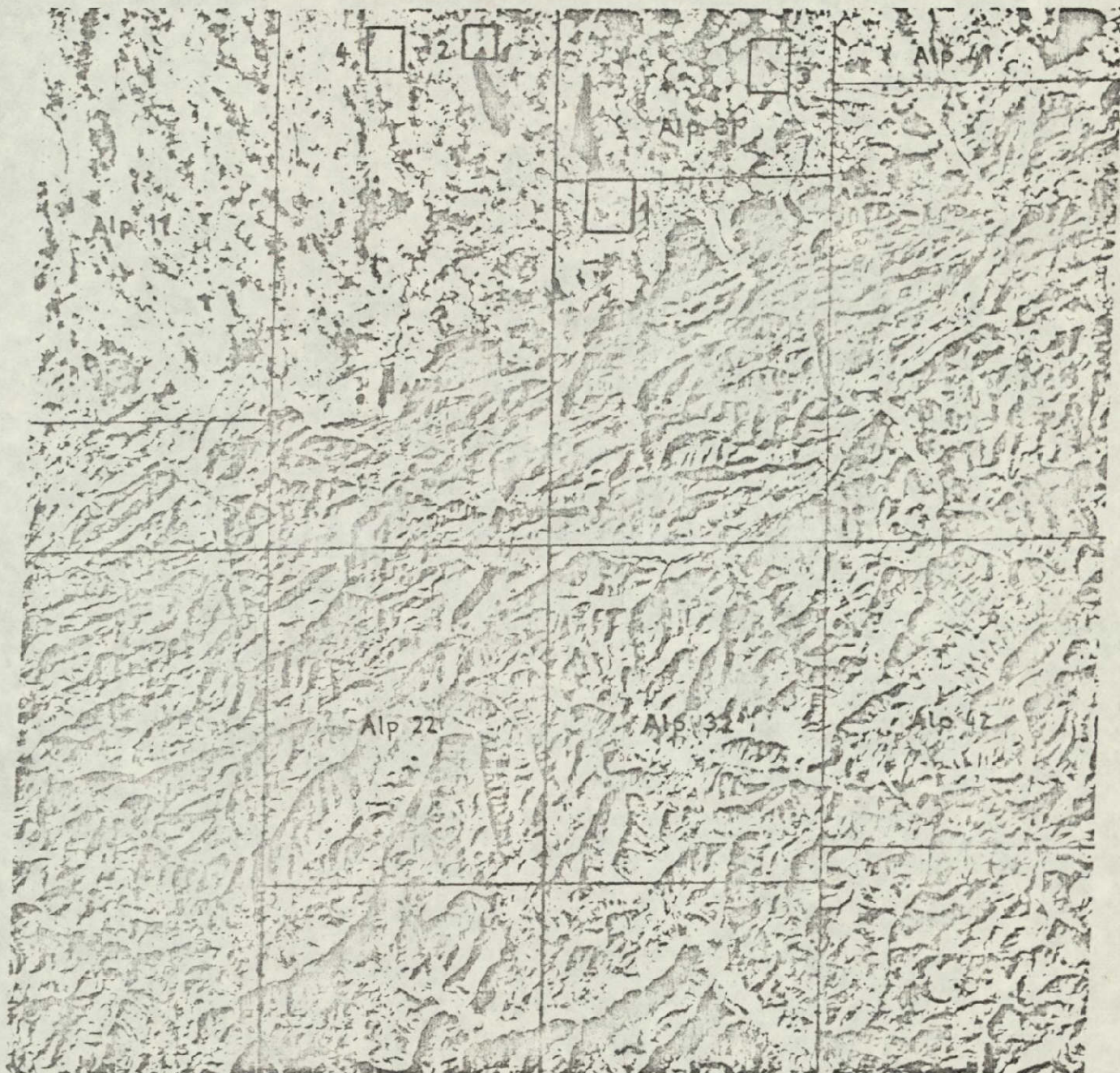
Fig. 45   LANDSAT-scene ID 1021-09380 with test areas
for the statistical evaluation
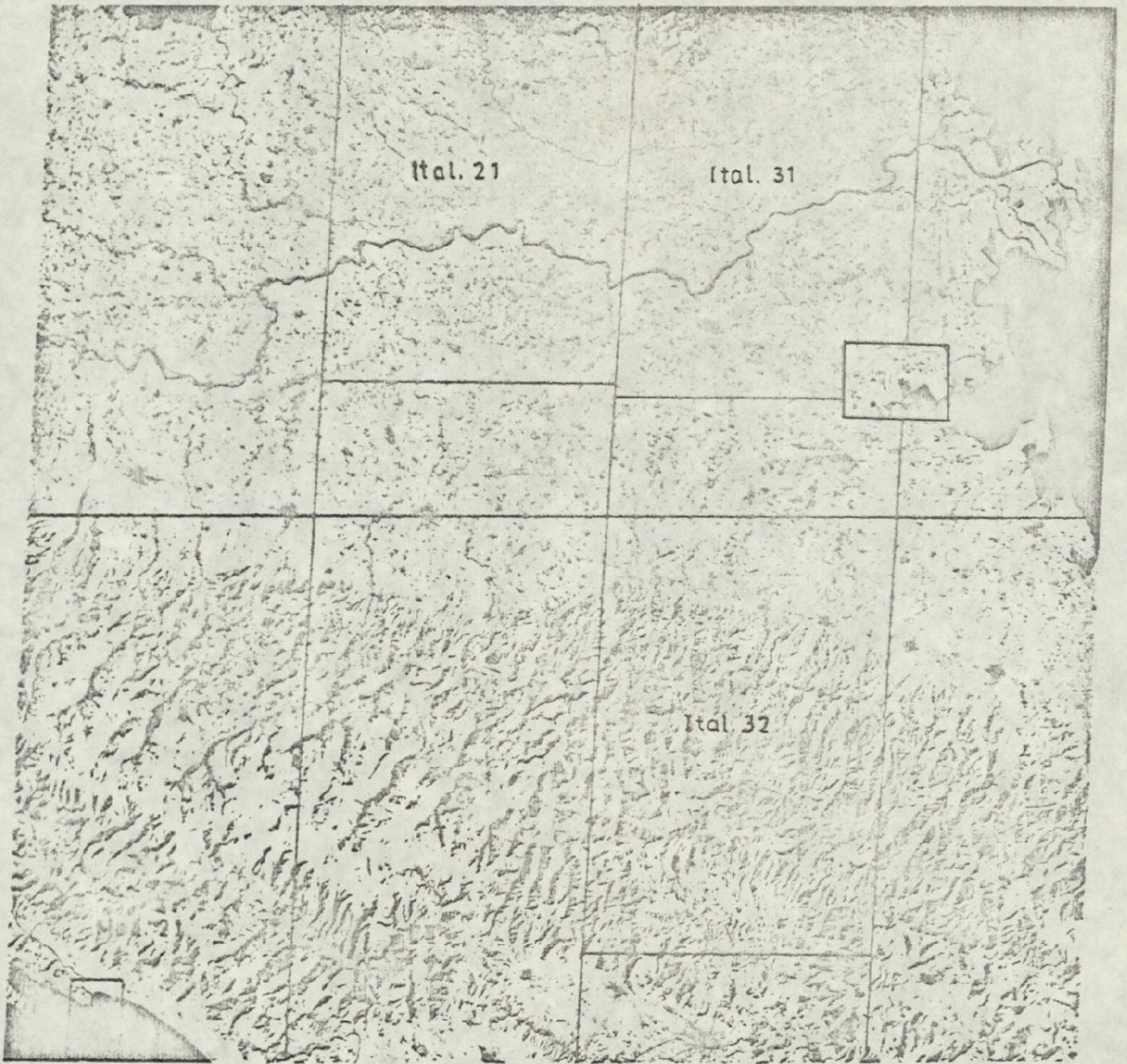
Fig. 46   LANDSAT-scene ID 1218-09341 with test areas
for the statistical evaluation

Scene Nr.	Area Features
1.	Lakes, Marsh land, Coniferous forest, Pastures, Agricultural Areas
2.	Lakes, Reed Grass, Coniferous Forests, Leaf Tree Areas
3.	Agricultural Areas, Meadows, Mixed Forest Types
4.	Mixed Forest Type, Agricultural Areas
5.	Rice fields
6.	**Coast area**

In order to look at the statistics of the multispectral scanner data additional larger areas out of above LANDSAT scenes were selected (**Fig.** 46 - **ALP**)

3. Statistical Evaluation

The statistical evaluation began with an intensity (dynamic range) comparison of different data channels to obtain some idea of the intensity population of a typical Central European scene, represented by the Starnberg Lake area. By plotting these data for two MSS channels in a Cartesian coordinate system, a distinct linear relationship between the intensities of ERTS infrared channels MSS 6 and MSS 7 became evident (Fig. [47]).

Assuming a straight line as the best correlation curve for the data set, the constants A_1 and A_2 in the linear equation for channels 6 and 7

$$I_6 = A_1 + (A_2 * I_7)$$

were found to be 5.3059 and 1.5101, respectively, for this particular region.
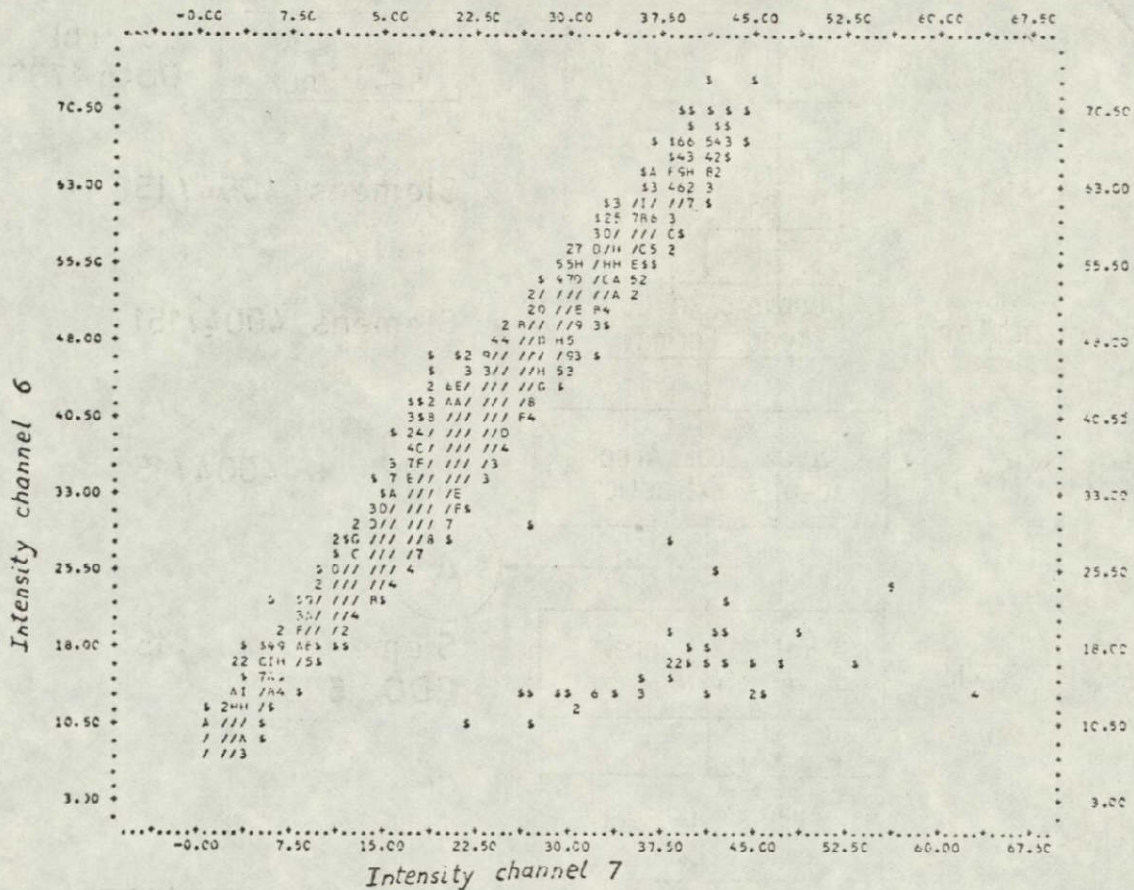
Fig. 47   Intensity Plot, MSS 6 versus MSS 7

These constants were obtained by a least-squares method
on the basis of the following relations:

$$A_1 = \frac{(\Sigma I_6)(\Sigma I_7^2) - (\Sigma I_6)(\Sigma I_6 I_7)}{N\Sigma I_6^2 - (\Sigma I_6)^2}$$

$$A_2 = \frac{N\Sigma I_6 I_7 - (\Sigma I_6)(\Sigma I_7)}{N\Sigma I_6 - (\Sigma I_6)^2}$$

The deviation in the measured intensity values and those
calculated with the above formula as a function of the
measured values of channel 7 is shown in Figure 48 . The
mean deviation was found to be 2,2 for a scale of 128
intensity values for LANDSAT MSS data.

$$S = \sqrt{\frac{\sum (I_{6,measured} - I_{6,Calc})^2}{N}}$$

$$S = 2.2$$

Number of Data Points
N = 11760

Region Starnberg Lake
ERTS-A   13. Aug. 1972

Difference
$D = I_{6,measured} - I_{6,Calc}$
Linear Correlation
$I_{6,Calc} = A_1 + (I_{7,measured} \times A_2)$
$A_1 = 5.3059$
$A_2 = 1.5101$
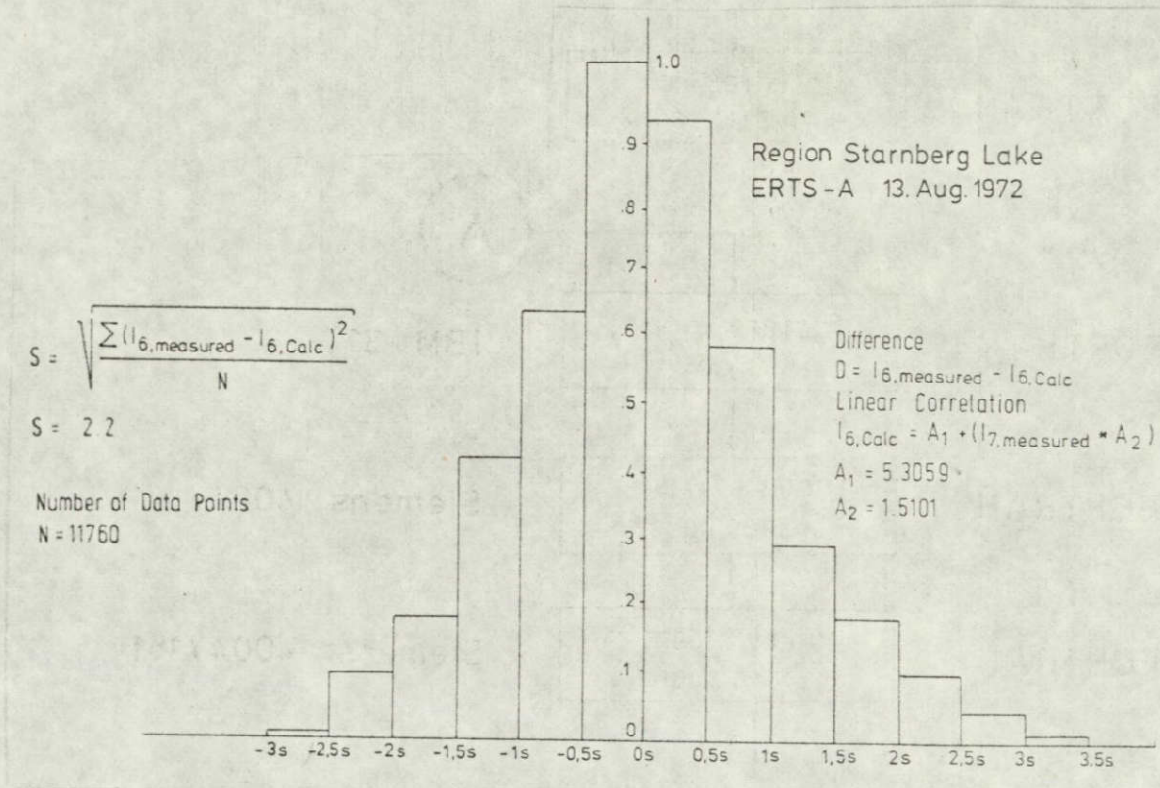
Fig 48   Population as a function of difference D

The graphical presentation shows very good agreement with
a normal distribution, with populations of:

- 68 % in the region of 0 ± 1 S
- 93 % in the region of 0 ± 2 S
- 98 % in the region of 0 ± 3 S

with

$$S = \sqrt{\frac{\sum (I_{6_1 \text{ measured}} - I_{6_1 \text{calc}})^2}{N}}$$

A histogram of the measured data of channel 6 and those
derived mathematically from the experimental values of
channel 7 shows almost an equivalent population distri-
bution to that presented in Figure 49 for the Starnberg
Lake are and the Italian Mediterranean scene.

$I_{7, measured}$

$I_{6, measured}$

$I_{6, Calc} = 5.3059 + (1.5101 \times I_{7, measured})$
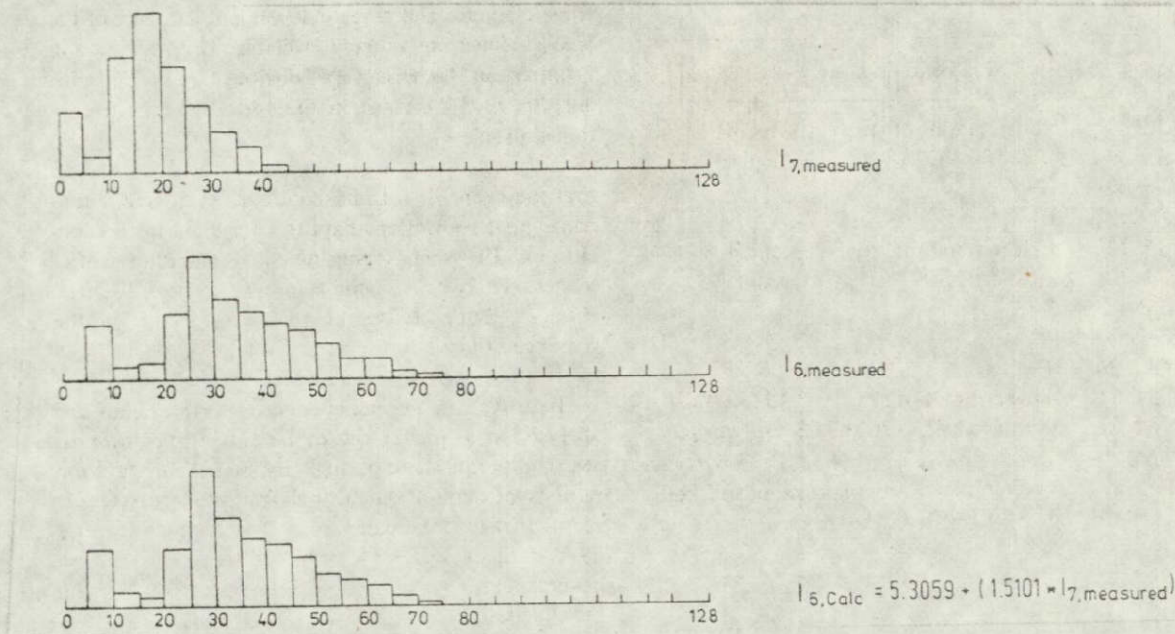
**Fig.49 Histogram of the population of experimental
and calculated values of $I_6 = f(I_7)$**

Based on these results, the analysis was subsequently
extended to complete Central European and Italian scenes
indicated in Tables 1 and 2 . Evaluation of these data
shows almost equivalent constants A_1 and A_2 for the same
type of landscape and landform.

Table 1.

Scene	Number of pixels	Channel 6		Channel 7		Linear equation		
		$\bar{I}_6$	S_6	$\bar{I}_7$	S_7	A_1	A_2	S
ALP 11	974400	35.75	10.83	18.79	6.8	0.28	1.84	10.35
ALP 31	324800	36.98	13.64	20.44	8.72	0.3	1.75	
ALP 41	97080	44.23	13.70	25.19	9.07	3.40	1.17	3.71
ALP 22	950040	38.21	16.55	20.03	9.22	0.3	1.85	26.55
ALP 32	950040	40.73	21.08	20.62	9.89	0.12	1.95	26.55
ALP 42	946533	37.71	16.57	20.26	9.54	3.54	1.11	10.18
ITAL 21	936767	22.96	6.55	12.18	3.95	0.13	1.84	12.1
ITAL 31	943467	24.12	3.86	11.82	2.45	0.11	2.0	17.57
ITAL 32	943879	25.41	4.16	13.08	2.88	0.14	1.91	16.19
MED 12	40000					5.01	0.0678	5.5

Table 2.

Scene	Identification		
ALP 11	Northern half of strips 1, 3 and 4		
ALP 31	of ERTS 1021-09380, 13 August 1973		
ALP 41			
ALP 22	Southern half of strips 2, 3 and 4,		
ALP 32	ERTS 1021-09380, 13 August 1973		
ALP 42			
ITAL 21	Northern half of strip 2	ERTS	
ITAL 31	Northern half of strip 3	1218-09341	
ITAL 32	Southern half of strip 3	26 February	
		1973	
MED 21	Mediterranean water surface of southern strip of ERTS 1218-09341, 26 February 1973		

Linearity alone, however, is not a sufficient identity
criterion. Much more important is the average deviation
between the measured intensities of channel 6 and those
derived mathematically from the experimental values of
channel 7 . The data obtained show that the average de-
viation for the equivalent landscape and land-use scenes
are almost identical. This is valid not only for the Cen-
tral European summer scene, but also for the Italian
winter scene. The additive and multiplicative constants
for the linear equation show a strong deviation for equi-
valent scenes only in those cases where the test area
considered largely contains a single uniform feature. This
was the case for scene ALP 41 (water surface of the Chiem-
see Lake), scene ALP 42 (mostly cloud covered), and MED 12
(uniform water surface of the Mediterranean). Applying
these results to a scene of the same type, but containing
several different features, results in a very wide deviation
between the measured and mathematically derived values of
channel 6.

From these results, it can apparently be concluded that a
strong correlation, and therefore redundancy, occurs bet-
ween the intensity values of channels 6 and 7 for each

individual data point. Such strong dependance has further
consequences which find their impact in the mathematical
procedures for feature recognition and identification.
The idea was to present the data from the four MSS channels
in four-dimensional mathematical space and, by identifica-
tion of particular characteristics to recognise the presence
of certain features in the scene.

The fact that there is a strong correlation between the two
infrared channels means that one set of data does not
really give new information, so that only three channels
and three independent data sets of the four assumed are
actually available. This reduction in information became
very obvious for the factor analysis and is evident in the
correlation matrix obtained (Table 3).

Although these results could be interpreted such that the
channels 6 and 7 could be considered redundant, great
restrictions have to be applied to this conclusions. The
scenes considered were either winter scenes (Italy) or mid-
summer scenes (Central Europe). Both landscapes are charac-
terised by the presence of highly uniform land-use patterns,
containing features of the harvest or post-harvest period.

To arrive at a definite conclusion, extension of this
analysis to a greater set of land-use types over all
seasonal periods, and particularly over the maturation
periods of certain agricultural fruits, is necessary.
It seems that in these cases , as well as for such
features as waters of different turbidity, cloud and
snow cover, there is no redundancy between the two infra-
red channels, and therefore one of them cannot be dis-
pensed with.

Table 3   Correlation coefficients LANDSAT MSS bands

	MSS-4	MSS-5	MSS-6	MSS-7
MSS-4	1.000	0,762	0,218	0,141
MSS-5	0,762	1,000	0,471	0,388
MSS-6	0,218	0,471	1,000	0,987
MSS-7	0,141	0,388	0,987	1,000

While working on the statistical evaluation of the Central
European and Italian scenes, an interesting feature con-
cerning only the water bodies became evident. While the
intensity level of European lakes ranged from 0 to 9 in
channel 7, the dynamic range for the Mediterranean water
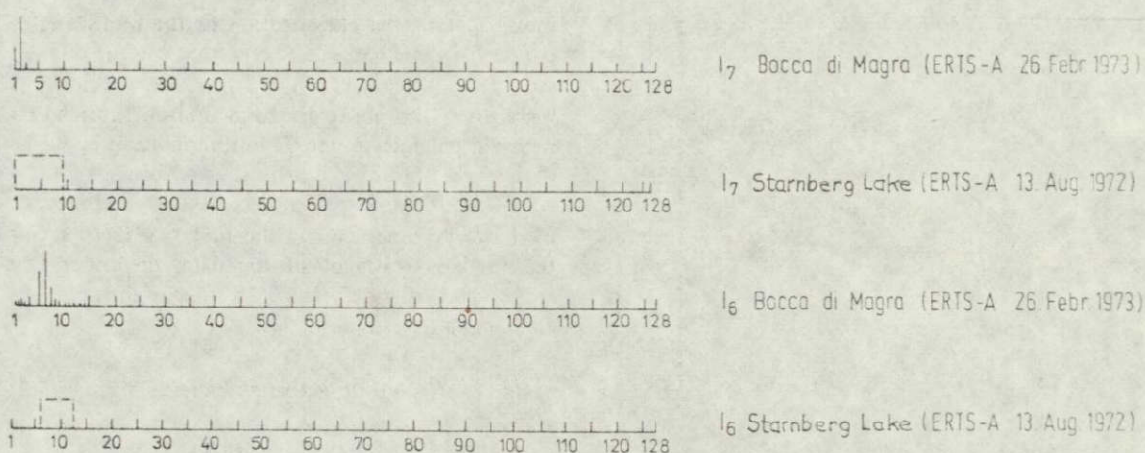body was 0 to 2 (Fig. 50.)

I_7 Bocca di Magra (ERTS-A 26 Febr 1973)

I_7 Starnberg Lake (ERTS-A 13 Aug 1972)

I_6 Bocca di Magra (ERTS-A 26 Febr 1973)

I_6 Starnberg Lake (ERTS-A 13 Aug 1972)

Fig 50 Compasrison of dynamic ranges
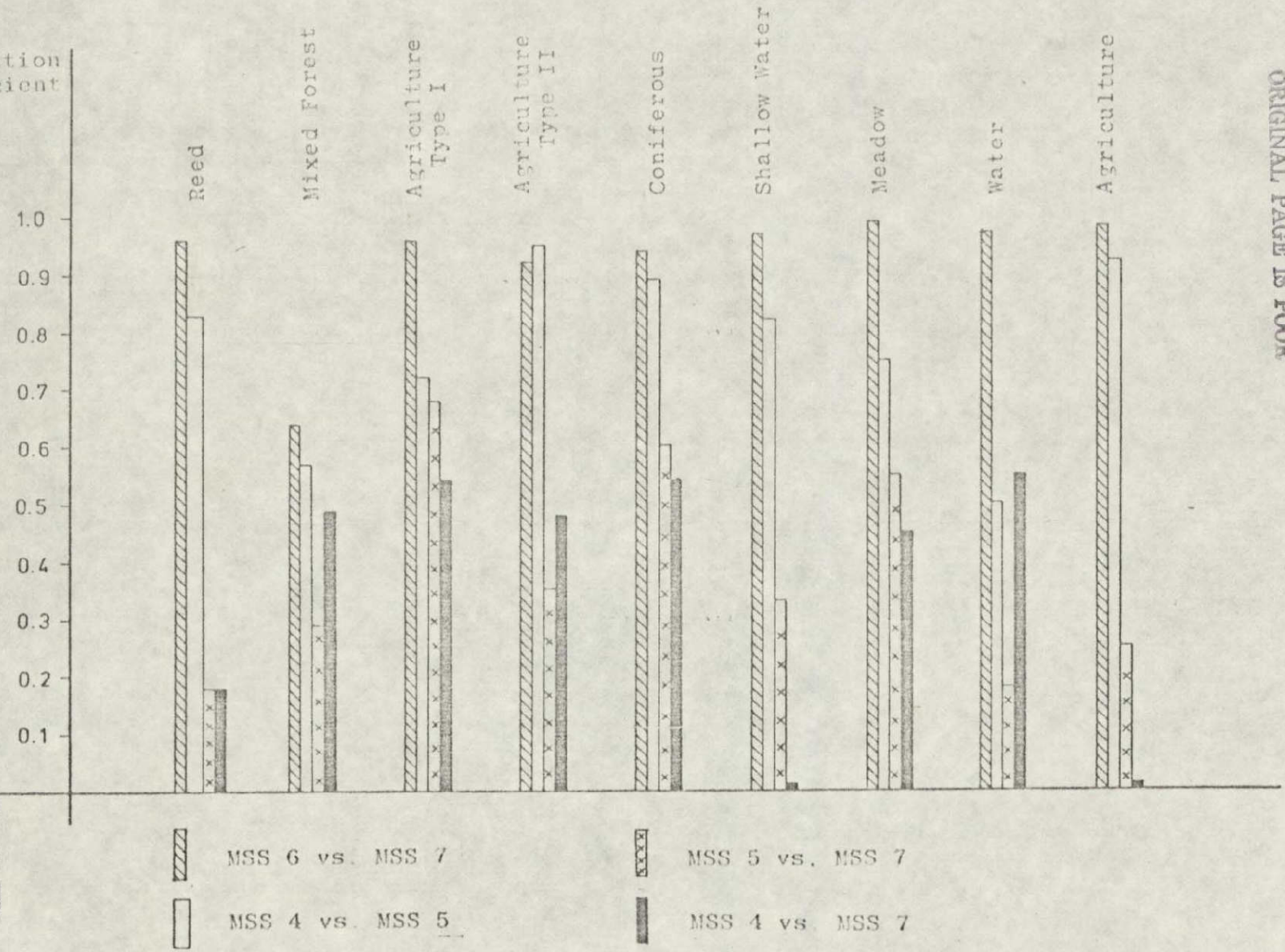
4.   Data Reduction

Above described phenomenon of the correlative property
of MSS bands led to a more detailed evaluation on the basis
of special selected surface features. Furthermore this
approach led us to discussions about the possibilities of
taking advantage of the correlative property by reducing
the redundant information for data compression purposes.
The selection of test areas has been directed at large homo-
geneous objects such as coniferous forest, water and
large homogeneous vegetated areas. Furthermore, surface areas
composed of different sub-categories of earth scientific
interest such as agricultural field pattern, were also
selected (Fig.51). The graphical representation, Fig. 51
illustrates the correlation of the LANDSAT bands with
the above-mentioned surface features.

Based on this comparison, the following conclusions can
be reached:

- A very high redundancy exists between the infra-
  red bands, expressed by a correlation factor
  above 0,9.
  The degree of correlation is approaching a uni-
  form value for all samples except for the mixed
  forest.

- The visible channels are also characterized by
  a relatively high redundancy. The absolute degree
  of correlation is more dependent on the various
  surface features.

- Low redundancy exists between the visible and
  infrared channels. The variations in correlation
  are strongly influenced by the selected samples.
  So minimum correlation can partly be observed
  between MSS 5 and MSS 7.

Correlation
Coefficient

Reed

Mixed Forest

Agriculture
Type I

Agriculture
Type II

Coniferous

Shallow Water

Meadow

Water

Agriculture

1.0
0.9
0.8
0.7
0.6
0.5
0.4
0.3
0.2
0.1

MSS 6 vs. MSS 7   MSS 5 vs. MSS 7

MSS 4 vs. MSS 5   MSS 4 vs. MSS 7

fig. 51 Correlation of different ERTS-1 bands with respect
to selected surface features

Blatt 97

These examples show very clearly that, at least on the
basis of LANDSAT, the significance of spectral bands is
strongly dependent on the surface feature, or more gene-
rally, on the earth scientific problem in question.

With respect to the relationship described above in general,
it is not possible to satisfy different earth scientific
requirements with only a limited number of spectral bands.
The result would be the implementation of a multispectral
scanner operating a high number of spectral bands. This
requirement leads to non-manageable data rates, especially
with respect to operational systems. On the other hand,
the more or less high degree of redundancy between multi-
spectral data enables the application of redundancy supression
techniques. The strong realtionship between correlation
factor and surface feature calls for a supression technique
that is carried out in relation to the corresponding user
oriented problem and that can be performed after data
acquisition and before data transmission.

4.1   Data Compression by Principal Components Transformation

A well known data compression technique is the so called
Principal Components Transformation. This statistical method
defines a new coordinate system describing maximum dis-
persion of the input data. The new coordinates or principle
components represent a linear combination of the original
coordinates or spectral channels.

Application of this technique on multispectral information
indicates, that the same information, described by the
entire range of spectral bands, can be expressed by a
very limited number of principal components. This effect
is primarily based on the correlative property of multi-
spectral data. With respect to the number (n) of available

variables represented by the spectral bands, the Principal
Components Transformation operates in an n-dimensional
space.
From a statistical point of view, the definition of the
new axis is based on the dispersion created by the chance
occurrence of N categories or data populations. Therefore
the dispersion or information content of a single popula-
tion and of under-represented populations of earth
scientific interest cannot be described in an optimum way.
Due to this effect, data reduction on the basis of the
Principal Components Transformation is of necessity a
compromise between the information content of the total
input data and the information content of minor popula-
tions.

4.2   Application Oriented Data Compression

The effect described above becomes crucial if the Principal
Components Transformation is considered as an in-flight
data compression technique for operational satellite
systems. Furthermore as a statistical method, it requires
elaborate computer hardware.

In reality an operational system evidently cannot satisfy
the entire multi-disciplinary user community, at least
not at the same time. It will be able, however, to cover
a limited number of relevant applications. For these
reasons in defining earth scientific problems, it is
necessary to have optimum information in terms of appli-
cation oriented low data rates. This requirement can be
partly fulfilled on the basis of a so-colled Supervised
Principal Components Transformation.

The basic idea of this method is, to define a priori (the
principal components of only a single- or a group of
features which is of interest) and to transform (reduce)
the incoming multispectral information with respect to
these defined components.

By means of this supervised reduction above-mentioned
"compromise-effect" of the Principal Components Trans-
formation is minimized with respect to the dispersion of
single or minor data populations. Furthermore, the super-
vised transformation does not require elaborate on-board
computer facilities. Therefore, from a technical point of
view, if offers a high potential as an in-flight data
caompression technique.

In order to demonstrate this kind of supervised transfor-
mation, as a first step, the loadings of the principal
axis of an inhomogene agricultural area and of a homogeneous
coniferous forest, were calculated.

Principal Components Factor Loadings

Agricultural area: Coniferous forest:

	I	II	III	I	II
MSS 4	o.815	-o.558	-o.158	o.898	-o.369
MSS 5	o.646	-o.749	-o.15o	o.927	-o.437
MSS 6	o.845	o.528	o.o16	o.448	o.311
MSS 7	o.754	o.652	o.o24	o.273	o.486

As calculated above, the three principal components for
the agricultural area contain 99,7 % of the total informa-
tion represented by the 4 MSS-bands. Because of the homo-
geneous signature of the coniferus forest, 96,3 % of the
total information can be described by only two factors
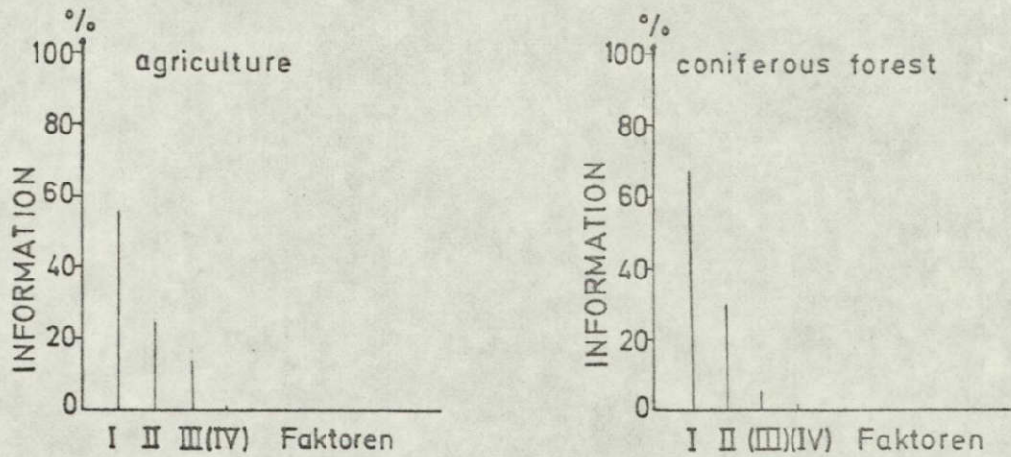(Fig. 52).

Fig. 52   Distribution of information on principal com-
ponents for agriculture and coniferous forest

In a second step the MSS data of the test area (Fig.53),
characterized basically by a coniferous- and mixed forest
cover and also by an agricultural area, was translated.

Fig. 53   Representation of the test-site (LANDSAT-MSS 7)

The quantized grey step image of fig. 54 represents a transformation due to the first principal component of the agricultural training set.
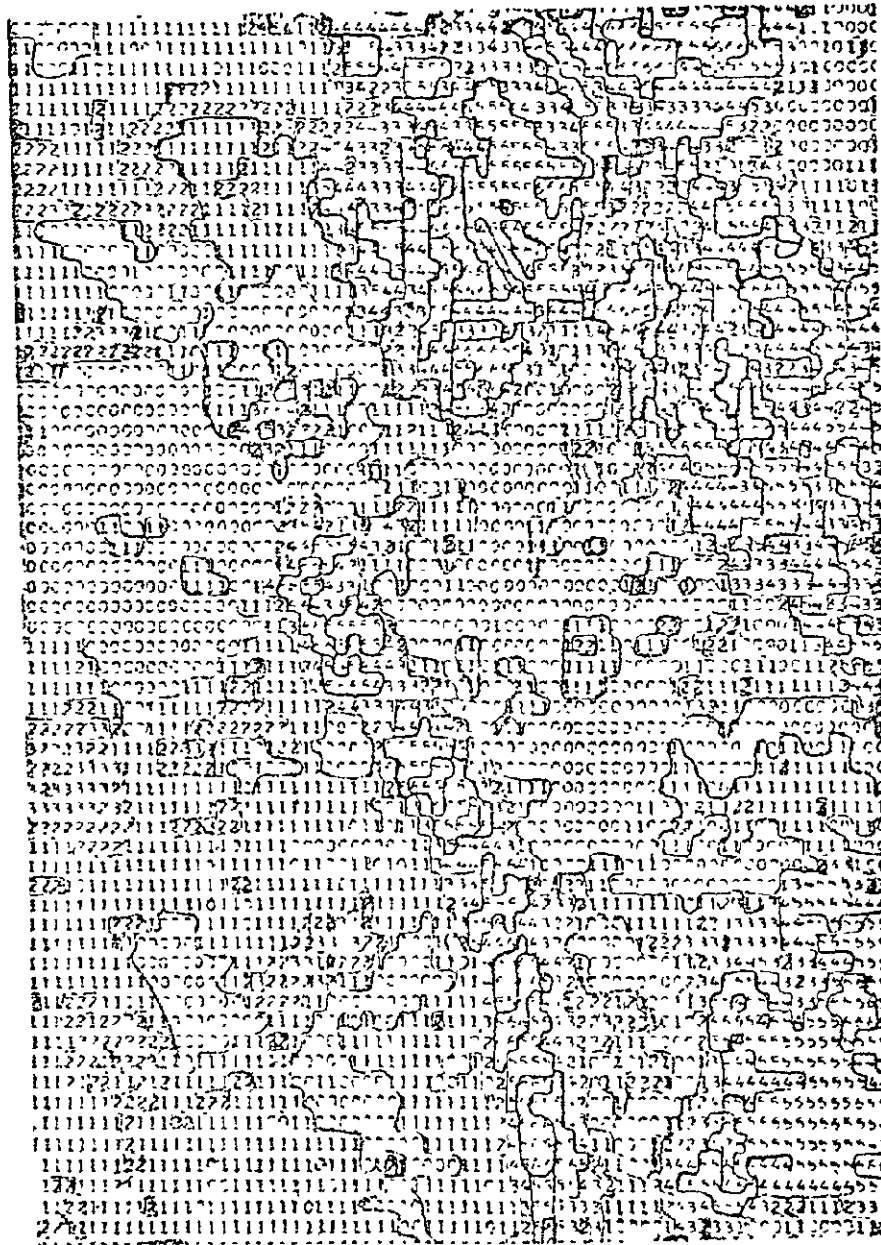

Fig. 54 Principal component image optimized for
         agricultural used areas

This transformation shows very detailed information on
field patterns; whereas, it is not possible to define
the homogenity of the coniferous forest.

A transformation of the same original data with the
loadings of the first factor representing coniferous samp-
les (fig. 55) was also carried out.
This time the forest cover appears very well defined and
the lack of information on agricultural areas is evident.
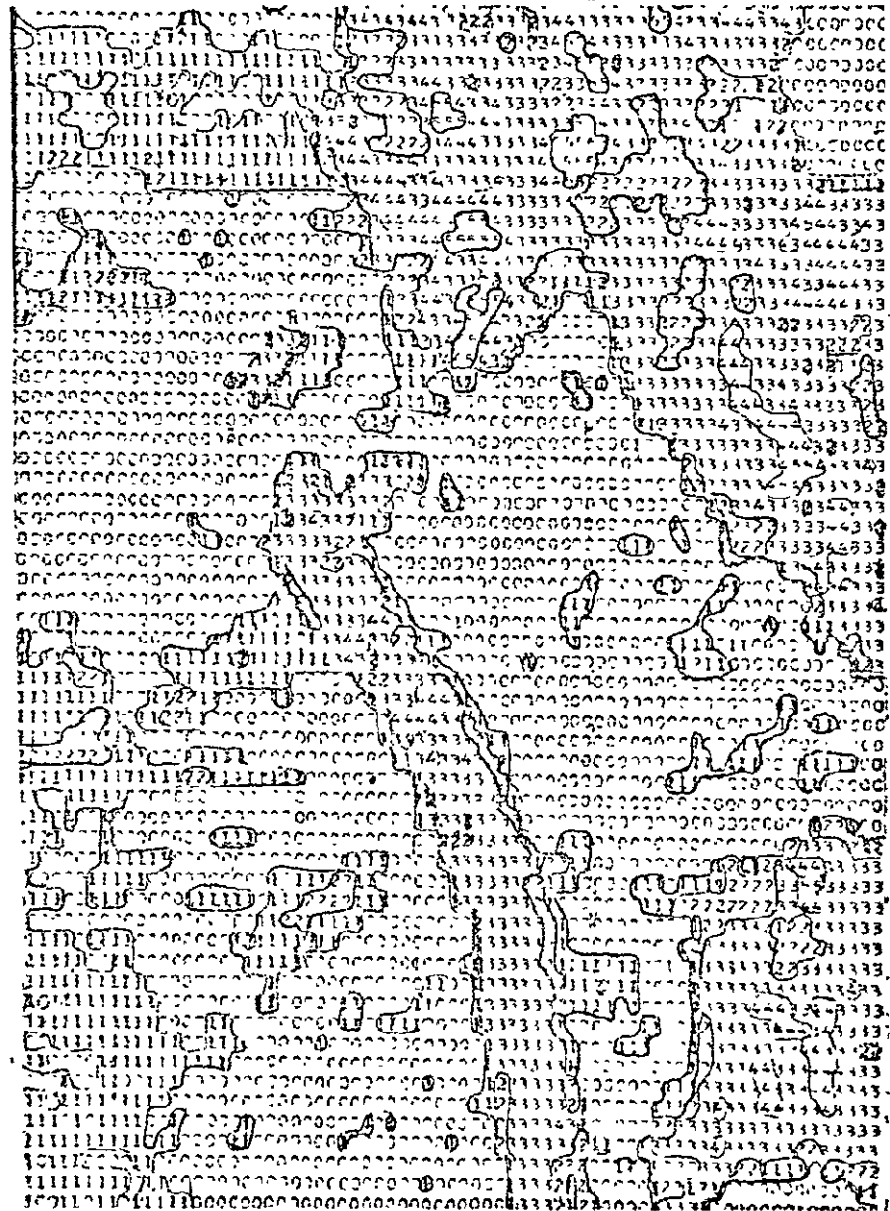
Fig. 55 Principal component image optimized for forested
        areas

By means of corresponding transformations of the original
data through available supervised factors, the new set of
data can be regarded as compressed input data with optimum
information content for specific applications.

Furthermore, by applying the remaining set of data (com-
ponents), a reduction of computer time in the ratio of
9:16 could be maintained with no reduction in classifi-
cation accuracy as the processing time required is a
quadratic function of the number of spectral bands.

Another type of data reduction can be obtained through
application of factor analysis (FAKTR), in order to select
those spectral channels with the highest degree of
significance for the identification of certain surface
features. Using this method for LANDSAT-data, it was found,
that only three out of the 4 bands showed sufficient and
linear independent information. The high degree of linear
dependence, as pointed out already above, between MSS 6
and MSS 7 should be restated.

5.   Automatic Classification

Multispectral data require by its nature of representing multivariate information advanced processing techniques.

Furthermore this data can be regarded as an optimum prémise to apply fully automated evaluation and classification algorithms.
On the basis of data representing Italian and South German scenes, both supervised and unsupervised algorithms were programmed and applied.

5.1   Supervised classification

In order to test and evaluate the supervised classification programs (Apendix 1) a test site near Munich (Fig.45 Scene 1) was selected. The classification was started with objects easily identifiable by their areal extension and spectral characteristics such as water bodies, coniferous forest, urban areas, and pastures. The result of such a supervised classification is demonstrated by fig. 56

In order to prove the reliability of above classification intensive ground checks and comparative studies based on aerial photographs were carried out.
From this it turned out, that some classes which are uniform from an earth scientific point of view could not be fully recognized by the automatic classifier. Marsh land for example, which is composed by different vegetated and non vegetated surface features could not be seperated. Training the computer with data, representing the unhomogeneous category "marsh" interference with other surface features such as coniferous forest occured.

Dividing the cluster of marshland into more subclusters it has not been possible to map the true areal extension of the marsh itself in spite of a high statistical accuracy in terms of separability. Such difficulties in defining special

Fig. 56 supervised classification: water= blue, urban=black
pastures=red, coniferous forest=green and
marshland=grey

surface features are not caused by the algorithms used.
Rather the reason for classification errors is the signi-
ficance of the available spectral information for solving
a particular lash.

Further difficulties arise especially with respect to the
resolution capabilities of the MS-scanner and the typical
pattern of agricultural used areas in Europe.

In contrast to the extensive land use, characteristic of
North America, we are faced with an intensive management of
our agricultural areas. This has resulted in very small
and inhomogeneous field pattern.
Due to this situation, it is necessary to make a very careful
selection of the picture elements for training the computer
with certain test features. A further problem is, that the
test site very often is much smaller than the dimension of
a resolution element leading to a mixture of different
spectral significances for one cluster. Furthermore this
results in a very poor separability crucial for automatic
classification purposes.

The same problem of gathering unhomogeneous spectral information
occurs at the borders of two significant surface features.
The degree of misclassification for this case can be mini-
mized by comparing neighbouring picture elements.

Due to above mentioned problem in classifying phenomena
"below the resolution" other approaches of automatic in-
formation extraction techniques should be taken into con-
sideration.
To carry out a spectral-statistical inventory of agricultural
used areas over one vegetation cycle in combination with
detailed ground truth reports may result in correlation which
allow a further use of Landsat data in terms of a pure
numerical evaluation. A premise for this approach has to
be a maximum repetitive LANDSAT coverage.

5.2 Non supervised Classification

For carrying out a non supervised classification two routines
were implemented.

The first routine stores all data necessary for an automatic
classification in core. As the numbers of storage elements
necessary for the classification depend on the number of
picture elements by n (n - 1)/2, its execution requires much
storage, but, on the other hand, is very fast.

The second routine has in core only the information of the
clusters found, and the information of the actual data points.
It is as fast as the first routine, but does not need as
much storage.

With these routines a separation of those clusters with
a very high degree of agreement has been obtained. It soon
became evident, however, that it was not meaningful to use
all data elements for the classification, because of the
great computer time necessary for these procedures. Therefore
the decision was made to use only a very small number of
preselected pixels of a specific significance or to select
the data points from a certain land-scape type by random
number access.

For classification purposes the Laguna die Comachio
south of the Po-delta was chosen (Fig. 46, Scene 1)

The area covers water bodies, large agricultural fields
with uniform plant soil association characterized by ex-
treme changes in soil moisture and shallow water   in
irrigated rice cultures.

By applying AUKLA and AUKLB it was possible to seperate
four typical categories. The computer print out of the
evaluated area (Fig. 57) shows the following categories:
deep water, shallow water, channels, water covered fields
or areas with extremely high soil moisture, fields with
fresh vegetation, dry area with vegetation.

Fig. 57

5.3 The "Slope Method"

With respect to the computer time consuming classification operations the possible information gain has to be carefully examined. Even for a pure scientific data handling computer time often becomes a critical factor which calls for operating may be less complex processing software or analog equipment.

A very easy and still effectful possibility of digital evaluation of multispectral data is, taking into account the reflection properties of some dominant surface features within the spectral range covered by the ERTS-MSS scanner.

Some basic spectral properties are the reflection capabilities of plants and water in the near region of the infrared spectrum. In general, reflection characteristics depend on the spectral range or wavelength of the surface considered. For the particular case of the LANDSAT-data the slope has been defined as

$$\alpha = f \quad \text{(contribution of visible — contribution of infrared part of the spectrum)}$$

$$\alpha = \frac{I_4 + I_5}{2} - \frac{I_6 + I_7}{2}$$

This technique is not based on a statistical approach. Each picture point, represented by 4 Variables – the 4 spectral measurements – is classified with respect to say an certain angle intervalls, and assigned with a corresponding symbol and printed into the maps. This simple decision making program, does not require large amounts of computer time, and storag and can be regarded as a kind of digital quick look operation (fig. 58).

The idea of the slope technique is not to imitate density slicing techniques but to have the possibility to perform a certain kind of preselection of surface features.
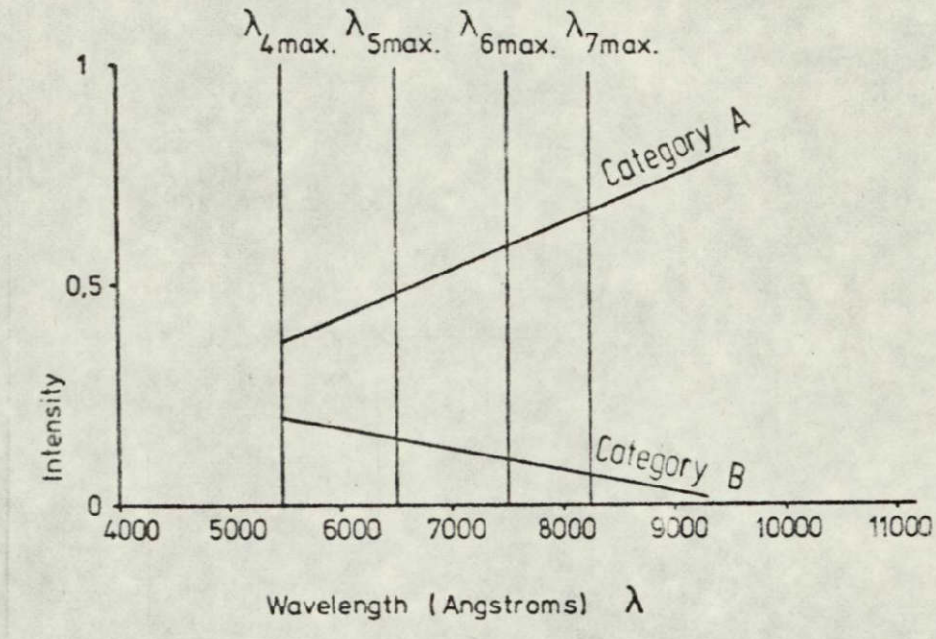
Fig. 58 **Spectral slope method**

Under this aspect, it is possible to get a distribution
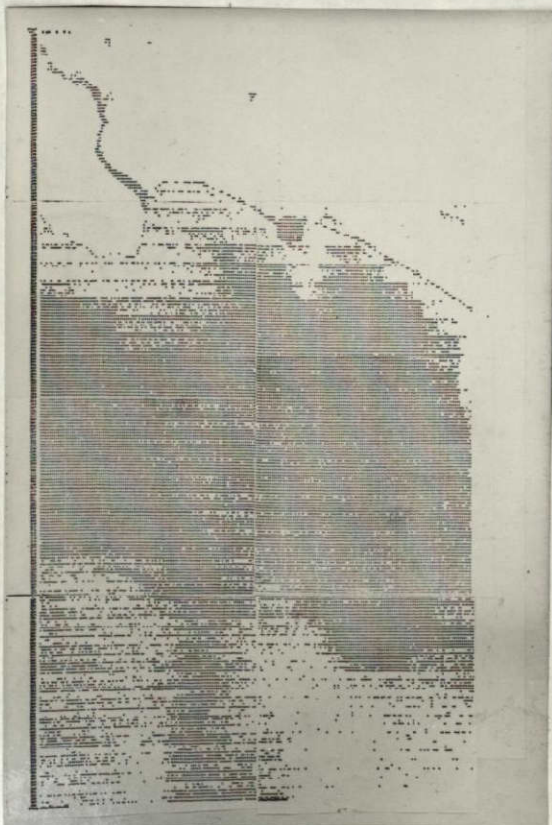display of different water bodies but no idea about its
relative degree of pollution.

Fig. 59 Color composite re-
presenting 3 classes
of turbid water

In Fig. 59 the Versilian coast is evaluated using this
method. Three different classes of turbid water bodies are
distinguished. Main pollution surces SE of the harbour
basin of Marina di Carrara, the distribution, transporta-
tion and degree of pollution in Thyrrenian Sea can be re-
corded in relation to different slope angles. Decreasing
slope is a function of the reflection and absorption pro-
perties within the visible and near infrared portion of
the spectrum.

B   Analog/Digital Treatment of Multispectral Data

The results of fully automated classification procedures
are data in maplike form which consists of averaged infor-
mation with respect to the information content of the ori-
ginal data. By this the user is confronted with a final
data product which does not permit anymore any further inter-
pretations.

Taking into account, the interference and complexity of
earth-scientific phenomena and the difficulties described
above for many applications the researchers know how is
indispensible.

Especially in an experimental phase it is of utmost import-
ance of being able to evaluate multispectral data by combining
the advantages of statistical techniques and the interpreters
know how.

From an earth scientific point of view a possible solution
to take advantage of both can be achieved via the following
steps.

a) statistical enhancement of class separability

b) combination of transformed data by operating in color space

c) interpretation

By this technique decision making algorithms which actually
result in an averaging of data is left to the interpreters
interaction.

1.   a) Enhancement of class seperability

This preprocessing technique represents a necessary first
evaluation step for both the fully automated classification
and the combined digital and analog treatment of multispectral
data.

The separability of surface classes represented by data
clusters in an N dimensional space is commonly increased
by applying the principal component transformation. Since
a linear transformation of all data points considers the
weighted intensities of the original bands, new dimensions
or components can be determined. Due to the enhanced
separability of the clusters, the pictural representation
of the new components offers enhanced maximum contrast.
In order to obtain principal component images which show
maximum information for selected phenomena or applications,
the transformation must be optimized. The optimization is
carried out by applying this technique on selected training
areas (as it is demonstrated on page   ).
The image of fig.61 represents a weighted transformation of
the original bands (fig. 60). It is evident that none of
the original bands (MSS 4,5,6 and 7) have a comparable con-
trast in the region of field patterns.

With respect to the various application-dependent require-
ments, it should be possible to define standard transforma-
tion by taking into account also changing environmental
parameters. Therefore this approach has to be based on
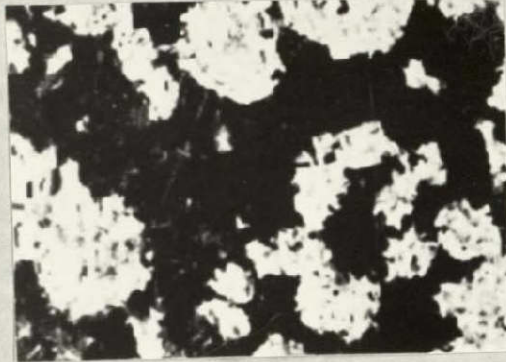along term experimental remote sensing measurement program.
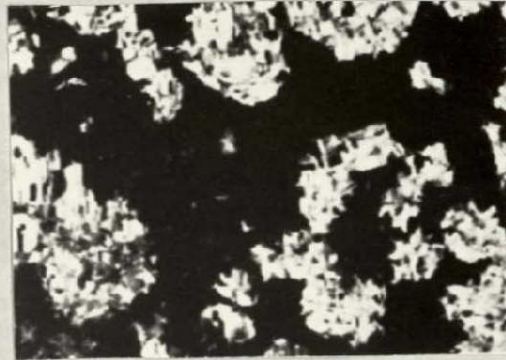

Fig. 60   LANDSAT-MSS 4
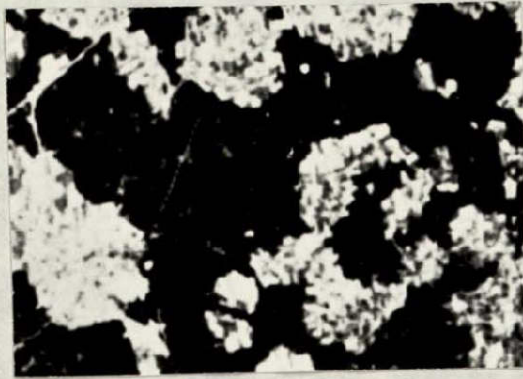
a
(MSS 5)

b
(MSS 6)

c
(MSS 7)
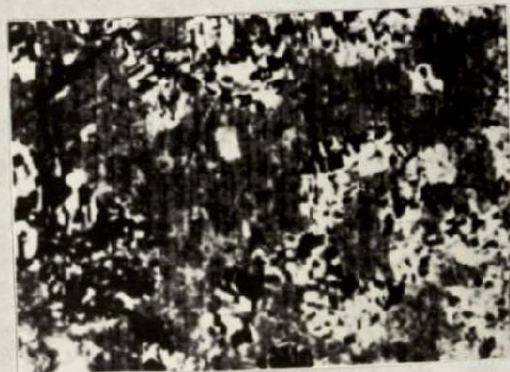
Fig. 60 a,b,c LANDSAT-MSS 5,6 and 7

Fig. 61   Transformed image (first principal component)

2. Color Coding by operating in the three-dimensional color space

The transformed spectral information now can be used as a
basis for a further automatic classification. With respect
to a further analog treatment, a selection of three trans-
formed images (either the first three principal components
or a selection of optimized transformations) can be used
for the generation of color composites. With respect to the
expanded information content of the black and white input
images the resulting perceptable color differences are very
indicative of the distribution of characteristic surface
signatures.

For demonstration some areas out of an ERTS-frame showing the
Alps between Munich and Bozen were selected (fig. 62 , frame **1**
and **2**). The image of fig. 63 illustrates the enlarged region
of the Murnauer Moos. The image is composed from MSS band 4
(blue), 5 (green) and 7 (red). This false color image shows
a relatively low degree of differentiation. Two main cate-
gories, grassland (light red) and bog areas can be seperated.

Fig. 62
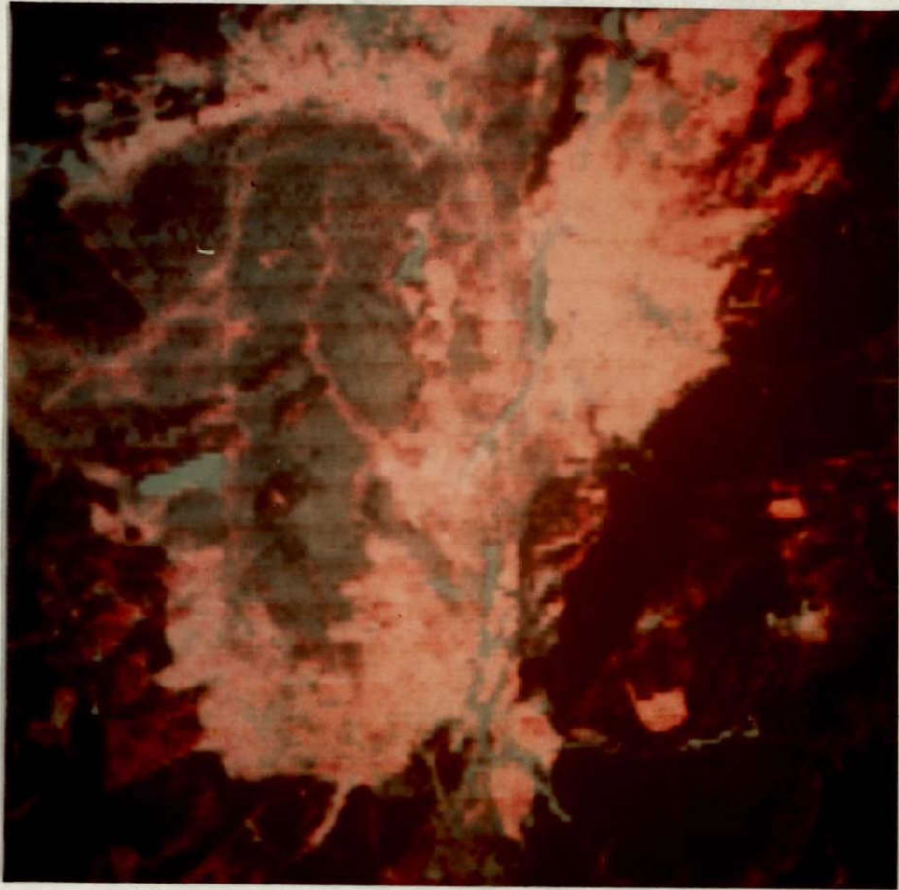
Fig. 63 False color composite "Murnauer Moos"

The color composite (fig.64) derived from statistically
transformed data is characterized by a much higher contrast
and an enlarged "spectrum" of colors.

Plant ecologists could derive from the transformed image
very good information on the areal distribution of raised-
bog (blueish) and trasition bog (brown). A differenciation
which could not be obtained on the false-color presentation.
Furthermore two types of meadows, light brown and green can
be seperated.
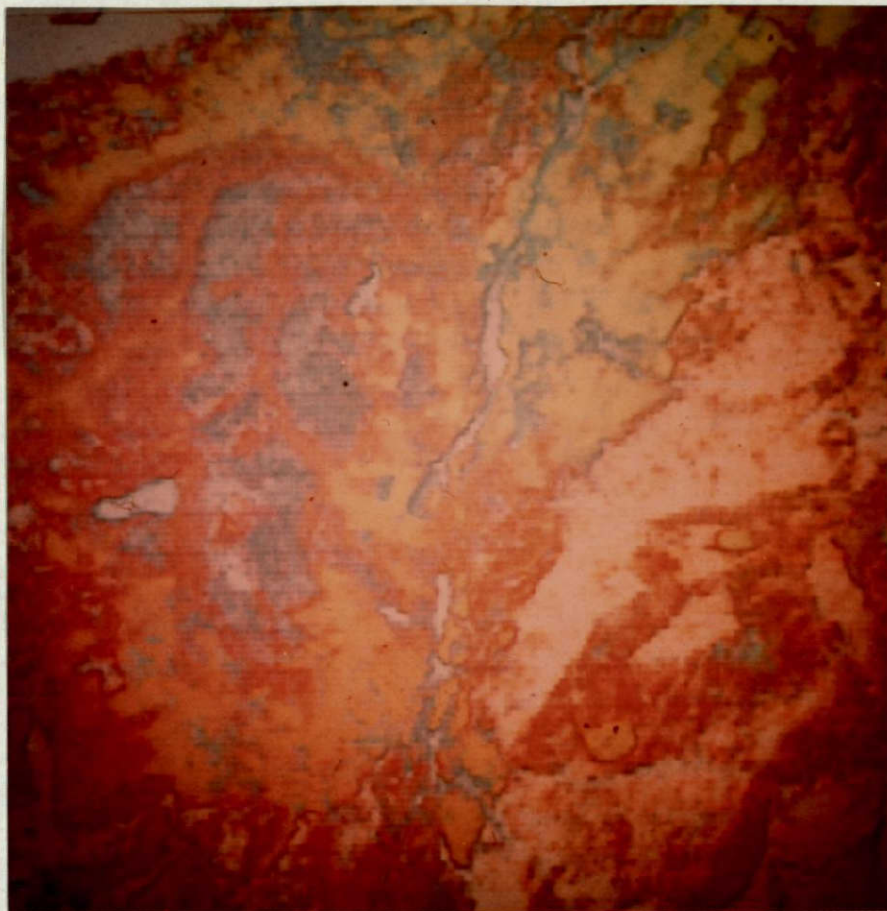
Fig.64   **Color transformation on the basis of statistically
preprocessed data**

Due to the momentaneous experimental status, it would be
desirable to quantify and standardize color coding of opti-
mized information on the basis of 3 dimensional color space.
The term standardization means a transformation into per-
ceptable color differences.

Quantification means a reproducable relationship between a
distinct phenomena and color. Such relationships are for
example red color tones indicating vegetation if false color
images are interpreted.

Such "quantified data" can be obtained if the input
data are derived from statistically optimized preprocesses.
For demonstration the data of test area 2 (Fig.62)
were selected.
The following color transformations show enhanced infor-
mation due to different surface phenomena (Fig. 65,66,67)

Fig. 65

Fig. 66

Fig. 67

Fig. 68 Aerial photograph exhibiting the same scene

On the basis of above processed information the user would be
provided with optimum data. In comparison to the computerized
classification technique, the transformation into the color
space procedure, results in data still "untouched" by decision
making errors or averaging effects.

The decision making aspect still left to the interpreter
could be carried out via isochrome mapping techniques or
even by an interpretation based on the earth scientific
know how.

3.   Analog Electronic Data Evaluation

The increased interest of scientists in Landsat data and
their requirements towards easy to operate and interactive
data processing possibilities led to the implementation of
an analog data processing system (Phase I, completet July
1975), which will be interfaced to a minicomputer (Phase
II, completed beginning of 1976).

By means of the interface combination, the system offers
hybrid capabilities. For quick look data evaluation based
on photographic LANDSAT-data-products it is possible to
operate the analog electronic circuits seperately. The
System has the following standard evaluation functions:

I Analog Electronics

    - point-wise density reading
    - density slicing
    - line by line intensity level analysis of the
      whole image including selection of particular
      features
    - combination of multispectral and sequential data
      with respect to following algorithms
          ratios; products, sums, differences

- color space operations with original or preprocessed
  data
- electronic representation of scatter diagrams of
  any two data sets.

The digital operating circuits will be supported by problem
oriented software routines covering the following function.

- CCT input capabilities
- geometric correction of LANDSAT data
- classification statistics
- basic image enhancement.

The results obtained by a pure digital treatment of data can
be displayed on a line printer or via the analog electronic
circuits.
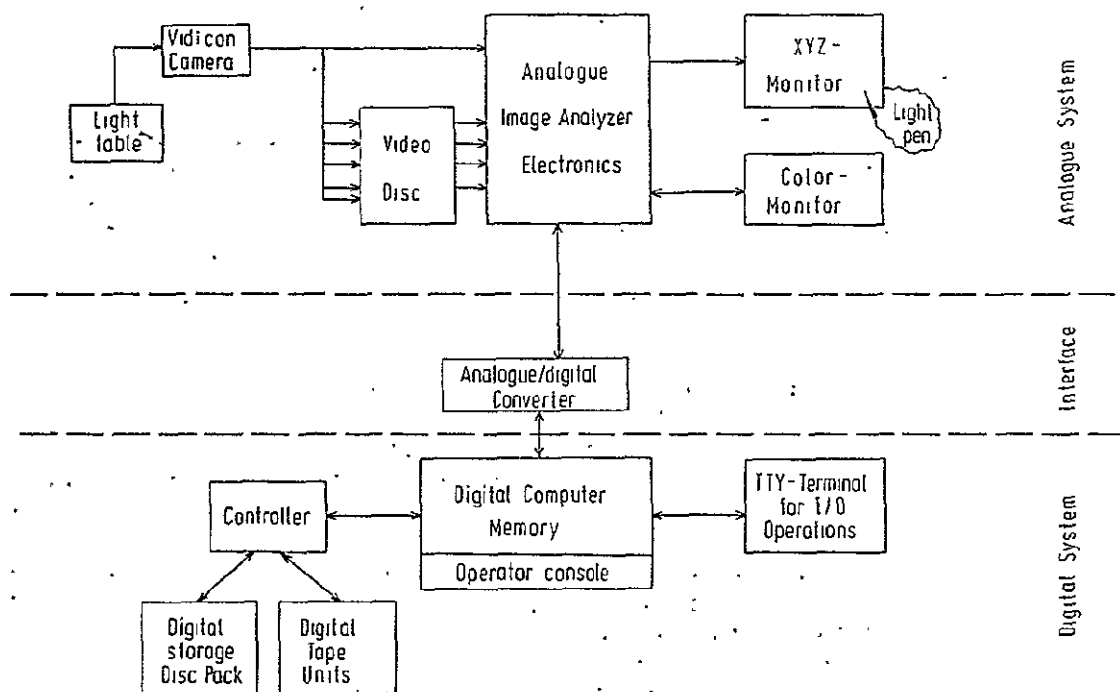
Fig. 69   Scheme of an analog/digital data processing
          system

C   Fourier analytical evaluation of LANDSAT data by

    an optical computer

During the last year coherent optical processing tech-
niques were applied on LANDSAT-data under various aspects.
The optical bench used is available at the Institut für
Nachrichtentechnik at the Technical University of Munich.

Optical processing was carried out for the following
purposes:

         − image manipulation

         − quantitative measurement of spectra

1. Image manipulation

    Image manipulations were done with an experimental system$
    exhibited by Fig. 7o

Fig. 7o   Schematic representation of optical bench

Using a coherent light source and a corresponding lens -
system, the two-dimensional pattern (Image) of the input
plane is transformed into the Fourier transform (fre-
quency plane). Now it is possible to remove spatial fre-
quencies from the Fourier spectrum by applying optical
filters.
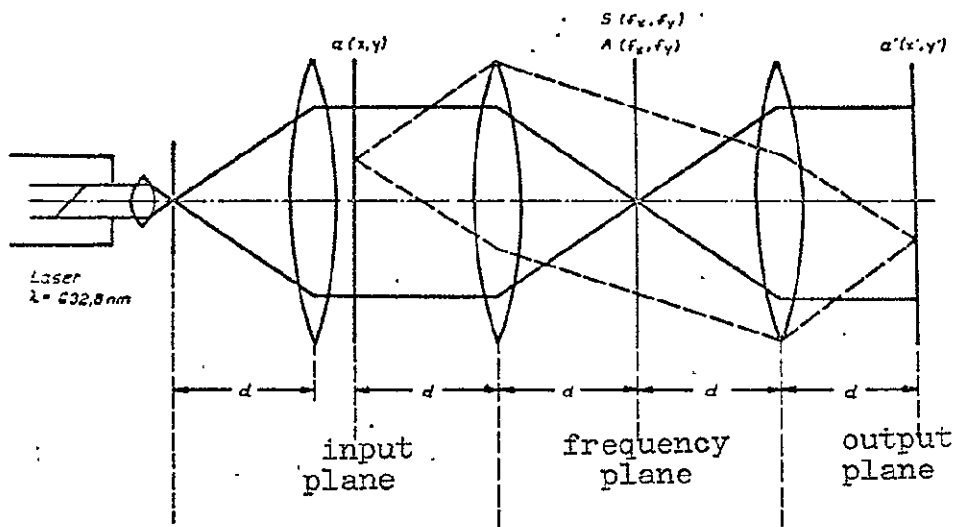Afterwards the filtered image can be optically rebuilt
(output plane) which again requires a corresponding lens.

By applying high- or low pass filters image enhancement in
terms of contrast manipulations can be carried out.

More intersting for geological applications is the so called
directioneal filtering.

For this purposes a 10° wedge filterwas used to remove
those directions which are easily detectable by the eye
and which may camouflage minor directions.

By using an S 190 A enlargement representing the Apenine
foreland between Pascara and Ancona (Fig. 71 a), an
attempt was made to remove especially those directions
that are not necessarily of tectonic origin in terms of
fracture control. The orientation indicated is due pri-$
marily to the drainage system dirested perpendicular to
the Adriatic coast (Fig.71a). The reconstruction (Fig.71b)
shows very distinctly the prolongations of the main line-
ations which cut the Apenines in an ENE and anaESE direc-
tion (Fig.71c).Furthermore, a secondary system acompany-
ing the main structures can be detected, especially in the
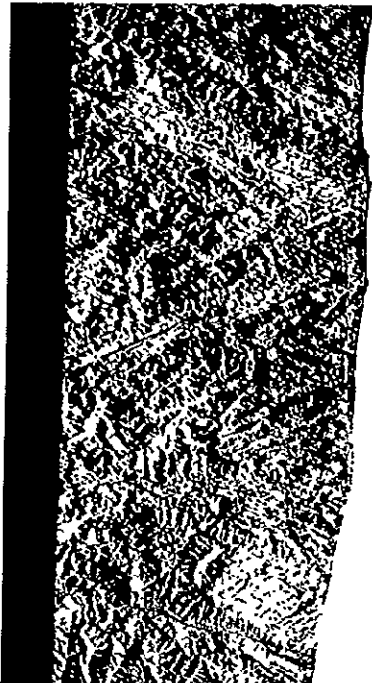northern part of the area selected.

Ancona

Eastern Apennine foreland
between Ancona and
Pescara
SKYLAB S 190 A, Sept. 73
(Detail)
Reconstruction from an
optical Fourier trans-
form

Adriatic
sea

(a)

Pescara

(b)
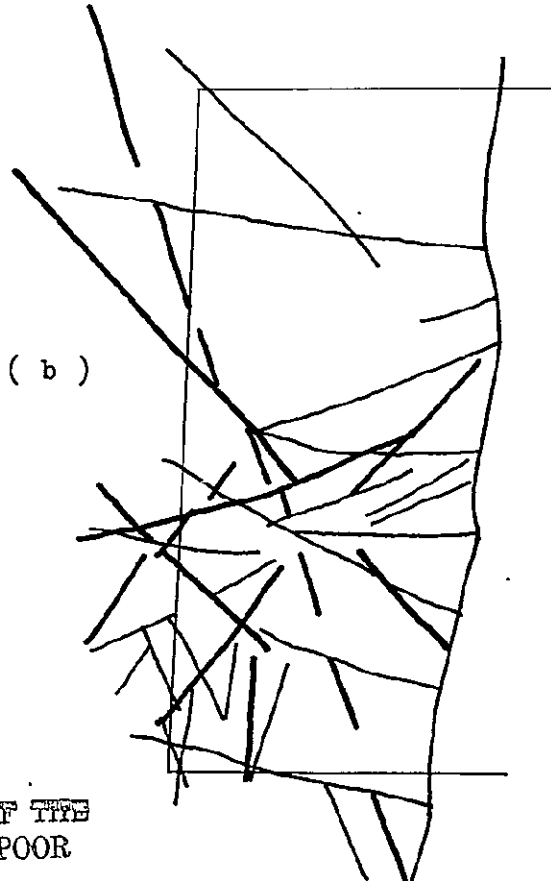
(c)

2. Quantitative measurements

Of special interest for tectonical applications is to ob-
tain a quantitative measure of the directional distri-
bution of linear features.
The conventional way of obtaining such information re-
quires time consuming evaluations and measurements of length
and direction of each single lineament.The results are
then statistically plotted in form of rose diagrams.

In order to evaluate the two-dimensional spectrum in a
quantitative way, the relative brightness of the spectrum
has to be measured.
The information of brightness - distribution was obtained
by using a photo multiplier which was connected to the
frequency plane. By a step wise rotation of a narrow wedge
filter the intensities can be easily recorded with respect
to the direction.

In order to obtain information on the accuracy of this tech-
nique a lineament(Fig. 72) was optically evaluated.
The result was compared with a conventional evaluation.
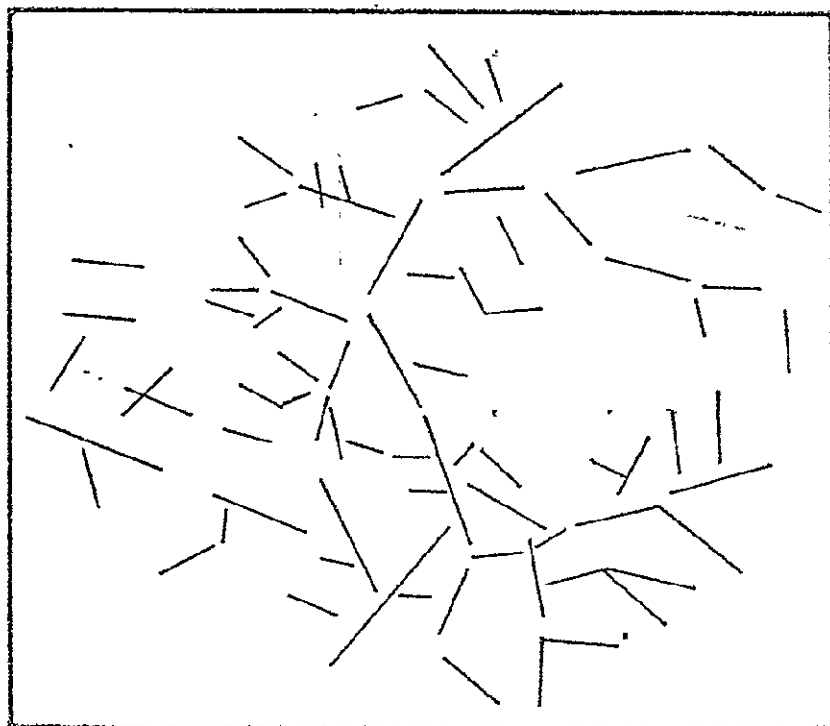
Fig. 72 Example of a lineament map

The comparison is exhibited by Fig.73 and shows a far-reaching agreement especially in the directional distribution of main lineaments.
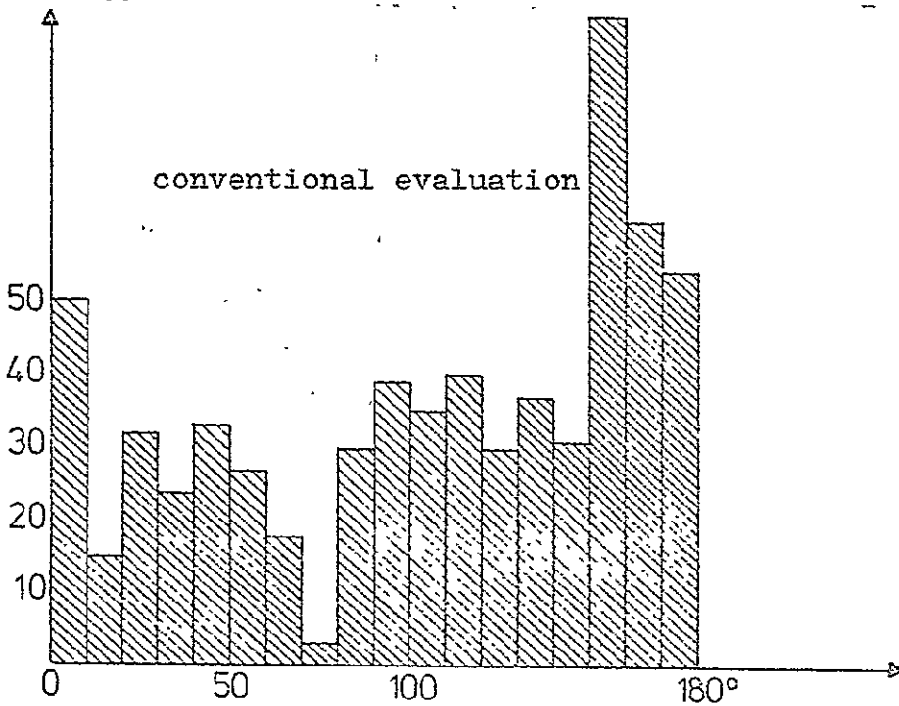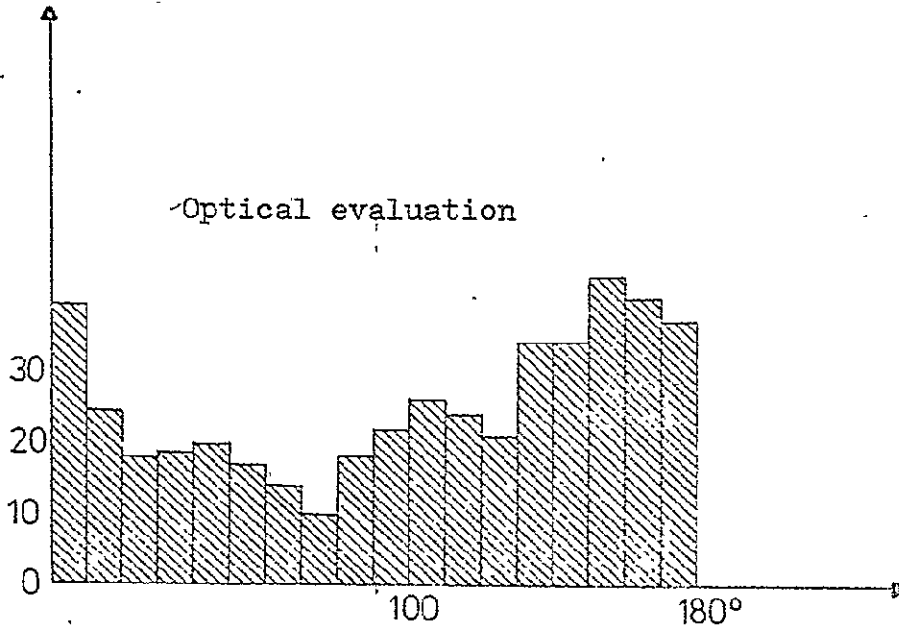
Fig. 73 Comparison optical/hand evaluation of a lineament map

In a next step a small part out of a LANDSAT scene (Fig.74)
was used. The distribution of image frequencies were di-
rectly measured and again compared with the lineament-
distribution obtained by a pure interpretation.(Fig.75).

Fig. 74 LANDSAT MSS-6 Rhine Graben with test site
for optical processing
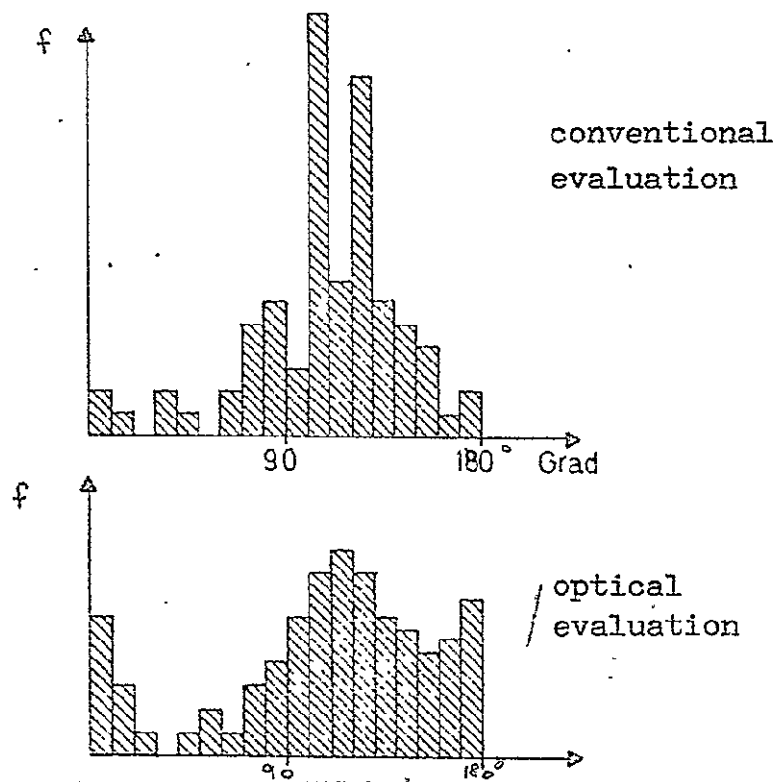
Fig. 75 Comparison optical/hand evaluation of testsite

This figure demonstrates again, that it is possible to obtain information at least on the distribution of dominant linear features by applying optical processing techniques.

Above described good possibilities led to a more detailed evaluation taking into account the frequency distributions which can be derived from different spectral bands. Fig. 76 demonstrates the frequency distributions of the same test area (Fig.74)with respect to MSS bands 4,5,6 a.7. A good comparisons af above readings is given by the characteristic peaks originated from the scan-lines. An effect which is distinctly expressed on MSS 4.

rel. Intens./10° Sektor

MSS 7

MSS 6

MSS 5

MSS 4

0 40 80 120 160 200 240 280 320 360

Drehwinkel
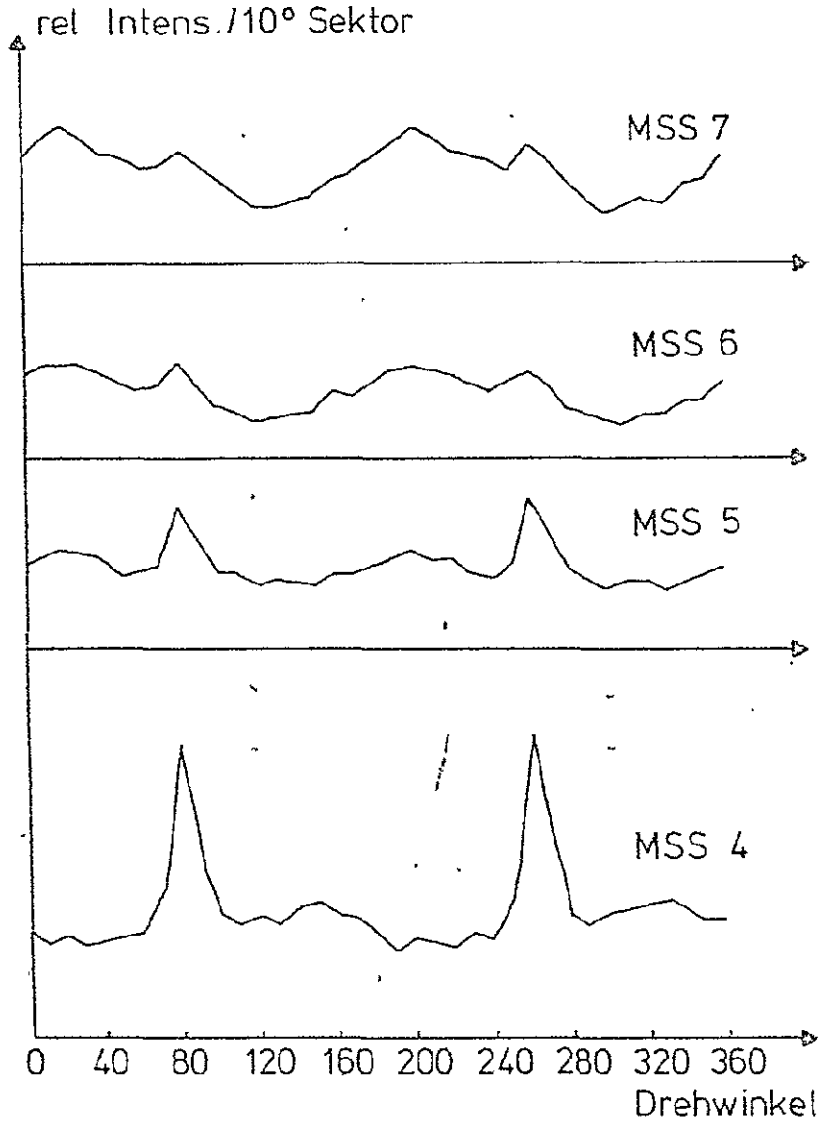
Fig. 76 Frequency distribution derived from
MSS bands 4, 5, 6 and 7

A comparative evaluation between MSS 7 and MSS 4 (Fig. 76)
shows that two directions can be identified with respect to
relative brightness differences.

Category I : Intensity MSS 7   MSS 4

Category II : Intensity MSS 7   MSS 4
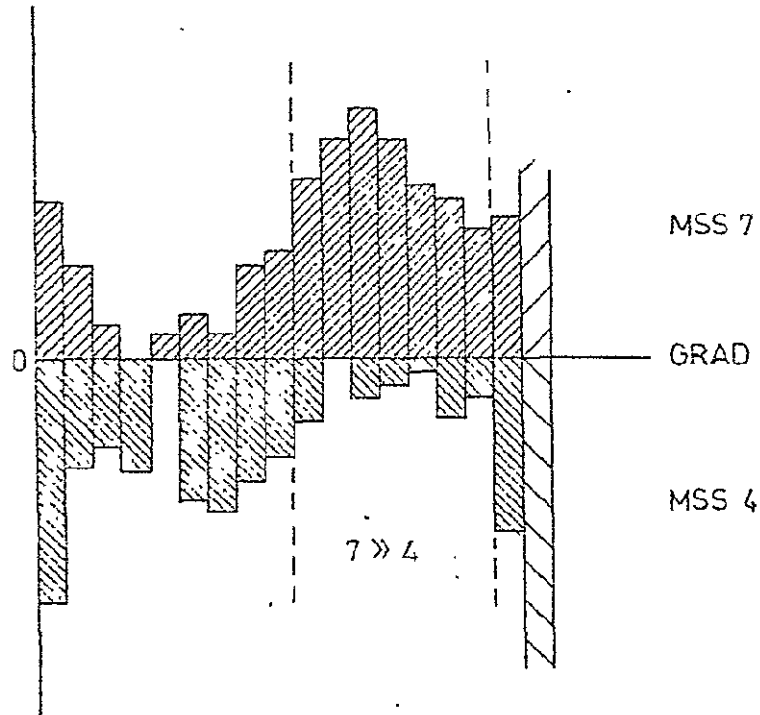
Fig. 77 Comparison Intensities band 7 versus band 4

These two characteristic intervals could be related to the
dominant fracture system in the vicinity of the Rhine Graben.
Category I corresponds to the Rhine Graben-parallelfracture
system and Category II to the lineations which are ± per-
pendicular to the parallel strucures.

This example has to be regarded as an attempt to com-
bine multispectral- with spatial- information on a more
quantitative way.

References to Part I, B: Geo-tectonic studies in Eastern Alps

Anderson, E.M.,   1951   The Dynamics of Faulting and Dyke-
                                       Formations with Application to Britain.
                                       Oliver and Boyd, Edinburgha, secd. ed.
                                       pp.10-11

Aubouin, J.,   1964   Esquisse Paleogeographique et Structu-
                                       rale des Chaines Alpines de la Medite-
                                       rranee Moyenne. Geol. Rdsch vol 53,
                                       pp.480-534.

Bodechtel, J. and   1973   New aspects on the tectonics of the
Lammerer,B.   Alps and the Appennines revealed by
                                       the ERTS-1 data. Proc. Symp. Signifi-
                                       cant Results Obtained from the ERTS-1
                                       Goddard Space Flight Center, Maryland
                                       March 5-9,1973,vol. I, Tech.Presentatio
                                       Sect.A, pp.493-499.

Bodechtel, J. and   1974   Geologigisch-tektonische Auswertung
Nithack, J.   von ERTS-1 und SKYLAB Aufnahmen von
                                       Nord- und Mittelitalien.Geoforum 20,
                                       pp.11-24.

Carte tectonique internatioale de l'Europe, 1 : 2,500,000, No.10,
Moscow, 1962.

Ernst, W.G.,   1975a   Systematics of large-scale tectonics
                                       and age progressions in Alpine and
                                       cicum-Pacific blueschist belts.
                                       Tectonophysics, 26, pp.229-246.

Ernst, W.G.,   1975b   Interpretative synthesis of metamor-
                                       phism in the Alps. In :W.G.Ernst(Editor)
                                       Subduction Zone Metamorphism ; Bench-
                                       mark papers in Geology /19; Dowden
                                       Hutchinson & Ross Inc. , pp. 406-431.

Farmer, I.W.,   1968   Engineering Properties of Rocks
                                       E.&F.N.Spon Ltd. London, pp. 58-59.

Freden, S.C. and   1973   Symposium on Significant Results Obtai-
Mercanti, E.P.   ned from Earth Resources Technology
                                   Satellite - 1 , vol. III, Discipline
                                   Summary Reports, 118 p., Goddard Space
                                   Flight Center,Greenbelt, NASA, Washing-
                                   ton, D.C.

Freden, S.C.,   1974   Third Earth Resources Technology Sympo-
Mercanti, E.P,and   sium,vol.III, Discipline Summary Reports
Friedman, D.B.,   155 p., Goddard Space Flight Center,
                                   Greenbelt,NASA, Washington,D.C.

Gansser, A.,   1968   The Insubric Line - a major geotectonic
                                   problem. Schweiz. Minerlog. Petrograph.
                                   Mittlgn.,vol. 48, pp.123-143.

Illies, H.,   1974   Intra-Plattentektonik in Mitteleuropa
                                   und der Rheingraben. Oberrhein. Geol.
                                   Abh., 23, pp. 1-24.

                           1975   Intraplate tectonics in stable Europe
                                   as related to plate tectonics in the
                                   Alpine system. Geol.Rdsch., vol. 64,
                                   pp. 677-699.

Laubscher, H.P.,   1971   The large-scale kinematics of the west-
                                   ern Alps and the western Apennines and
                                   its palinspastic implications, Am. Jour.
                                   Sci., vol. 271, pp 193-226.

Laubscher, H.P.,   1973   Alpen und Plattentektonik-das Problem
                                   der Bewegungsdiffusion an kompressiven
                                   Plattengrenzen. Z. Deutsch. Geol. Ges.
                                   vol. 124, pp. 295-308.

Price, N.J.,   1959   Mechanism of jointing in rocks. Geol.
                                   Mag., vol. 96, pp. 149-167.

                           1966   Fault and Joint Development in Brittle
                                   and Semi-Brittle Rock. Pergamon Press,
                                   Great Britain.

Ranalli, G., and   1975   The stress field in the Upper Crust as
Chandler, T.E.,   determined from in-situ measurements.
                                   Geol. Rdsch., vol. 64, pp. 653-674.

Ritsema, A.R.   1969   Seismo-tectonic implications of a
                                   review of European earthquake mechanism.
                                   Geol. Rdsch. vol.59, pp. 36-56.

Senftle, E., and   1973   Resente Hebung der hohen Tauern und
Exner, Ch.,   geologische Interpretation. Verh. Geol.
                                   Bund. Anst.,Vienna, No. 2, pp. 209-234.